SCALABLE MODULAR ANTENNA ARRAY FOR MASSIVE MIMO ANTENNA

A MASTER'S THESIS

A THESIS SUBMITTED TO
MASTER OF ELECTRICAL ENGINEERING STUDY

By

SALWA SALSABILA

2101212060

IN PARTIAL FULFILMENT OF THE REQUIREMENTS
FOR THE DEGREE OF MASTER ENGINEERING

MASTER OF ELECTRICAL ENGINEERING

TELKOM UNIVERSITY

BANDUNG

2023

APPROVAL PAGE

SCALABLE MODULAR ANTENNA ARRAY
FOR MASSIVE MIMO ANTENNA

This thesis is approved and authorized to be filled in the Graduate Program of Electrical Engineering, The School of Electrical Engineering, Telkom University

By:

Salwa Salsabila
2101212060

Bandung, 19 August 2023

First Advisor	Second Advisor
Dr. Bambang Setia Nugroho, S.T., M.T.	**Dr. Levy Olivia Nur, S.T., M.T.**
NIP: 99760035	**NIP: 14780033**

SELF DECLARATION AGAINST PLAGIARISM

In this thesis report entitled:

SCALABLE MODULAR ANTENNA ARRAY
FOR MASSIVE MIMO ANTENNA

At this moment author declares that information in this document has been obtained and presented following academic rules and conduct. Furthermore, the author has fully cited and reference all material and results that are not original to this work.

19 August 2023

Salwa Salsabila

Signature: 

19 August 2023

First Advisor: Dr. Bambang Setia Nugroho, S.T., M.T.

Signature: 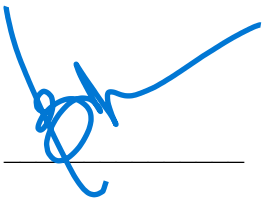

19 August 2023

Second Advisor: Dr. Levy Olivia Nur, S.T., M.T.

Signature: _____

ABSTRACT

High-speed 5G communication system technology (up to 1Gbps) for mobile internet use requires a large capacity. Multiple Input Multiple Output (MIMO) technology is used in antenna design which aims to get a larger capacity. Driven by the need for very high speed of 5G technology, a large-scale MIMO Antenna was designed or called a Massive MIMO Antenna. Massive MIMO antennas with a very large number of arrays can provide significant efficiency improvements.

Massive MIMO Antenna Design results in a very large antenna size that hinders the design process. The arrangement of Massive MIMO Antennas which consists of many antenna elements is a challenge in the design process due to the limited capability of the simulation software and the complicated process. Thus, a scalability technique is used to predict the results produced by a Massive MIMO Antenna with a certain configuration based on a simple MIMO Antenna compared with 4 elements, 16 elements, 64 elements MIMO configuration, etc. exponential increments.

This research will discuss the scaling process to predict the specifications of a Massive MIMO Antenna. The designed MIMO antenna arrangement is based on the design of a rectangular antenna with a truncated corner and yield the formula of $y = 6.6384x^{0.3069}$ of gain and $y = 100.33x^{-0.481}$ of HPBW, while a circular antenna with an X slot and yield the formula of $y = 6.8514x^{0.3027}$ of gain and $y = 100.72x^{-0.485}$ of HPBW for further design with various types of configurations that work at a frequency of 3.5 GHz.

Keywords: Massive MIMO Antenna,5G technology, scalability technique.

DEDICATION

بِسْمِ اللهِ الرَّحْمنِ الرَّحِيْمِ

All praise belongs to Allah SWT. who has given mercy and guidance and His gift, so that with His permission the author is given the opportunity to be able to complete the final project with the title "Scalable Modular Antenna Array For Massive Mimo Antenna" smoothly without any obstacles. Sholawat and greetings may always be bestowed upon the Prophet Muhammad SAW. who is a role model for mankind.

As for the preparation of this final project as one of the requirements to obtain a Master of Engineering (M.T) degree in Graduate Program of Electrical Engineering, The School of Electrical Engineering, Telkom University.

For the sake of perfecting the writing of this thesis, with all humility the author accepts constructive criticism, suggestions and responses as a guide in further writing to make it better. Hopefully this final assignment can be used as a form of application of knowledge that has been obtained during the learning process and can be used as a reference by future researchers.

Bandung, 19 August 2023

Author

ACKNOWLEDGEMENTS

In completing this Final Project, the Author realizes that it is inseparable from the assistance and guidance of various parties. Therefore, on this occasion, with all humility, the Author would like to express heartfelt gratitude and the highest respect to:

1. Allah SWT., for His abundant mercy and grace, enabling the Author to complete this final project and Prophet Muhammad SAW., as a role model for the Author in navigating this life;
2. Beloved parents, Mr. Tahqiq Faried (Papah) and Mrs. Ai Siti Fatimah (Ibu), for their unwavering support, advice, prayers, and shared efforts, which always kept the Author motivated throughout the academic journey;
3. Beloved siblings, Fatwa Mulhan Nabila (De Fatwa) and Tazkia Sayyidatunnisa (De Kia), who served as motivation and solace during the Author's lowest points in life;
4. Dr. Bambang Setia Nugroho, S.T., M.T., as the first Supervisor, and Dr. Levy Olivia Nur, S.T., M.T., as the second Supervisor, who generously agreed to be the Author's mentors, providing guidance, directions, and motivation, which greatly contributed to the smooth progress of the Thesis;
5. Mrs. Ir. Luk Lu'ul Ilma (Tante Lulu), a figure the Author respects and admires, who serves as a constant motivation for the Author to strive for excellence;
6. Rijal Habibulloh, who always accompanied and assisted the Author in overcoming various challenges, especially during the compilation of the Final Project;
7. Namira Fasya Rahim, a friend who has been a constant companion and aid to the Author since the early days of study until the end;
8. Friends and the entire academic community of Telkom University, whose support and contributions have been invaluable, even though they cannot all be individually named.

The Author acknowledges the tremendous help, guidance, and encouragement received from the aforementioned individuals and the broader academic community. Their contributions have significantly enriched the completion of this Thesis.

LIST OF CONTENTS

LIST OF TABLES

LIST OF FIGURES

LIST OF ABBREVIATIONS

ABBREVIATIONS	DEFINITIONS
AF	Array Factor
LHCP	Lefth Hand Circular Polarization
MIMO	Multiple Input Multiple Output
RHCP	Right Hand Circular Polarization

LIST OF SYMBOLS

SYMBOLS	DESCRIPTION
W_p	Width of patch
ε_r	Relative permittivity
f_r	Resonant frequency
c	Speed of light
L_p	Length of patch
ε_{reff}	Effective permittivity
h	Thickness of substrate
w	Width
L_{eff}	Effective length
L	Length
Q_0	Unloaded quality factor
S	Dimension of truncated corner
Δ	Delta
a	Radius of circular patch
π	Phi
W_g	Width of substrate and gain
L_g	Length of substrate and gain
G_S	Single gain
G_F	Field gain
θ	Thetea
$\emptyset$	Psi
L_g	Length of ground plane and substrate
$^\circ$	Degre
%	Percent
dB	Desibel

I. INTRODUCTION

1.1 Background

The development of mobile internet to meet the needs of future data growth is the reason for increasing network capacity, transmission rate, and efficiency compared to 4G cellular communication technology [1]. The use of wireless communications bands is increasingly congested as a result of data growth so we need a technology to increase data throughput. This poses a new challenge to research the solution technology to be developed. The Federal Communications Commission (FCC) has announced the frequency spectrum for 5G communication technology which explains that mobile internet-based electronic devices can not only take advantage of faster throughput speeds than 4G technology, but also have low latency that can be utilized in various cellular communication applications [2]. In this case, technology is used with the Multiple Input Multiple Output (MIMO) system on Massive MIMO Antennas (Massive MIMO) which is one of the core technologies in the 5G communication system used as multi-antenna transmission which can provide increased channel capacity and increase signal strength by reduce the multipath effect. Massive MIMO with a very large number of antennas is known to produce a significant increase in efficiency [3], [4].

The use of MIMO technology in antennas (MIMO antennas) causes mutual coupling to occur between single antenna elements, as well as multipath components that can affect wave propagation. This can be overcome by providing a high isolation value between single antenna elements [5]–[8]. The MIMO antenna configuration scheme needs to be considered in antenna design. Based on [9], it is explained that simple MIMO antenna configuration schemes (such as 4 elements, 16 elements) are still not suitable for 5G communication needs because of their predicted speed of 1,000 times faster than 4G and better reliability. As a result of the need for 5G communication, the antenna configuration scheme that is carried out is the design for the Massive MIMO Antenna model. Interest in [10]–[12] explains that Massive MIMO Antenna can increase channel capacity and wider coverage of electromagnetic wave radiation emission. However, the design of Massive MIMO Antennas results in a larger size that hinders the antenna design process.

The following is a picture of a massive MIMO antenna system that acts as a massive multi-transmission [8].

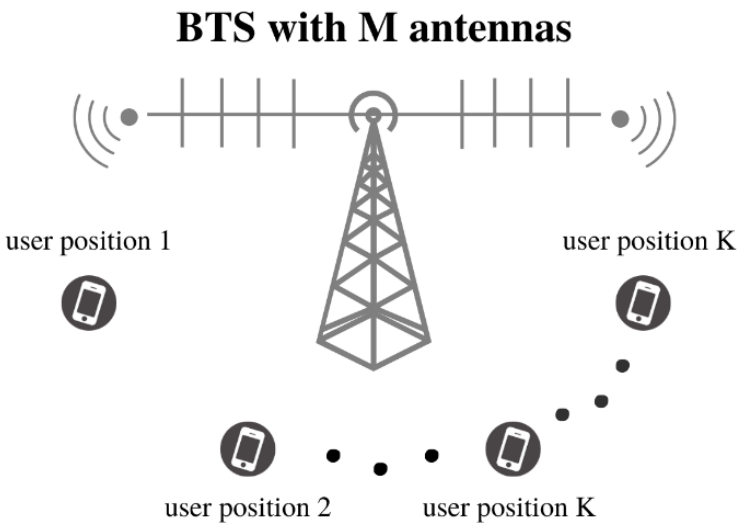

Figure 1. 1 Massive MIMO system.

Designing a large-scale antenna with a massive MIMO scheme is certainly a new challenge in the antenna simulation process. The antenna simulation process is limited because the capabilities of the simulation software are taken into consideration in the design process. However, the need for massive MIMO technology that continues to increase has forced the design of Massive MIMO Antennas to be carried out. Based on this, the authors propose the use of Scalable Techniques to predict the specification performance of Massive MIMO Antennas based on simple MIMO antennas using Array Factor (AF) Theory.

AF theory is used to calculate the overall antenna pattern by considering the element distance and element type for scalability purposes [13]. In [14] the impact of several elements on the AF for a uniform antenna arrangement is described. Another study proposed by [15] investigated the radiation parameters of large antenna arrays by combining the AF and active element patterns. The results also show that the AF pattern increases linearly with the number of antenna elements.

The MIMO system with the beamforming approach has dedicated communication capabilities between BTS and users. This happens because the MIMO Antenna work system has multipath propagation. Multipath propagation on

MIMO antennas makes it difficult to know the extent of the antenna's overall coverage when it transmits electromagnetic waves, in a MIMO system it is difficult to see how far BTS can reach users. An array antenna is used which has one propagation path and it can be seen how far the antenna can radiate. Thus, the predicted performance that can be achieved on the Massive MIMO Antenna is calculated based on its modular Array Antenna with the Array Antenna simulation scheme based on the MIMO configuration.

MIMO antenna with high isolation requires modification in its design. Modification of the MIMO antenna design is carried out by placing the port position on the antenna which will produce the polarization in opposite directions between antennas that are close to each other, including the Right Hand Circular Polarization (RHCP) and the Left Hand Circular Polarization (LHCP) [16]–[18]. Antenna design with RHCP and LHCP radiation patterns was carried out in 2 types of patch antennas that is rectangular antennas with truncated corners [19]–[21] and circular antennas with slot x [22].

1.2 Problem Identification

This research will focus on the design of Massive MIMO Antennas to predict the performance parameters generated by scalability techniques. However, the arrangement of MIMO antennas that make the antennas close each other can affect the performance between single antennas with the resulting mutual coupling effect. In addition, the scalability technique that is carried out needs to be reviewed further to predict the achievable specifications value.

The performance between adjacent MIMO antennas will not affect each other if adjacent antennas have high isolation value [16]–[18]. To produce high isolation value between adjacent antennas, a port placement modification technique is used to produce RHCP-LHCP polarizations between adjacent antennas. Modifications to produce RHCP-LHCP were carried out in the design of rectangular truncated corner antenna [19]–[21] and circular slotted x antennas [22].

The design that will be carried out on rectangular truncated corner antenna and circular slotted x antenna is each carried out by modifying the port position to produce RHCP-LHCP and simulating uniform antenna for each type of patch. Thus,

the effect and performance resulting from each type of patch will be compared and analysed to prove the scalability technique studied.

1.3 Objectives

The research will result in scaling the Massive MIMO Antenna design using scalability techniques. Antenna scalability is carried out on MIMO antennas by calculating predictions of the specifications that will be obtained by a Massive MIMO antenna based on a simpler MIMO antenna by simulating a simple modular array to scale it up into a Massive MIMO Antenna.

MIMO antenna can make the performance of adjacent antennas influence each other, so a solution is needed to make the antenna have a high isolation value. High antenna isolation values can be achieved by using an antenna type that produces RHCP-LHCP polarization. In this case, a rectangular patch antenna with a truncated corner and a circular patch antenna with x slot are used.

The simulation results of MIMO antenna configurations on rectangular patch antennas with truncated corners and circular patch antennas with x slots will be compared to ensure the scalability technique used to further calculate the Array factor to find out the pattern of increasing the performance of the antenna.

1.4 Scope of Research

Scope of research in this study are as follows.

1. This study focuses on discussing the simulation process of 5G MIMO antenna design and scalability.
2. The design method used for the single element antenna is a rectangular truncated corner patch antenna and a circular patch antenna with x slots for RHCP-LHCP circular polarization.
3. This study focuses on the calculation and scalability of a massive MIMO antenna for 5G Antenna based on a simple modular array antenna configuration.

1.5 Hypothesis

Massive MIMO antenna design was carried out to meet the needs of 5G technology with a large channel capacity and a predicted speed of 1000 times greater than 4G technology [9]–[11]. Massive MIMO antennas are known to

increase channel capacity and wider coverage of electromagnetic wave radiation [10]–[12]. However, Massive MIMO antennas with very large configuration schemes are a challenge due to the limited capability of the simulation software in the design process. Thus, a scalability technique is carried out to predict the parameter performance that will be produced by a Massive MIMO Antenna based on a simpler MIMO antenna arrangement by simulating on modular array antenna [23].

1.6 Research Methodology

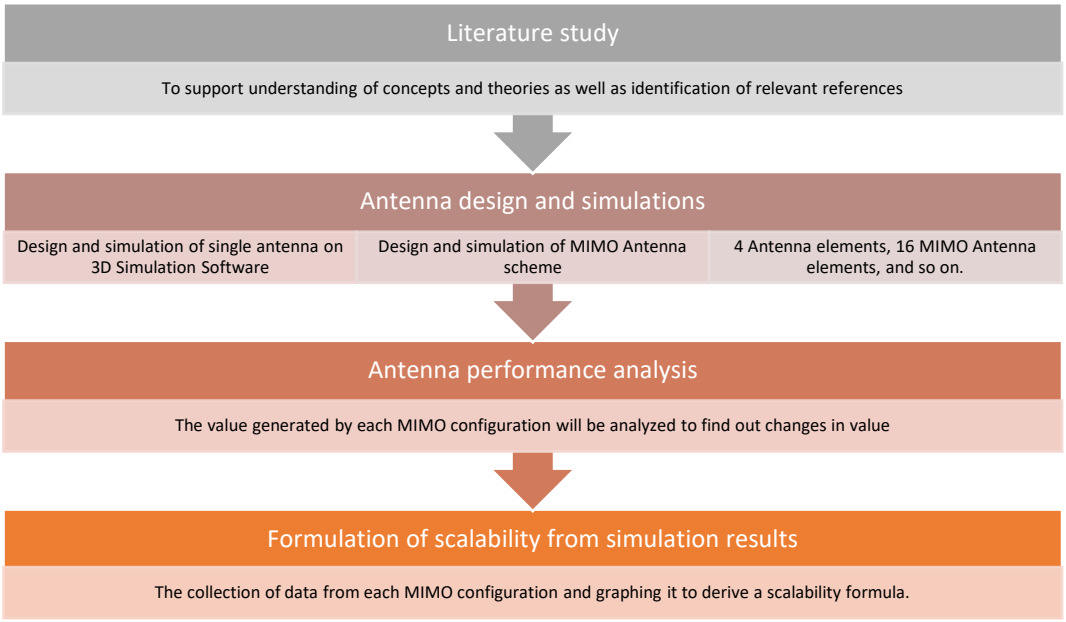

The research process begins with a literature study to support understanding of concepts and theories as well as identification of relevant references related to the development of 5G technology and Massive MIMO Antennas. Next, antenna design and simulation are carried out using a simple MIMO Antenna scheme in CST simulation software. The first stage of design and simulation is the design, simulation, and optimization of single patch rectangular antenna elements with truncated corners for RHCP-LHCP until the resulting parameters are in accordance with specifications. Next, the 4 MIMO Antenna configuration is performed as a single element. After that, bigger and more complex configurations (16 elements, 64 elements, etc.) configurations are carried out in exponential increments. As a comparison and to ensure the scalability technique being carried out, a circular patch antenna with an x slot with RHCP-LHCP polarization was also designed. The

purpose of this study is to perform further calculations, aiming to predict the specifications that can be generated from a larger MIMO configuration based on the formula derived from simulation results.

1.7 Thesis Organization

In general, this thesis is divide into five chapter's discussion. The explanation as follows:

1. CHAPTER 2 BASIC THEORY

   This chapter contains the basic concept and theories related to this study.

2. CHAPTER 3 EXPERIMENTAL DESIGN

   This chapter is consist of antenna design for RHCP-LHCP polarization MIMO configuration with a rectangular patch antenna with a truncated corner and a circular patch antenna with an x slot.

3. CHAPTER 4 ANALYSIS

   This chapter consist of analysis for scalability techniques that measure the antenna design of rectangular patch antenna with truncated corner and circular patch antenna with x slot.

4. CHAPTER 5 CONCLUSION AND SUGGESTION

   This chapter consist of conclusion of this research and the suggestion to develop it.

II. BASIC THEORY

2.1 5G Technology for Wireless Communications

The 5G technology is not just an advanced technology from 4G, but also a new technology that complements telecommunications. 5G technology with high-level features has a bandwidth that is at least 1000 times wider than 4G, a speed of up to 10 Gbps and a latency of less than 5ms.

Because of necessitates of compatibility and agile, modular architecture for expeditious low-cost deployment and smooth technical augmentation in the future, the 5G architecture is proposed to be fundamentally different from the 4G network architecture [24].

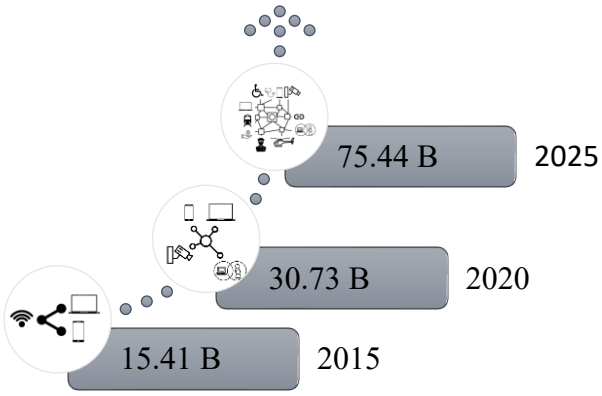

Figure 2. 1 The number of connected gadget prediction in year.

2.2 3.5 GHz 5G Band

GHz 5G Band (n78 3500 MHz) or commonly referred to as C-band 5G is a working frequency that is widely used in testing the development of 5G technology. In this case the 3.5 GHz frequency is used for simple wireless communication in the 3.3 GHz – 3.8 GHz spectrum with several channel bandwidths supported including 10,15,20,30,40,50,60,70,80,90,100 in MHz with the use of channel widths is in a Figure 2.2 [25].

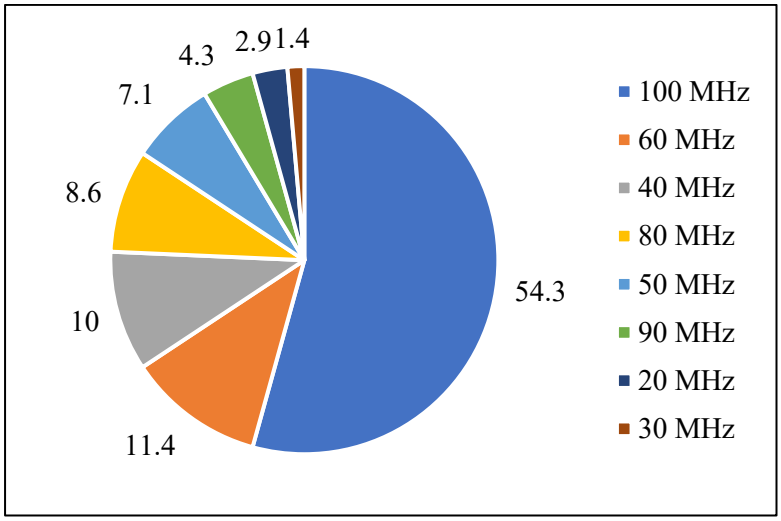

Figure 2. 2 5G Channel Widths.

The n78 coverage is naturally limited by the propagation characteristics of the higher frequencies, however the effect has in some ways been mitigated by advanced processing techniques such as massive MIMO, beamforming, and beam-tracking.

2.3 Multiple Input Multiple Output Antenna

Multiple Input Multiple Output (MIMO) technology is used in the antenna design process which aims to obtain a larger capacity. Driven by the need for very high speed of 5G technology, a MIMO Antenna on a large scale or called a Massive MIMO Antenna was designed. Massive MIMO antennas with a very large number of arrays can deliver significant efficiency improvements while supporting today's 5G technology requirements [3], [4].

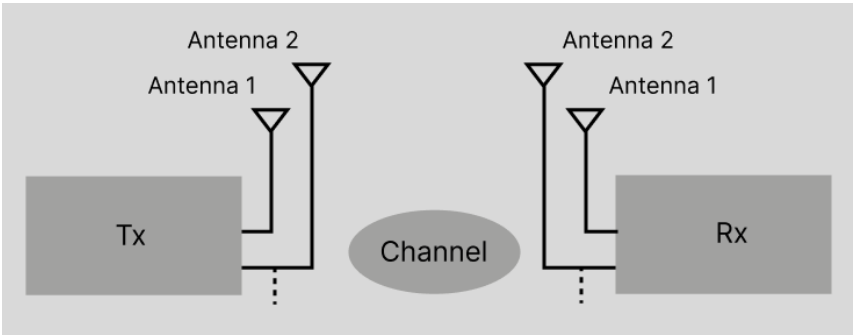

Figure 2. 3 Block diagram of MIMO Antenna performance.

Electromagnetic waves between the Transmitting Antenna and the Receiving Antenna create a multipath propagation direction which can affect the strength of each radiation beam. There is also interference which limits the performance of

individual antenna systems. In this case, MIMO technology can handle the transmission and reception of signals over multipath channels and the reduction of mutual coupling effects. The concept of MIMO technology also has several uses including wide area coverage, high speed, increased capacity, and good circular polarization. Circular polarization aims to ensure maximum signal reception in both the vertical and horizontal directions [8].

In the performance of MIMO antennas, the characterization of the mutual coupling is first carried out before reducing the mutual coupling. Mutual coupling on an antenna is related to the s-parameter parameter $S_{1,1}$ and the isolation parameter $S_{1,2}$. However, the s-parameter and isolation parameters cannot characterize, so the Envelope Correlation Coefficient (ECC) parameter is used which uses all s-parameter parameters and isolation parameters from different ports for characterization purposes. The International Telecommunication Union (ITU) has set the ECC value for cellular communications of 0.5.

Massive MIMO technology is a 5G technology system to serve a very large number of terminals. Massive MIMO technology research is known to provide data rates of 10 Gbps for the generation of wireless communication systems. Massive MIMO has been integrated with LTE and IEEE 802.11 wireless technology. Massive MIMO technology with its reliability that can measure information for each channel directly makes it a scalable technology.

2.4 Massive MIMO Performance

Massive MIMO systems are considered where the base stations are equipped with a large number (tens to hundreds) of antennas. An interesting feature of massive MIMO is based on optimistic assumptions about propagation conditions in combination with the availability of a large number of antennas. Massive MIMO can reduce interference between users served in the same time frequency source, because the focus is on the power transmitted to the desired user. The basic idea is because the number of base station antennas is getting bigger [26].

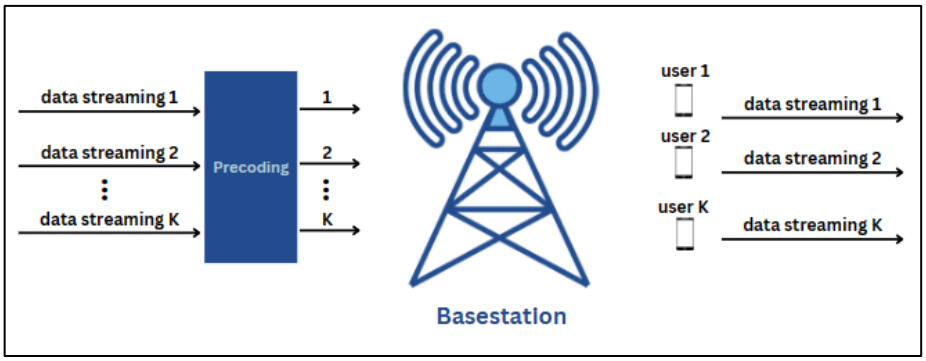

Figure 2. 4 Massive MIMO System.

Massive MIMO refers to the use of antenna arrays with many antenna elements for large-scale performance. In addition, the higher frequency bands provide the ability to design antenna arrays with a large number of antennas. That is, large-scale antenna arrays are a system requirement for 5G higher frequency band communication systems [27].

2.5 Microstrip Antenna

Microstrip antenna is a type of antenna that is small and relatively inexpensive. The microstrip antenna consists of three main constituent structures including the patch as the radiating element, the substrate as the dielectric component, and the ground plane as the reflector.

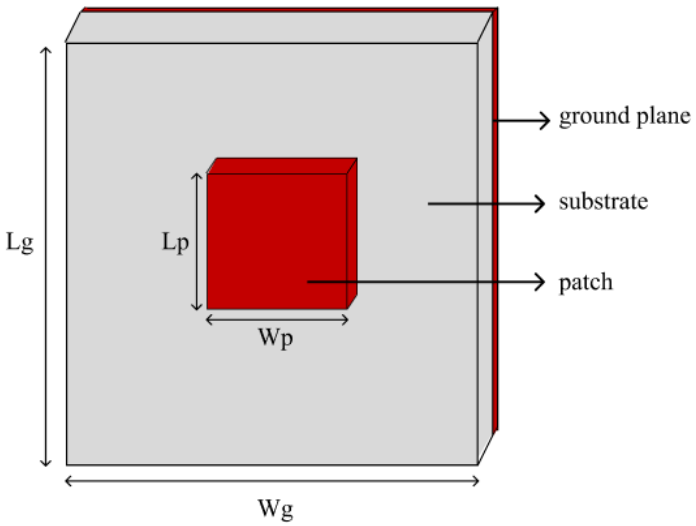

Figure 2. 5 Microstrip antenna front view.

Figure 2. 6 Microstrip antenna side view.

Substrate selection in microstrip antenna design can affect the performance of the antenna. Antenna designs with good performance usually have dielectric constant values (ε_r) in the range of $2.2 \leq \varepsilon_r \leq 12$. Thick substrates with low dielectric constant values can produce better efficiency and wider bandwidth than thin substrates with high dielectric constant values. However, thin substrates with high dielectric constant values can reduce unwanted radiation and mutual coupling effects [28].

2.5.1 Patch

The patch on a microstrip antenna is a radiating element that is placed on a substrate and is made of a conducting material. Patches can be made of various shapes and sizes. The size of the patch is determined by the resonant frequency acting on a microstrip antenna and the type of substrate material used. Patch shapes on microstrip antennas generally can consist of various shapes such as squares, rectangles, dipoles, circles, or various other shapes.

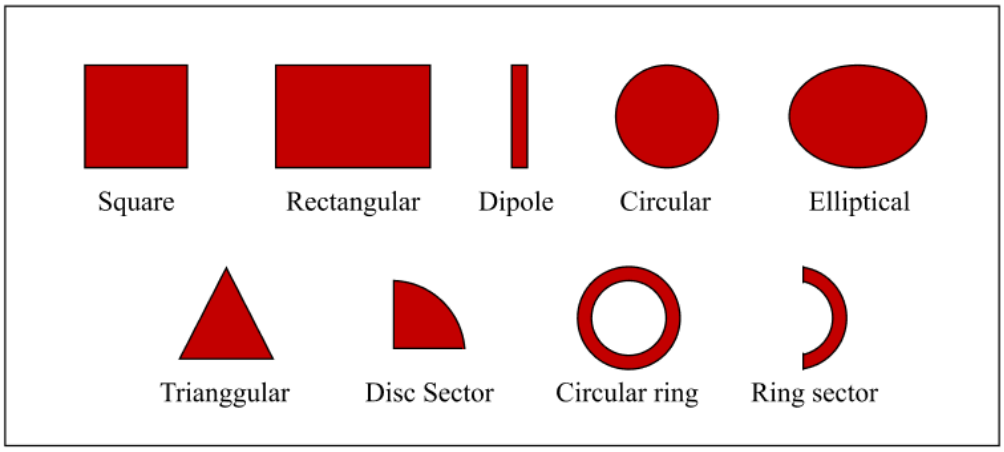

Figure 2. 7 The shape of patch of microstrip antenna.

In this research, a rectangular patch with a truncated corner and a circular patch with an X slot at a resonant frequency of 3.5 GHz.

2.5.1.1 Rectangular Patch with Truncated Corner

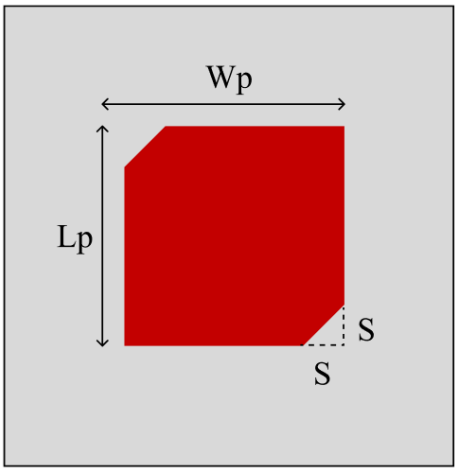

Figure 2. 8 Rectangular patch with truncated corner.

Based on [28], here is the formula for determining antenna dimensions:

- Width of Patch (W_p)

$$W_p = \frac{c}{2f_r}\sqrt{\frac{2}{\varepsilon_r + 1}} \tag{2.1}$$

Where W_p is the value of the patch width (mm).

- Length of Patch (L_p)

$$\varepsilon_{reff} = \frac{\varepsilon_r + 1}{2} + \frac{\varepsilon_r - 1}{2}\left[1 + 12\frac{h}{w}\right]^{-1/2} \tag{2.2}$$

$$L_{eff} = \frac{c}{2f_r\sqrt{\varepsilon_{reff}}} \tag{2.3}$$

$$\Delta L = 0{,}412\, h\, \frac{\left(\varepsilon_{reff} + 0{,}3\right)\left(\frac{w}{h} + 0{,}264\right)}{\left(\varepsilon_{reff} - 0{,}258\right)\left(\frac{w}{h} + 0{,}8\right)} \tag{2.4}$$

$$L_p = L_{eff} - 2\Delta L \tag{2.5}$$

Where L_p is a length of patch (mm), c is a speed of light in a free space (3×10^8 m/s), f_r is a resonant frequency (Hz), ε_r is a constant dielectric of substrate and h is a thickness of substrate (mm).

- Truncated Corner

Truncated Corner is a method to produce circular polarization on the antenna. This method is done by cutting the end of the patch which is located as shown in Figure 2.6.

To determine the dimensional value of S, calculations are performed using the following equation [20].

$$Q_0 = \frac{c\sqrt{\varepsilon_r}}{4f_r h} \tag{2.6}$$

$$\frac{\Delta s}{s} = \frac{1}{2Q_0} \tag{2.7}$$

$$S = L_p\sqrt{\frac{\Delta s}{s}} \tag{2.8}$$

Where Q_0 is a value of unloaded quality factor, $\frac{\Delta s}{s}$ is a cutting ratio, and S is the length of truncated corner.

2.5.1.2 Circular Patch with X Slot

Circular patch with X slot is designed to obtain the circular polarization RHCP-LHCP with the characteristic of the design is in the Figure 2.9. The dimension of X slot is obtained from carrying out the sweep parameter to the best s-parameter value at a frequency of 3.5 GHz.

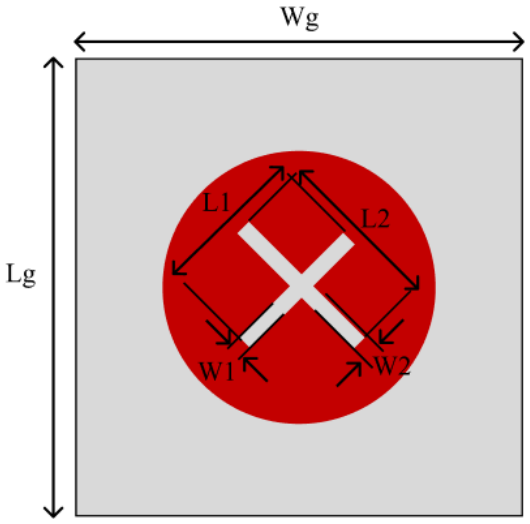

Figure 2. 9 Circular patch with X slot.

- Radius of Patch (a)

$$a = \frac{F}{\left\{1 + \frac{2h}{\pi\varepsilon_r F}\left[\ln\left(\frac{\pi F}{2h}\right) + 1.7726\right]\right\}^{1/2}} \quad (2.9)$$

where

$$F = \frac{8.791 \times 10^9}{f_r\sqrt{\varepsilon_r}} \quad (2.10)$$

Where a is a radius of patch (mm).

2.5.2 Dielectric Substrate

The substrate is a dielectric element that is between the two conductor elements in a microstrip antenna. The substrate on the microstrip antenna has a certain characteristic of ε_r . The value of ε_r determines the efficiency and bandwidth that can be generated. To produce good efficiency and wide bandwidth, it is necessary to use a thick substrate with a small $\varepsilon_r$value. The substrate used in this study is FR-4 Epoxy with $\varepsilon_r = 4.4$ with a thickness of 1.6 mm.

2.5.3 Ground Plane

The ground plane is the lowest part of a microstrip antenna arrangement which functions to reflect the radiation emitted from the radiating elements. The dimensions of the ground plane of a microstrip antenna will depend on the dimensions of the patch. These dimensions can be determined by the following formula:

- Width of Substrate (W_g)

The dimensions of ground and substrate are the same.

$$W_g = 6h + W_p \quad (2.11)$$

Where W_g is the substrate width value (mm).

- Length of Substrate (L_g)

$$L_g = 6h + L_p \quad (2.12)$$

Where L_g is the substrate length value (mm).

2.6 Circular Polarization

Circular polarization of a microstrip antenna can be generated by adjusting the dimensions of the antenna and modifying the feed, be it a single feed or more. For simplicity, a single feed can be used with the configuration of placing the feed on a part that can produce right circular polarization or left circular polarization [29], [30].

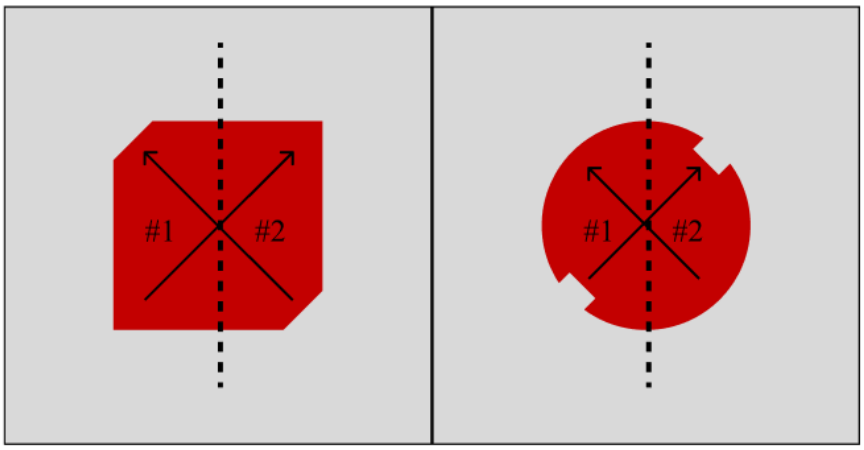

Figure 2. 10 Circularly polarized microstrip antenna.

2.7 Field Gain

Field Gain is indicating an antenna's ability to focus electromagnetic wave radiation into a desirable field pattern, is the gain value in the electromagnetic wave radiation field from the antenna. By combining the gains from each antenna element in the MIMO array, Field Gain may be used in MIMO system design to determine the overall gain of the MIMO system. The gain values in the MIMO setup method are then generated using these values as a reference after first calculating the Field Gain of each MIMO antenna element.

Field Gain is the value of gain in the electromagnetic wave radiation field produced by an antenna that can assess the antenna's ability to concentrate wave radiation into a specific field pattern. By combining the gains from each antenna element in the MIMO array, Field Gain can be utilized in the design of MIMO systems to determine the system's overall gain. This time, the Field Gain of each MIMO antenna element is computed first, and the gain values for the MIMO configuration scheme are then calculated using these values as a guide.

The following is the formula for calculating field gain [31].

$$G_F = \sqrt{n} \times G_S = \frac{10 \log n}{2} + G_S \quad (2.13)$$

When G_F is $Field\ Gain$ and G_S is $Single\ Gain$ is the gain value of single antenna.

2.8 The Difference Between Array Antenna and MIMO Antenna

The difference between Array Antenna and MIMO Antenna can be outlined as follows:

An antenna array is a configuration of multiple individual antenna elements arranged in a specific pattern to enhance signal reception or transmission performance. Its main goal is to strengthen signal directionality, improve communication efficiency, and combine signals from several antennas within the array. The key advantages include superior beamforming capabilities, increased resistance to signal interference and attenuation, and the reduction of multi-path fading effects. Antenna arrays are commonly used in communication and radar systems to direct signals towards specific directions or to isolate signals from angles [32].

On the other hand, MIMO antenna involves the utilization of multiple transmission and reception antennas within a communication device to send and receive multiple streams of data simultaneously. The primary objective is to enhance system capacity and mitigate the adverse effects of fading channels, which are rapid changes in signal strength. The notable advantages of MIMO include improved spectral capacity, better signal reliability, enhanced signal quality, and the ability to counteract multi-path fading effects. This technology is commonly applied in wireless technologies such as Wi-Fi, LTE, 5G, and other communication systems to enhance data throughput and overall communication quality [33].

2.9 Array Factor

By factoring the array formula, we can achieve some of the characteristics of a planar array. Furthermore, the scaling method can find out the relationship between small planar arrays and large planar arrays. Similarity of characteristics between the displayed arrays [28].

For a uniform M × N planar array element in which all elements have the same excitation amplitude, the normalized array factor is formulated as follows:

$$AF_n(\theta, \emptyset) = \left\{\frac{1}{M}\frac{\sin\left(M\frac{\psi x}{2}\right)}{\sin\left(\frac{\psi x}{2}\right)}\right\}\left\{\frac{1}{N}\frac{\sin\left(N\frac{\psi y}{2}\right)}{\sin\left(\frac{\psi y}{2}\right)}\right\} \quad (2.14)$$

Where:

$$\psi x = kd_x \sin\theta \cos\emptyset + \beta_x$$

$$\psi y = kd_y \sin\theta \cos\emptyset + \beta_y$$

The solid beam angle of the planar array can be obtained as:

$$\Omega_A = \theta_h \emptyset_h \text{ atau } \Omega_A = \frac{\Delta\theta_x \Delta\theta_y}{cos^2\theta_0\sqrt{\left[sin^2\emptyset_0 + \frac{\Delta\theta^2 y}{\Delta\theta^2 x}cos^2\emptyset_0\right]\left[sin^2\emptyset_0 + \frac{\Delta\theta^2 x}{\Delta\theta^2 y}cos^2\emptyset_0\right]}} \quad (2.15)$$

θ_0 and $\emptyset_0$ represents the direction of the main lobe, $\Delta\theta_x$ is an HPBW value of a wide linear array where the number of M elements and excitation amplitude is equal to the x-axis linear array forming a rectangular planar array whereas $\Delta\theta_y$ is an HPBW value of a wide linear array where the number of N elements and the excitation amplitude are equal to the y-axis linear array forming a planar array.

The array factor will be calculated based on a simple antenna array pattern and continues to a larger antenna array in a MIMO antenna array. AF calculation starts from the 2 elements of antenna MIMO antenna array (vertical arrangement scheme and horizontal arrangement scheme) as a reference for AF calculations for 4 elements of antenna, 16 elements of antenna MIMO antenna arrays and so on. As in Figure 2.11 an AF calculation pattern based on a phased array scheme.

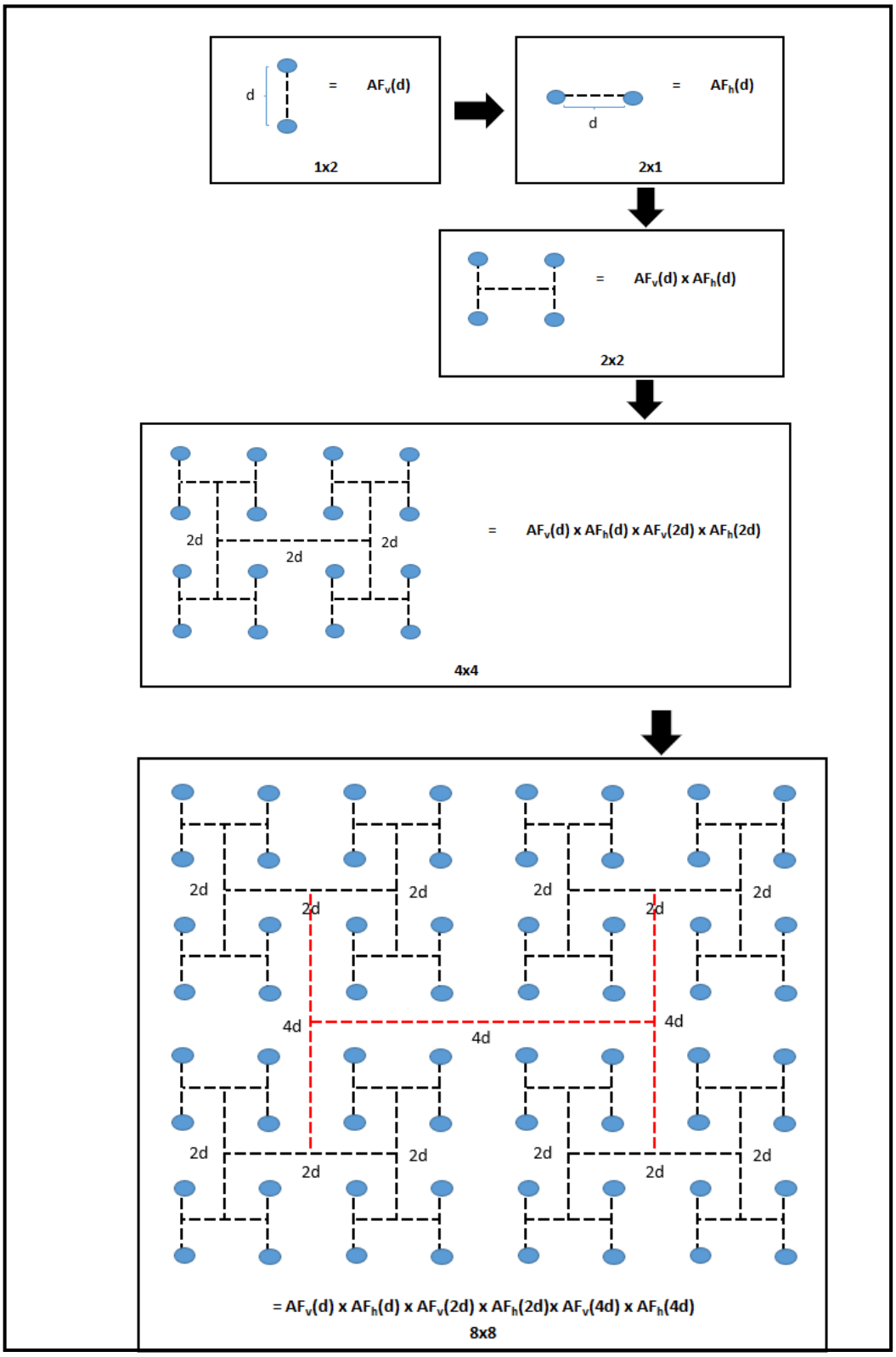

Figure 2. 11 AF Calculations Pattern.

III. EXPERIMENTAL DESIGN

3.1 Design Method

A rectangular patch microstrip antenna is designed with a truncated corner and a circular patch with an x slot to determine the size of the antenna before simulating it and creating a MIMO configuration. The following is a step-by-step MIMO Antenna design method starting from the single patch design stage up to the MIMO configuration.

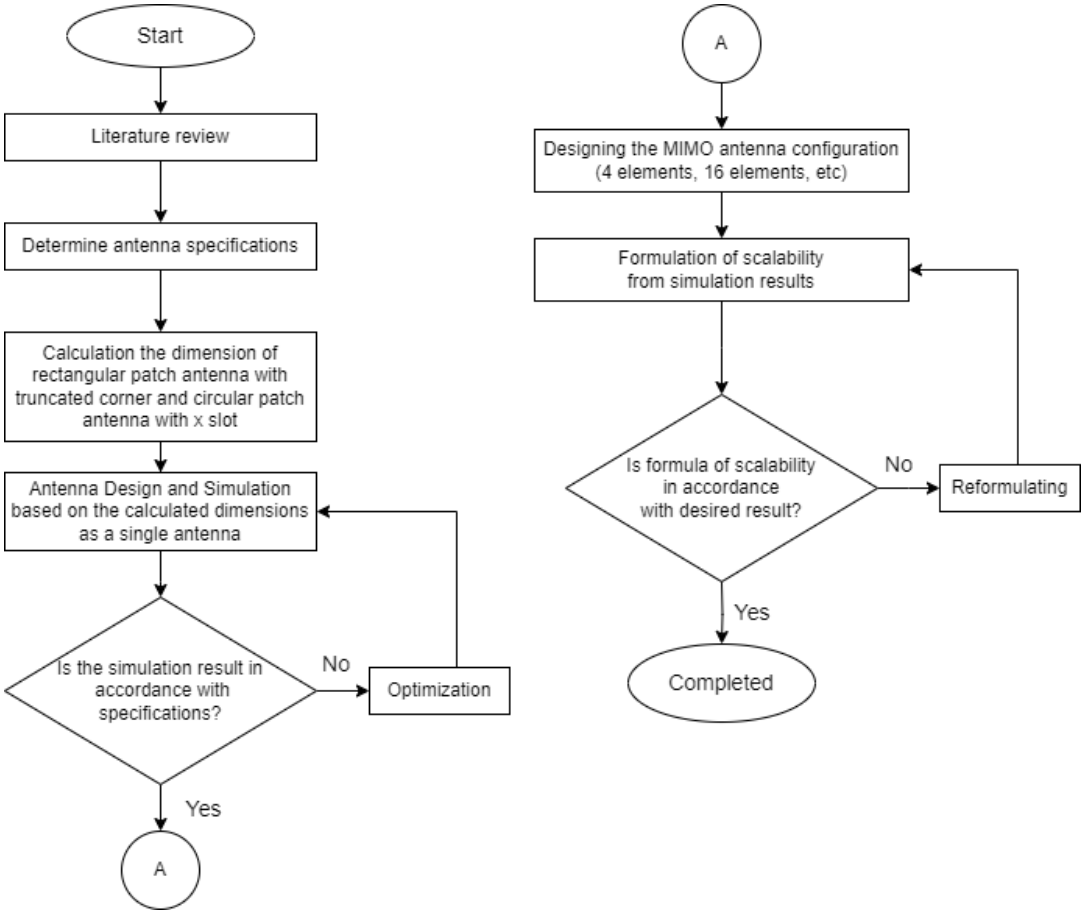

Figure 3. 1 Flowchart of the research.

The design method in Figure 3.1 is carried out in stages starting with a literature study. A literature study was carried out by collecting references to support understanding of concepts and theories regarding the effect of using the truncated corner method on rectangular patch antennas and the effect of using the x slot on circular antennas prior to MIMO configuration.

After understanding the concept and theory, the next step is to determine the antenna specifications. In order for the antenna to meet these specifications, antenna dimensions are calculated before carrying out the design and simulation.

In this study, the design and simulation process consisted of two stages, namely the design and simulation of rectangular patch antennas with truncated corners and circular patch antennas with x-slots until the simulation results match the specifications and continued with the stages of preparing the MIMO configuration.

The preparation of the MIMO configuration is carried out in stages starting from 2 elements of antenna, 4 elements of antenna, 16 elements of antenna and 64 elements of antenna until the simulation results show that the value tends to increase and the increase is in a certain pattern. The pattern of increasing value is then analyzed to be compared with the theoretical calculation so that it can be proven whether the scalability technique can be known or not.

3.2 Antenna Specifications

Antenna specifications are determined as an initial stage of initiation prior to calculating the dimensions and design of an antenna. Determination of antenna specifications is an important step before further antenna design and simulation is carried out. The antenna specifications listed in the table is a single antenna specifications as a reference that antennas can work well on a single antenna scheme prior to MIMO modeling. Following are the antenna specifications in Table 3.1 with an input impedance value of $Z_0 = 50\ \Omega$.

Table 3. 1 Antenna Specifications.

Parameter	Specifications
Resonant Frequency	3,5 GHz 5G Band
Gain	$> 3\ dB$
VSWR	< 2
Polarization	Circular
Bandwidth	50 MHz

3.3 Characteristics of Antenna Component Materials

The single patch antenna element is designed using FR-4 Epoxy material as a substrate and copper material as a patch and ground plane with the material characteristics in Table 3.2.

Table 3. 2 Materials Characteristic.

Component	Materials	Thickness
Patch and ground plane	Copper	t = 0.1 mm
Substrate	FR-4 Epoxy	h =1.6 mm

3.4 Antenna Dimension

The calculation of antenna dimensions refers to the resonant frequency that has been determined when determining the antenna specifications. The resonant frequency value of an antenna is inversely proportional to the dimensions of the antenna. The higher the resonant frequency value, the smaller the antenna dimensions will be, and vice versa.

3.5 Single Line Feed

The single line feed technique for microstrip antennas is used to create circular polarization. By using a single connected transmission line, the resulting electromagnetic field generates circular polarization. This involves designing the transmission line, radiating element, and ground plane to create the desired effect. The outcome is a microstrip antenna capable of transmitting and receiving electromagnetic waves with a defined rotational field orientation, useful in wireless communication, radar, and satellite systems. Single line feed is used to obtain the desired circular polarization of RHCP and LHCP with the modification of feed that shown in the Figure 3.2.

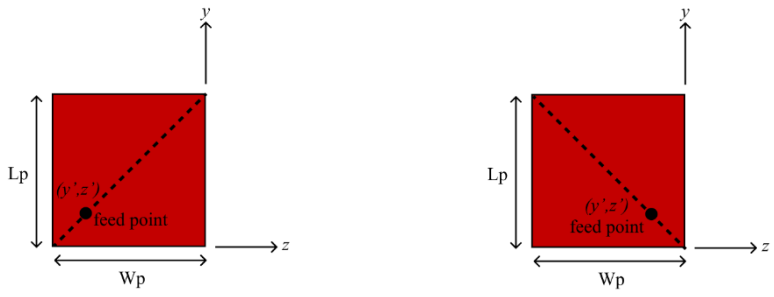

Figure 3. 2 Single feed arrangement for circular polarization (a) LHCP, (b) LHCP.

3.5.1 Dimension of Rectangular Patch with Truncated Corner

- Width of patch (W_p)

  Width of patch is calculated using the equation (2.1):

$$W_p = \frac{c}{2f_r}\sqrt{\frac{2}{\varepsilon_r + 1}}$$

$$W_p = \frac{3 \times 10^8}{2 \times 3.5 \times 10^9}\sqrt{\frac{2}{1.6 + 1}}$$

$$W_p = 37.58\, mm.$$

- Length of patch (L_p)

  Length of patch is calculated using the equation (2.5):

$$L_p = L_{eff} - 2\Delta L$$

$$L_{eff} = \frac{c}{2f_r\sqrt{\varepsilon_{reff}}} \text{ dimana } \varepsilon_{reff} = \frac{\varepsilon_r+1}{2} + \frac{\varepsilon_r-1}{2}\left[1 + 12\frac{h}{w}\right]^{-1/2}$$

$$\varepsilon_{reff} = \frac{1.6 + 1}{2} + \frac{1.6 - 1}{2}\left[1 + 12\frac{0.05}{3.758}\right]^{-1/2}$$

$$\varepsilon_{reff} = 1.58$$

$$\Delta L = 0.412\, h\, \frac{\left(\varepsilon_{reff} + 0.3\right)\left(\frac{w}{h} + 0.264\right)}{\left(\varepsilon_{reff} - 0.258\right)\left(\frac{w}{h} + 0.8\right)}$$

With the result that,

$$L_p = \frac{c}{2f_r\sqrt{\varepsilon_{reff}}} - 2\left(0.412\, h\, \frac{\left(\varepsilon_{reff} + 0.3\right)\left(\frac{w}{h} + 0.264\right)}{\left(\varepsilon_{reff} - 0.258\right)\left(\frac{w}{h} + 0.8\right)}\right)$$

$$L_p = \frac{3 \times 10^8}{2 \times 3.5 \times 10^9 \times \sqrt{1.58}} - 2\left(0.412\,(0.5 \times 10^{-3})\, \frac{(1.58 + 0.3)\left(\frac{3.758}{0.05} + 0.264\right)}{(1.58 - 0.258)\left(\frac{3.758}{0.05} + 0.8\right)}\right)$$

$$L_p = 33.53\, mm.$$

- Truncated corner

The dimension of truncated corner is calculated using the equation (2.8):

$$Q_0 = \frac{c\sqrt{\varepsilon_r}}{4f_r h}$$

$$Q_0 = \frac{3 \times 10^8\sqrt{1.6}}{4 \times 3.5 \times 10^9 \times 10^{-3}}$$

$$Q_0 = 27$$

$$\frac{\Delta s}{s} = \frac{1}{2Q_0}$$

$$\frac{\Delta s}{s} = \frac{1}{2 \times 27}$$

$$\frac{\Delta s}{s} = 0.0185$$

$$S = L_p\sqrt{\frac{\Delta s}{s}}$$

$$S = 33.53 \times 10^{-3}\sqrt{0.0185}$$

$$S = 0.0045\ m = 4.5\ mm$$

3.5.2 Dimension of Circular Patch with X Slot

- Radius of circular patch (a)

The dimension of circular patch is determined by the radius of circular with calculation using the equation (2.9):

$$a = \frac{F}{\left\{1 + \frac{2h}{\pi\varepsilon_r F}\left[\ln\left(\frac{\pi F}{2h}\right) + 1.7726\right]\right\}^{1/2}}$$

where

$$F = \frac{8.791 \times 10^9}{f_r\sqrt{\varepsilon_r}}$$

$$F = \frac{8.791 \times 10^9}{3.5 \times 10^9\sqrt{4.4}}$$

$$F = 1.197$$

So,

$$a = \frac{1.197}{\left\{1 + \frac{2(1.6)}{\pi \times 4.4 \times 1.197}\left[\ln\left(\frac{\pi \times 1.197}{2(1.6)}\right) + 1.7726\right]\right\}^{1/2}}$$

$$a = 10.21\ mm$$

3.5.3 Dimension of Substrate and Ground Plane

- Width of ground plane and substrate (W_g)

Width of ground plane and substrate have the same value that calculated using the equation (2.11):

$$W_g = 6h + W_p$$

$$W_g = (6 \times 0.5 \times 10^{-3}) + (37.58 \times 10^{-3})$$

$$W_g = 40.58\ mm$$

The calculated W_g value is the minimum W_g value, so the W_g value can be enlarged up to $W_g = 2 \times W_p$. Thus, $W_g = 2 \times 37.58\ mm = 75.16\ mm$.

- Length of ground plane and substrate (L_g)

Length of ground plane and substrate have the same value that calculated using the equation (2.12):

$$L_g = 6h + L_p$$

$$L_g = (6 \times 0.5 \times 10^{-3}) + (33.53 \times 10^{-3})$$

$$L_g = 36.53\ mm$$

The calculated L_g value is the minimum L_g value, so the L_g value can be enlarged up to $L_g = 2 \times F_g$ Thus, $L_g = 2 \times 36.53\ mm = 73.06\ mm$.

The provided table encapsulates the values associated with key symbols, shedding light on crucial parameters. These values are instrumental in guiding the design and simulation process, enabling a comprehensive understanding of the underlying factors that contribute to the antenna's performance. The table serves as a valuable reference, facilitating accurate adjustments and refinements throughout the development stages. Based on the calculations that have been done, the antenna parameter values are obtained in Table 3.3 to be designed and simulated.

Table 3. 3 Calculated Antenna Dimensions.

Parameter	Value (mm)	Description
W_p	37.58	Width of rectangular patch
L_p	33.53	Length of rectangular patch
W_g	75.16	Width of substrate and ground plane
L_g	67.06	Length of substrate and ground plane
t	0.1	Thickness of patch
h	1.6	Thickness of substrate
S	4.5	Dimension of truncated corner
a	10.21	Radius of circular patch

3.6 Antenna Configuration

Antenna configurations suitable for massive MIMO start with modular antennas, followed by higher MIMO antenna configurations (ie, 2 elements, 4 elements, 16 elements, 64 elements, and so on in an exponential pattern). After finding a suitable MIMO antenna configuration, the scaling factor for each configuration will be modeled and developed based on the simulated array factor. The scaling factor will be used to predict the performance and characteristics of the larger array based on the smaller antenna configurations.

In this study, the notation of MIMO antennas, including 2 MIMO configurations, signifies the incorporation of two antenna elements. Furthermore, a 4 MIMO configuration implies the integration of four antenna elements, organized in a vertical array of two elements and a horizontal array of two elements. Similarly, the representation of a 16 MIMO antenna entails the arrangement of 16 elements, with four elements vertically and four elements horizontally. This judicious increase in antenna elements has a significant impact on the overall system performance, particularly in terms of enhancing spatial diversity and multipath mitigation. The ensuing analysis explores the implications of these configurations in optimizing MIMO system capacity and robustness. The progression in the number of antenna elements follows an exponential pattern, as depicted in Figure 3.3.

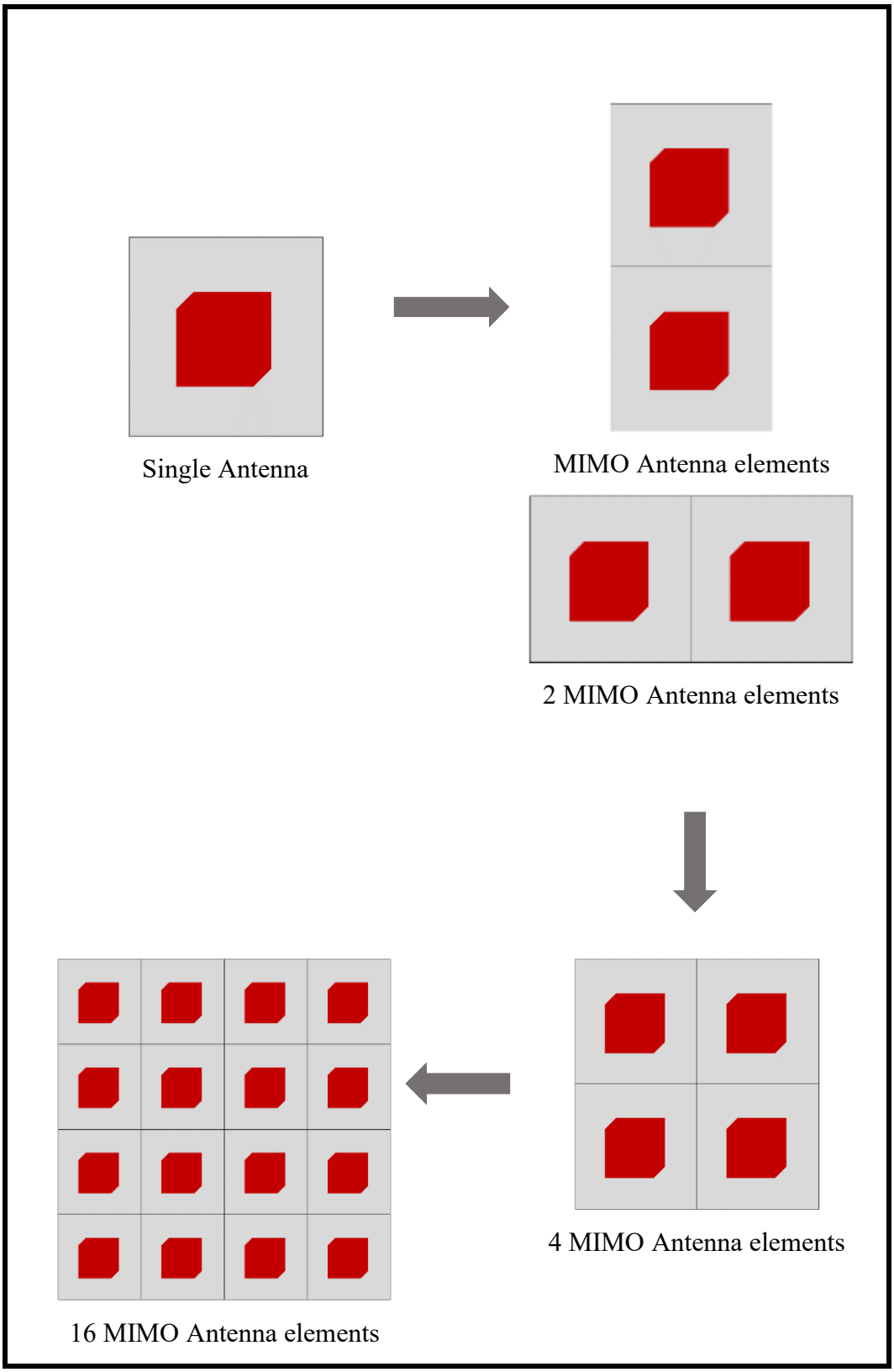

Figure 3. 3 MIMO antenna configurations.

3.7 Simulation of Rectangular Patch Antenna with Truncated Corner

The simulation for the rectangular antenna will be conducted in multiple stages, commencing with the single patch antenna simulation. Subsequently, simulations will progress to MIMO configurations. The MIMO configuration simulations will also be executed in several steps, starting with a 2-antenna element configuration, followed by a 4-antenna element configuration. The process will then advance to a 16-antenna element configuration, culminating in a final configuration with 64 antenna elements.

3.7.1 Simulation of Single Antenna

After obtaining the antenna dimension values according to the calculations, simulation and optimization is carried out on the single patch antenna to obtain the antenna parameters according to predetermined specifications.

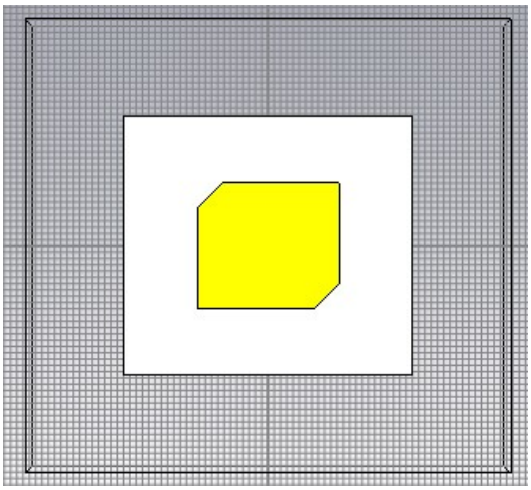

Figure 3. 4 Simulation of Single Rectangular Antenna.

Based on the simulation results in Figure 3.4, the following results are obtained.

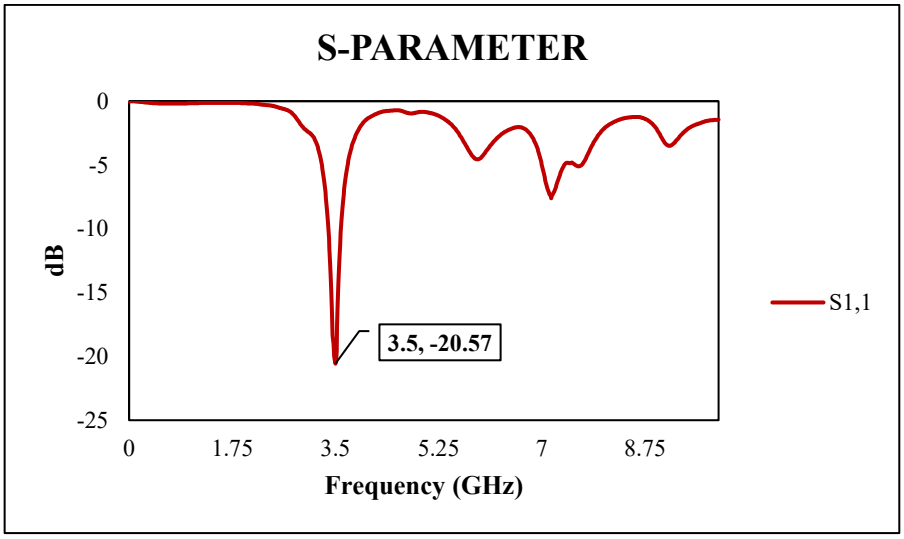

Figure 3. 5 S-parameter of Single Rectangular Antenna optimization.

The s-parameter value generated on a single antenna as shown in Figure 3.5 is -39.02 dB at the desired resonant frequency, this value already meets the specifications where the s-parameter is <-10 dB. Thus, a single antenna design has good performance when viewed from its s-parameter value.

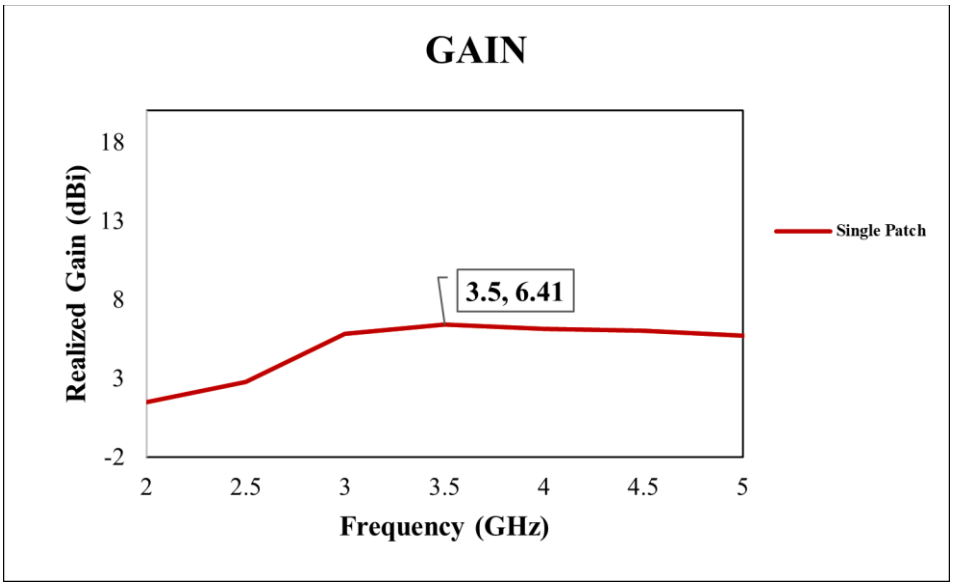

Figure 3. 6 Gain value of Single Rectangular Antenna.

The resulting value as shown in Figure 3.6 is 6.41 dB at the desired resonant frequency. The gain value has exceeded the specified specifications, namely gain > 3 dBi. Thus, a single antenna design has good performance based on the result of gain value.

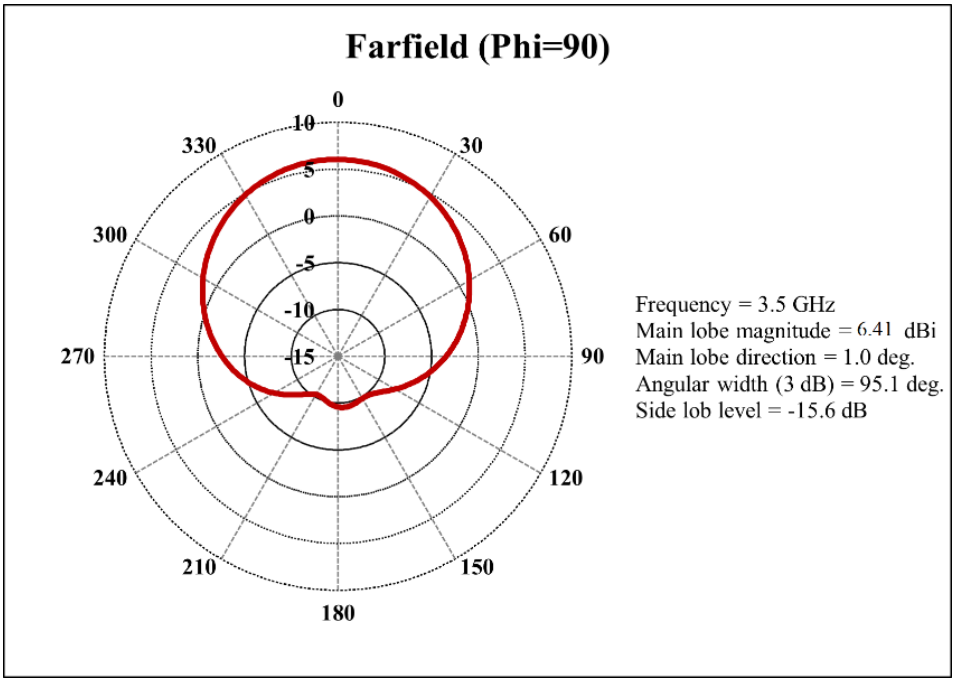

Figure 3. 7 Angular width of Single Rectangular Antenna.

Another characteristic that was tested and found to be its value was HPBW, in Figure 3.7 it is shown that the HPBW value obtained was 95.1°. The HPBW measured on this single antenna will then be used as a reference in designing MIMO antennas (both 2 elements, 4 elements, 16 elements, etc.) to then find out the pattern of changes in value.

The simulation results are indicated by three values including s-parameter, gain and HPBW. Figure 3.5 shows the s-parameter value of -29.02 dB which means that the antenna can work properly. Furthermore, the gain value in Figure 3.6 is 6.41 dBi and the HPBW value in Figure 3.7 is 95.1°.

3.7.2 Simulation of Vertical 2 MIMO Antenna Elements

Furthermore, a simulation is carried out with a Vertical 2 MIMO configuration for calculating the vertical Array Factor.

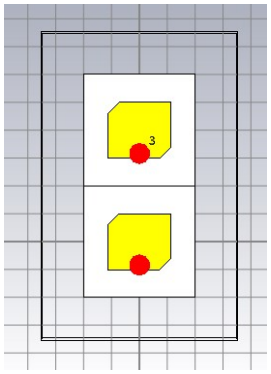

Figure 3. 8 Simulation of Vertical 2 MIMO Rectangular Antenna Elements.

Based on the simulation results in Figure 3.8, the following results are obtained.

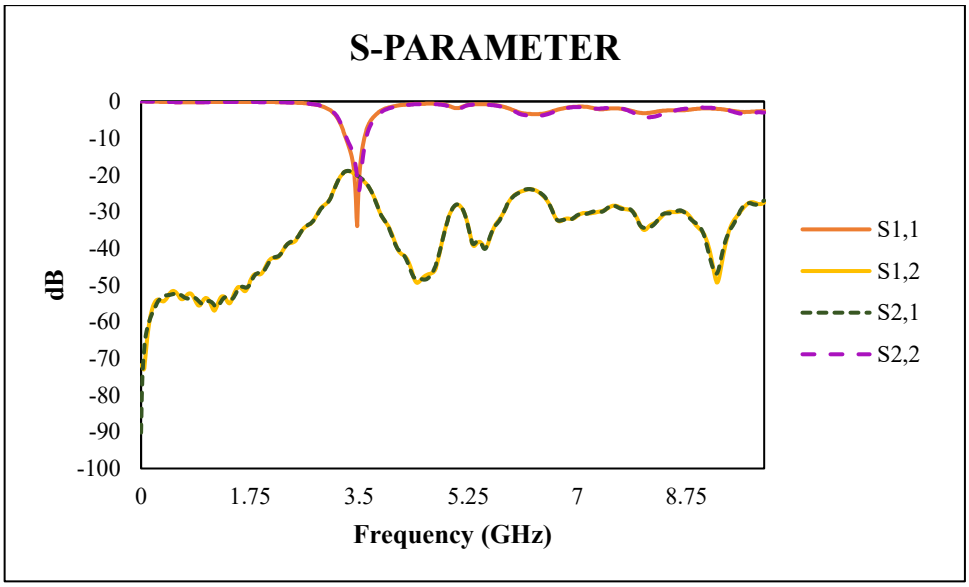

Figure 3. 9 S-parameter of Vertical 2 MIMO Rectangular Antenna Elements.

The s-parameter value generated on a vertical 2 MIMO antenna as shown in Figure 3.9 has a value of $S_{1,1}$, $S_{1,2}$, $S_{2,1}$, $S_{2,2}$ where the values of $S_{1,1}$ and $S_{2,2}$ indicate the value of s-parameter for each antenna element, while the $S_{1,2}$ value and $S_{2,1}$ value indicate mutual coupling between adjacent antennas. The overall s-parameter value generated at the resonant frequency has a value of <-10 dB so that the vertical 2 MIMO antenna design has good performance when viewed from the s-parameter value.

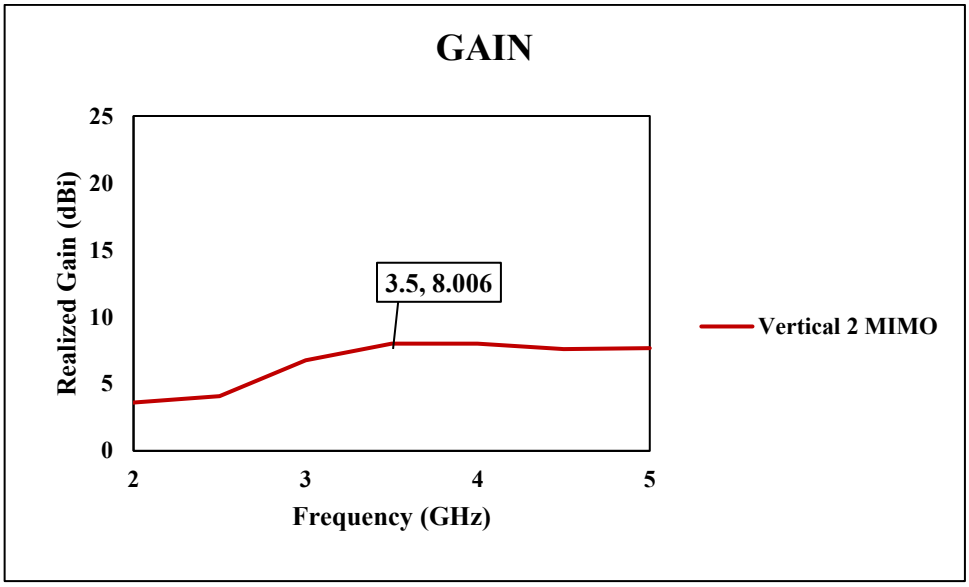

Figure 3. 10 Gain value of Vertical 2 MIMO Rectangular Antenna Elements.

The resulting gain as shown in Figure 3.10 is 8,006 dBi. This gain value is the gain value measured by the array antenna approach based on the designed MIMO scheme.

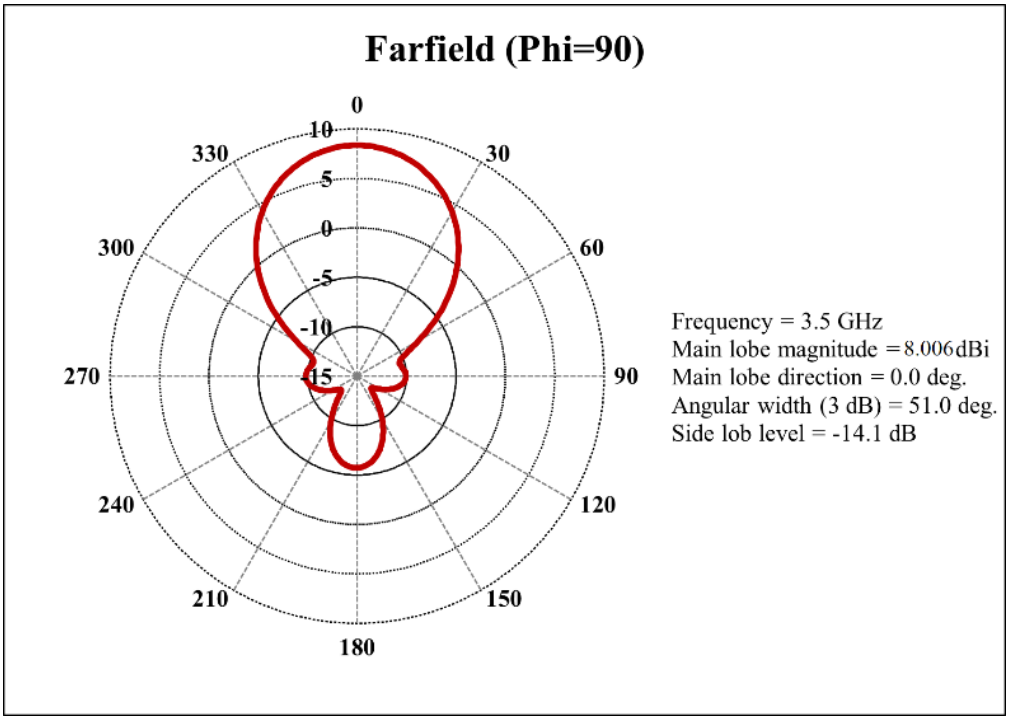

Figure 3. 11 Angular width of Vertical 2 MIMO Rectangular Antenna Elements.

The HPBW value generated in the vertical 2 MIMO Antenna design as shown in Figure 3.11 is 51.0°. The HPBW value generated in this design will then be

compared with the HPBW value for a single scheme and as a reference for further scheme MIMO designs.

The simulation results of vertical 2 MIMO Antenna are also indicated by three values including s-parameter, gain and HPBW. Figure 3.9 shows the s-parameter value of each antenna are $< -10\,dB$ which means that the antenna can work properly. Furthermore, the gain value in Figure 3.10 is 8.006 dBi and the HPBW value in Figure 3.11 is 51.0°.

3.7.3 Simulation of Horizontal 2 MIMO Antenna Elements

Furthermore, a simulation is carried out with a horizontal 2 MIMO configuration for calculating the horizontal Array Factor.

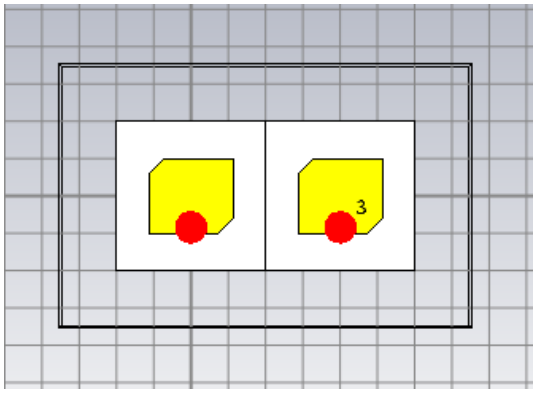

Figure 3. 12 Simulation of Horizontal 2 MIMO Rectangular Antenna Elements.

Based on the simulation results in Figure 3.12, the following results are obtained.

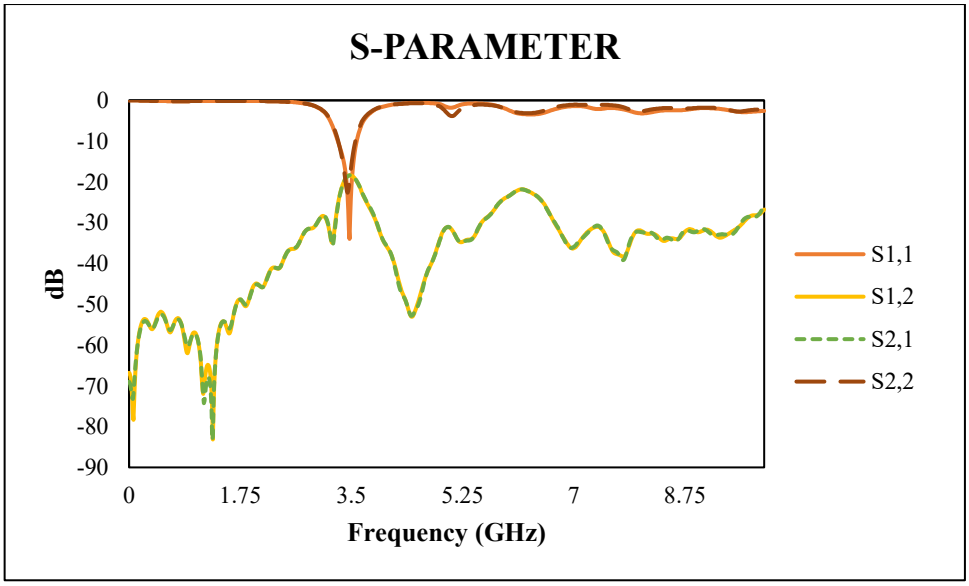

Figure 3. 13 S-parameter of Horizontal 2 MIMO Rectangular Antenna Elements.

The s-parameter values generated on the horizontal 2 MIMO antenna as shown in Figure 3.13 have values $S_{1,1}$, $S_{1,2}$, $S_{2,1}$, $S_{2,2}$ where the values $S_{1,1}$ and $S_{2,2}$ indicate the value of s-parameter for each element. antenna, while the $S_{1,2}$ and $S_{2,1}$ value indicate mutual coupling between adjacent antennas. The overall s-parameter value generated at the resonant frequency has a value <-10 dB so that the horizontal 2 MIMO antenna design has good performance from its s-parameter value.

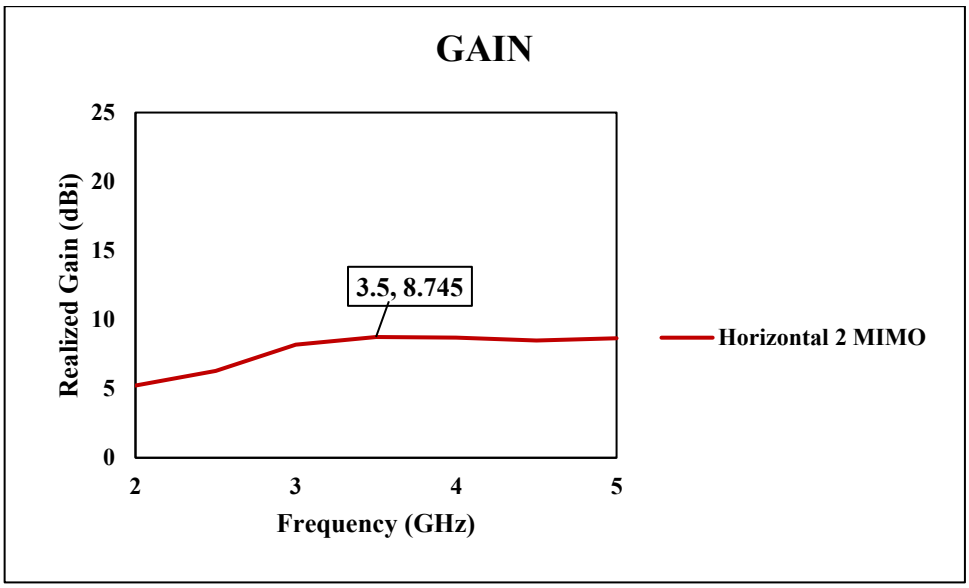

Figure 3. 14 Gain value of Horizontal 2 MIMO Rectangular Antenna Elements.

The resulting gain as shown in Figure 3.14 is 8,745 dBi. This gain value is the gain value measured using the stacking antenna approach based on the MIMO configuration designed.

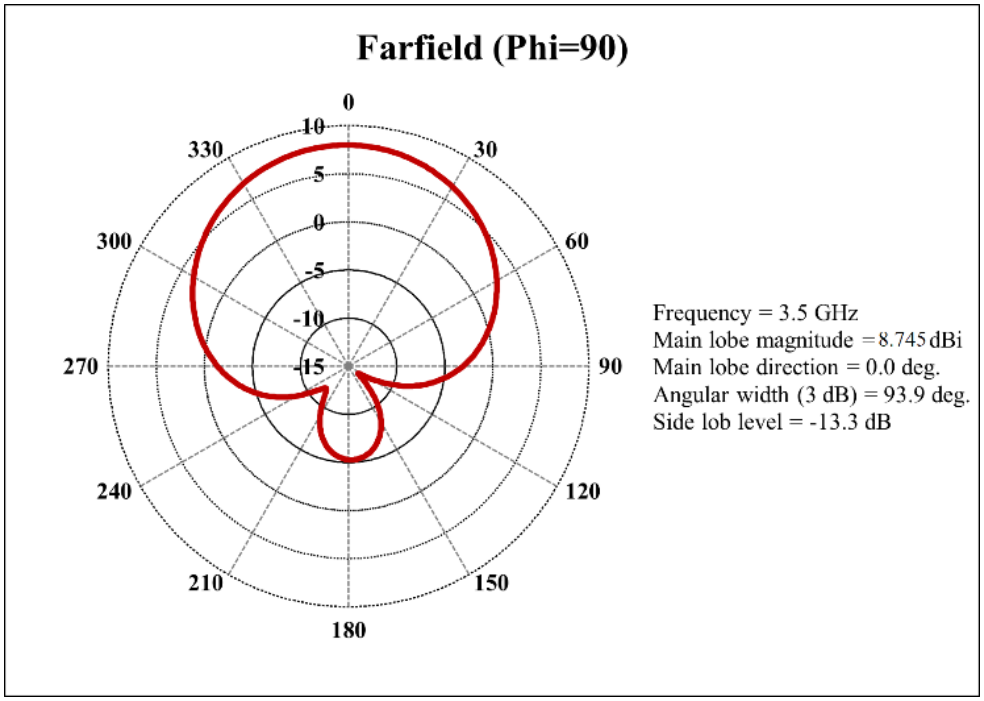

Figure 3. 15 Angular width of Horizontal 2 MIMO Rectangular Antenna Elements.

The HPBW value generated in the horizontal 2 MIMO Antenna design as shown in Figure 3.15 is 93.9°. The HPBW value generated in this design will then be compared with the HPBW value for a single scheme and as a reference for further scheme MIMO designs.

The simulation results of horizontal 2 MIMO Antenna are also indicated by three values including s-parameter, gain and HPBW. Figure 3.13 shows the s-parameter value of each antenna are $< -10\ dB$ which means that the antenna can work properly. Furthermore, the gain value in Figure 3.14 is 8.745 dBi and the HPBW value in Figure 3.15 is 93.9°.

3.7.4 Simulation of 4 MIMO Antenna Elements

Simulations were carried out for the 4 MIMO antenna configuration which refers to a single optimization antenna so that the antenna elements of the MIMO antenna are in accordance with the specified specifications.

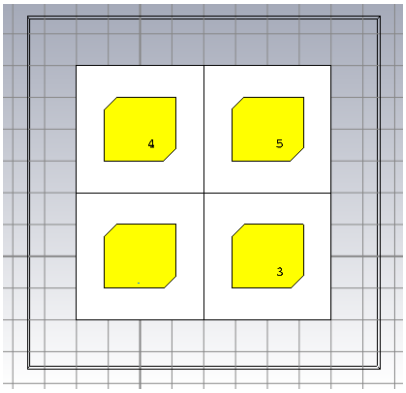

Figure 3. 16 Simulation of 4 MIMO Rectangular Antenna Elements.

Based on the simulation results in Figure 3.16, the following results are obtained.

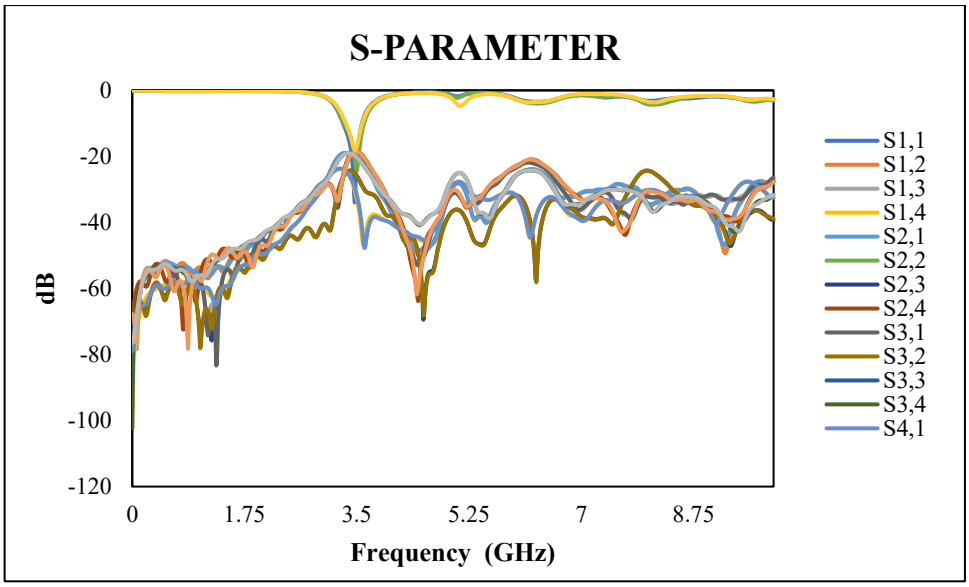

Figure 3. 17 S-parameter of 4 MIMO Rectangular Antenna Elements.

The s-parameter value generated on the 4 MIMO antenna as shown in Figure 3.17 has a value of $S_{1,1}$, $S_{1,2}$, …, $S_{4,3}$, $S_{4,4}$ where for the return value loss pattern $S_{N,N}$ ($S_{1,1}$, $S_{2,2}$, $S_{3,3}$, $S_{4,4}$) shows the value of s-parameter for each antenna element, while the value of s-parameter pattern $S_{N,M}$ (s-parameter other than the pattern $S_{N,N}$) shows mutual coupling between adjacent antennas. The overall s-parameter value generated at the resonant frequency has a value of <-10 dB so that the 4 MIMO antenna design has good performance when viewed from the s-parameter value.

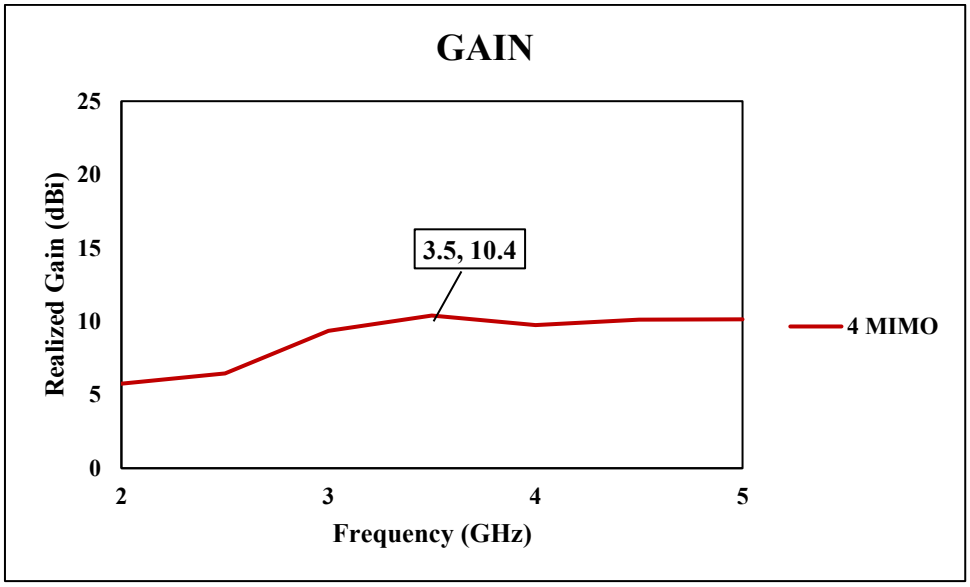

Figure 3. 18 Gain value of 4 MIMO Rectangular Antenna Elements.

The resulting gain as shown in Figure 3.18 is 10.4 dBi. This gain value is the gain value measured using the stacking antenna approach based on the MIMO configuration designed.

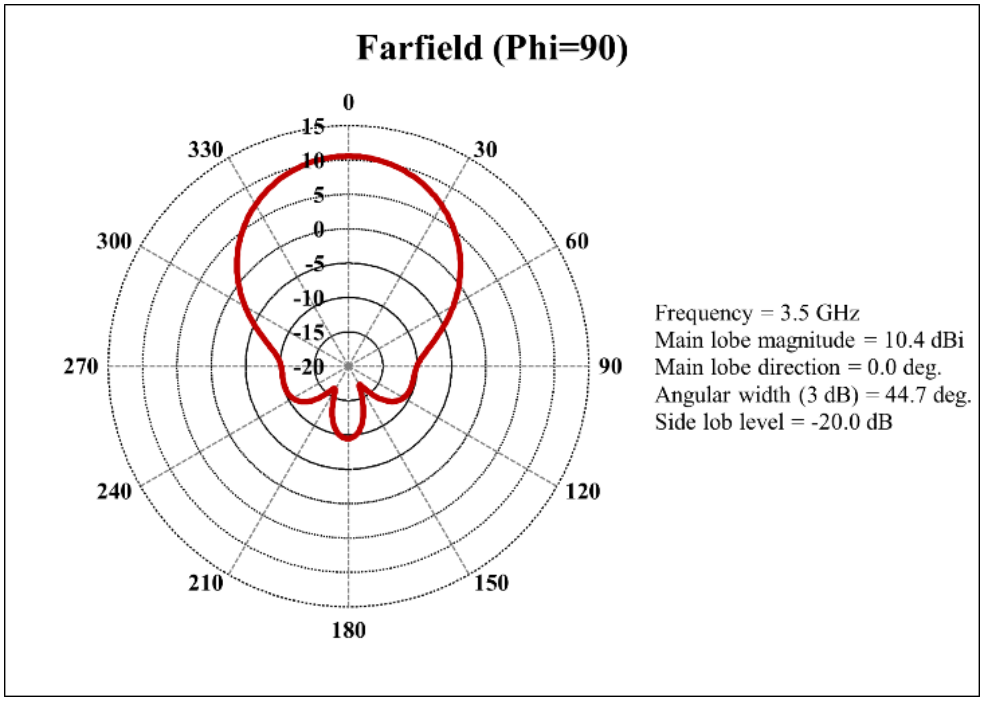

Figure 3. 19 Angular width of 4 MIMO Rectangular Antenna Elements.

The HPBW value generated in the 4 MIMO Antenna design as shown in Figure 3.19 is 44.7°. The HPBW value generated in this design will then be

compared with the HPBW value for a single scheme and as a reference for further MIMO configuration designs.

The simulation results of 4 MIMO Antenna are also indicated by three values including s-parameter, gain and HPBW. Figure 3.17 shows the s-parameter value of each antenna are $< -10\ dB$ which means that the antenna can work properly. Furthermore, the gain value in Figure 3.18 is 10.4 dBi and the HPBW value in Figure 3.19 is 44.7°.

3.7.5 Simulation of 16 MIMO Antenna Elements

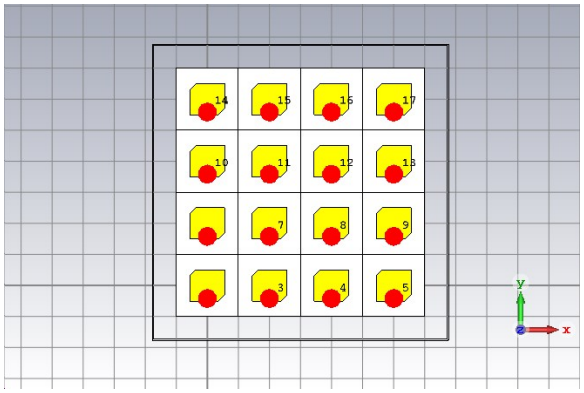

Figure 3. 20 Simulation of 16 MIMO Rectangular Antenna Elements.

Based on the simulation results in Figure 3.20, the following results are obtained.

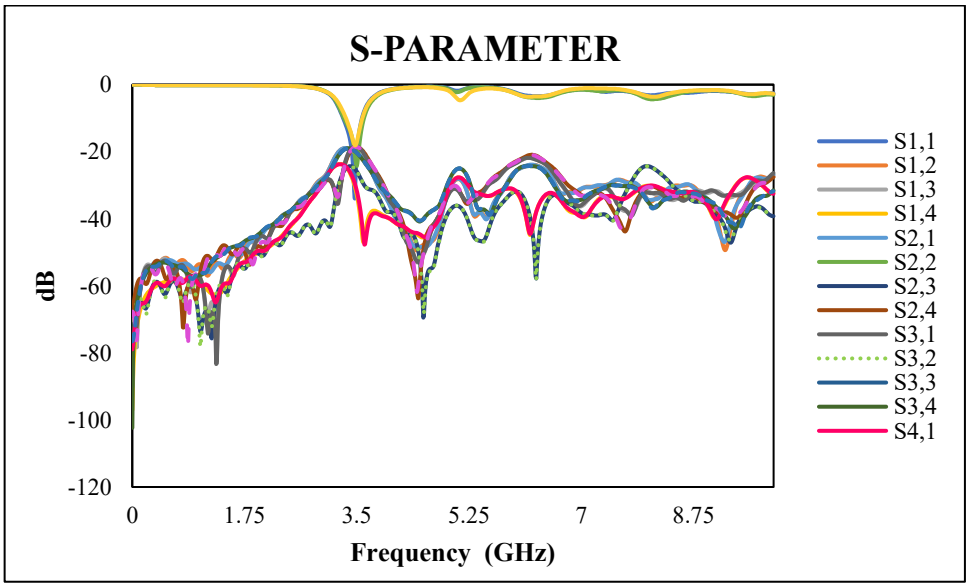

Figure 3. 21 S-parameter of 16 MIMO Rectangular Antenna Elements.

The s-parameter value generated on the 16 MIMO antenna as shown in Figure 3.21 has a s-parameter value where the $S_{N,N}$ patterned s-parameter value indicates

the s-parameter value for each antenna element, while the $S_{N,M}$ patterned s-parameter value (s-parameter other than pattern $S_{N,N}$) shows mutual coupling between adjacent antennas. The overall s-parameter value generated at the resonant frequency has a value of <-10 dB so that the 16 MIMO antenna design has good performance when viewed from the s-parameter value.

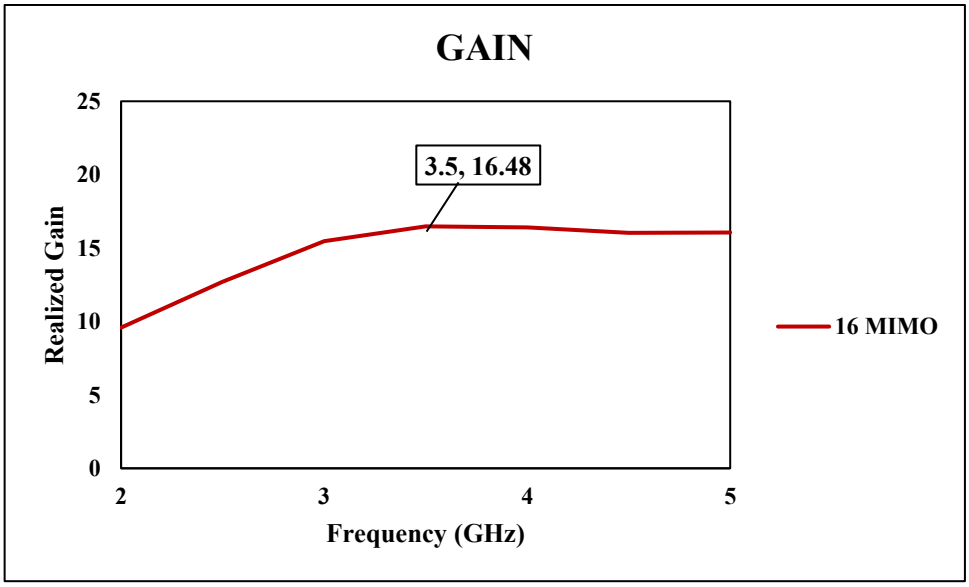

Figure 3. 22 Gain value of 16 MIMO Rectangular Antenna Elements.

The resulting gain as shown in Figure 3.22 is 16.48 dBi. This gain value is the gain value measured by the array antenna approach based on the MIMO configuration designed.

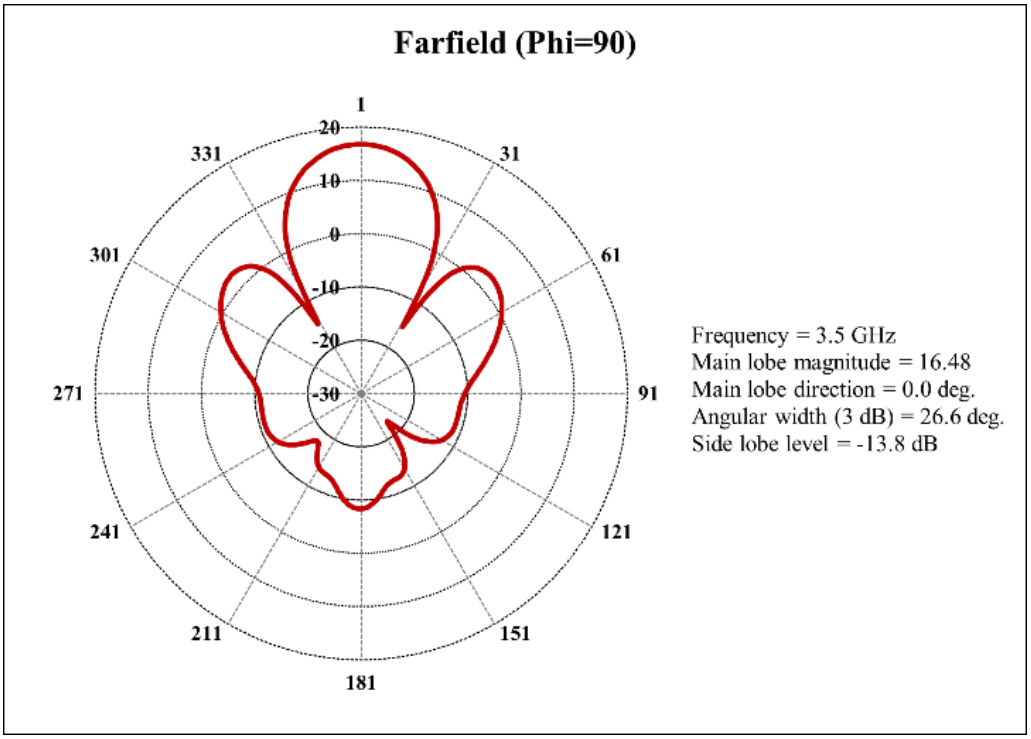

Figure 3. 23 Angular width of 16 MIMO Rectangular Antenna Elements.

The HPBW value produced in the 16 MIMO Antenna design as shown in Figure 3.23 is 26.6°. The HPBW value generated in this design will then be compared with the single scheme HPBW value and as a reference for further MIMO configuration design.

The simulation results of 16 MIMO Antenna are also indicated by three values including s-parameter, gain and HPBW. Figure 3.21 shows the s-parameter value of each antenna are $< -10\ dB$ which means that the antenna can work properly. Furthermore, the gain value in Figure 3.22 is 16.48 dBi and the HPBW value in Figure 3.23 is 26.6°.

3.7.6 Simulation of 64 MIMO Antenna Elements

The next step is the simulation on the MIMO Antenna 64 configuration as the final configuration which will be simulated and used as a reference for calculating the Array Factor. Antenna simulation can be seen in the Figure 3.24.

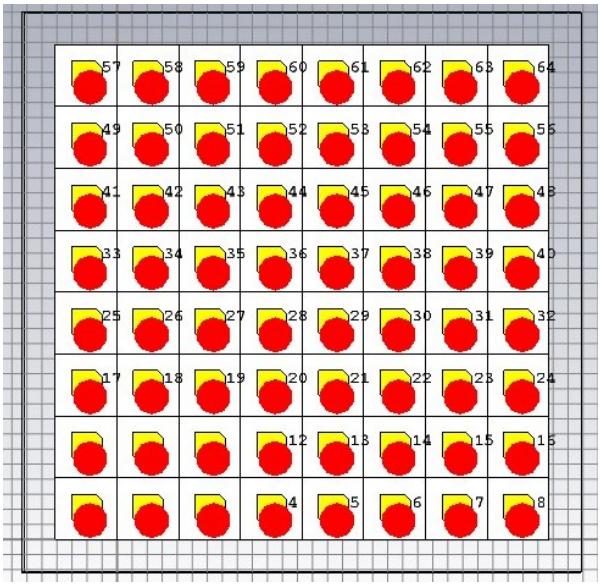

Figure 3. 24 Simulation of 64 MIMO Rectangular Antenna Elements.

Based on the simulation results in Figure 3.24, the following results are obtained.

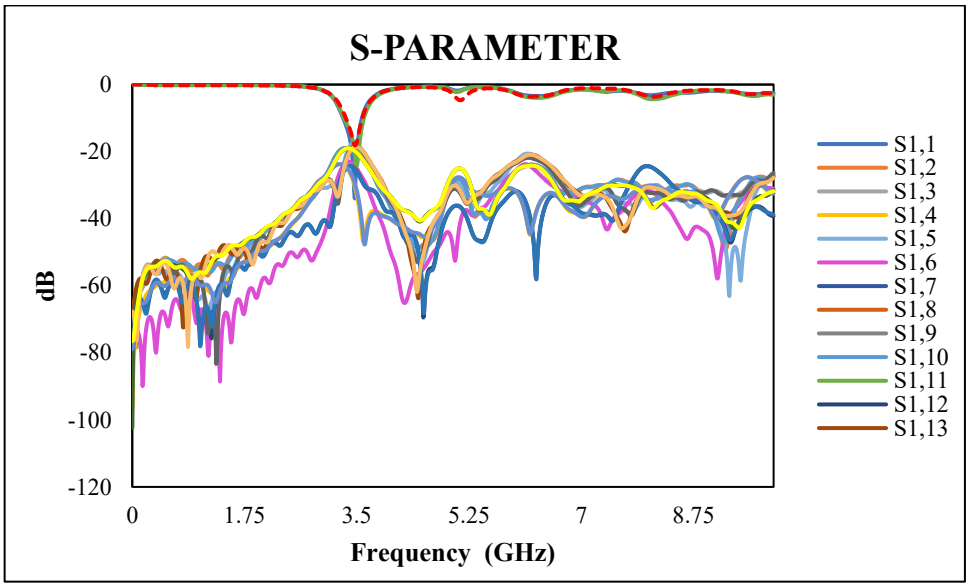

Figure 3. 25 S-parameter of 64 MIMO Rectangular Antenna Elements.

The s-parameter value generated on the 64 MIMO antenna as shown in Figure 3.25 has a s-parameter value where the $S_{N,N}$ patterned s-parameter value indicates the s-parameter value for each antenna element, while the $S_{N,M}$ patterned s-parameter value (s-parameter other than pattern $S_{N,N}$) shows mutual coupling between adjacent antennas. The overall s-parameter value generated at the resonant

frequency has a value of <-10 dB so that the 64 MIMO antenna design has good performance when viewed from the s-parameter value.

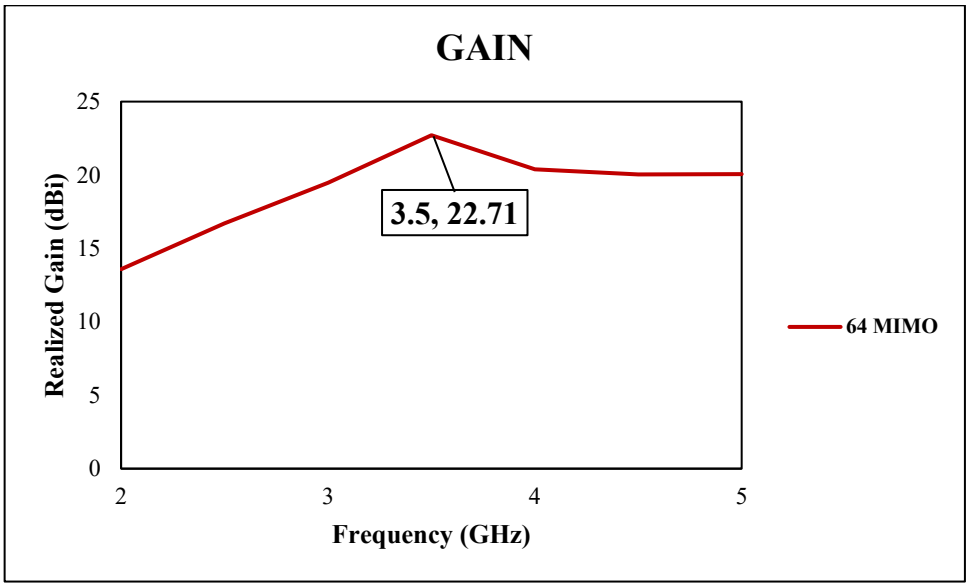

Figure 3. 26 Gain value of 64 MIMO Rectangular Antenna Elements.

The resulting gain as shown in Figure 3.26 is 22.71 dBi. This gain value is the gain value measured by the array antenna approach based on the MIMO configuration designed.

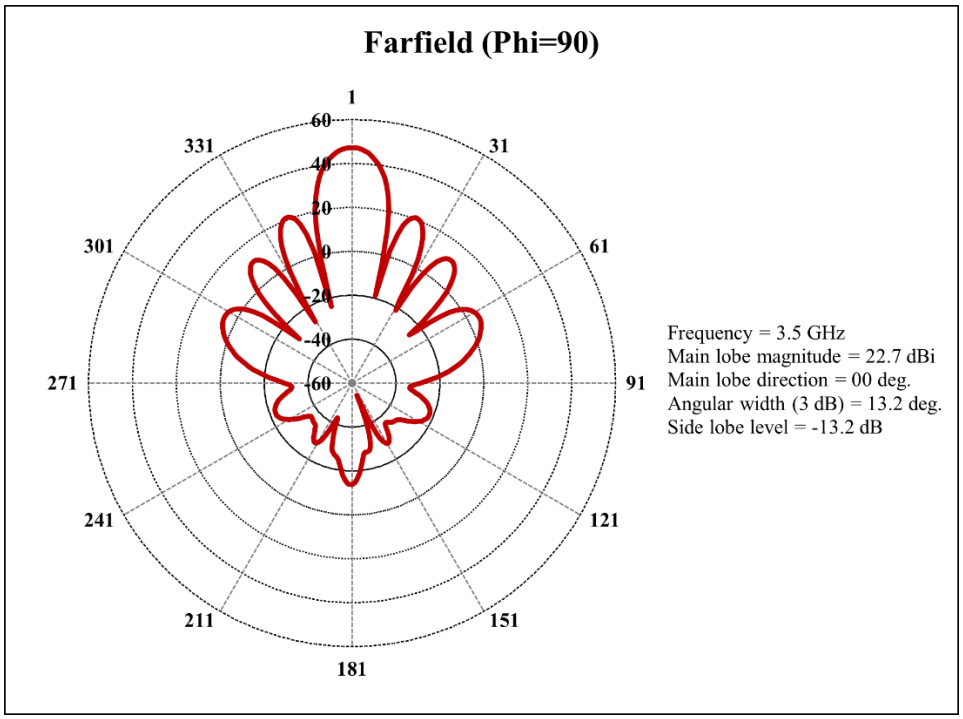

Figure 3. 27 Angular width of 64 MIMO Rectangular Antenna Elements.

The HPBW value produced in the 64 MIMO Antenna design as shown in Figure 3.27 is 13.2°. The HPBW value generated in this design will then be compared with the single scheme HPBW value and as a reference for further MIMO configuration design.

The simulation results of 64 MIMO Antenna are also indicated by three values including s-parameter, gain and HPBW. Figure 3.25 shows the s-parameter value of each antenna are $< -10\ dB$ which means that the antenna can work properly. Furthermore, the gain value in Figure 3.26 is 22.7 dBi and the HPBW value in Figure 3.27 is 13.2°.

3.8 Simulation of Circular Patch Antenna with X Slot

As a comparison, a Circular Antenna simulation with X slot is carried out as in the following simulations.

3.8.1 Simulation of Single Antenna

As with the rectangular antenna simulation, circular antenna simulations were also carried out with the antenna dimensions obtained from the calculation results. Antenna simulation can be seen in the Figure 3.28.

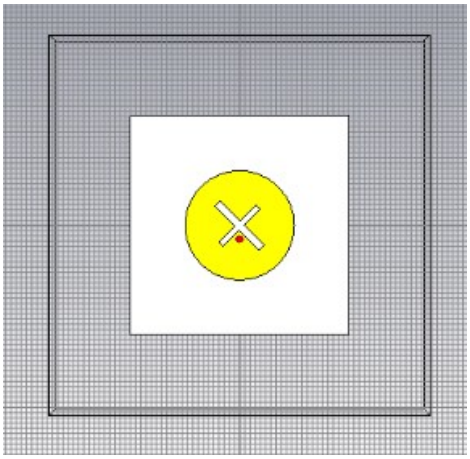

Figure 3. 28 Simulation of Single Circular antenna.

Based on the simulation results in Figure 3.28, the following results are obtained.

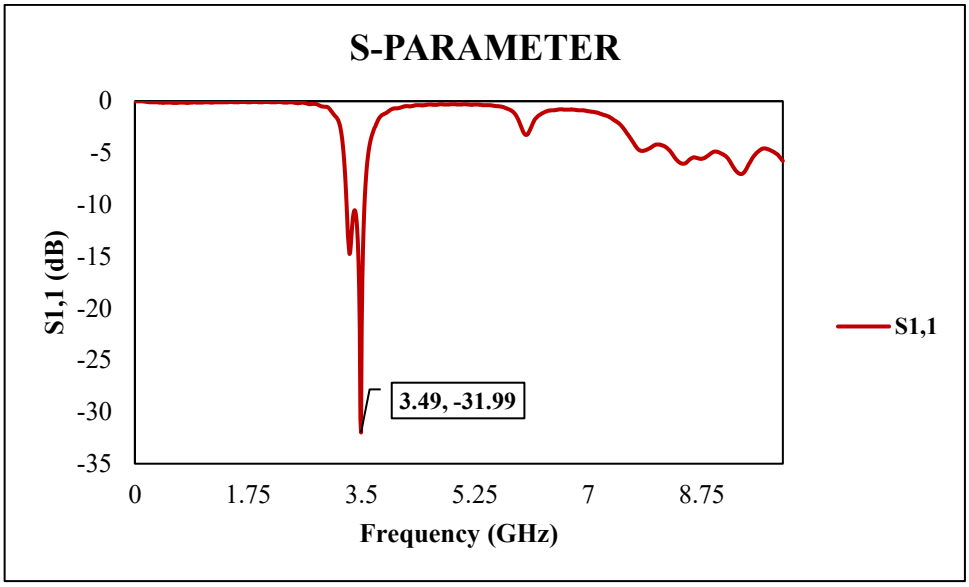

Figure 3. 29 S-parameter of Single Circular Antenna.

The s-parameter value generated on a single antenna as shown in Figure 3.29 is -31.99 dB at the desired resonance frequency, this value already meets the specifications where the s-parameter is <-10 dB. Thus, a single antenna design is said to have good performance when viewed of the s-parameter value.

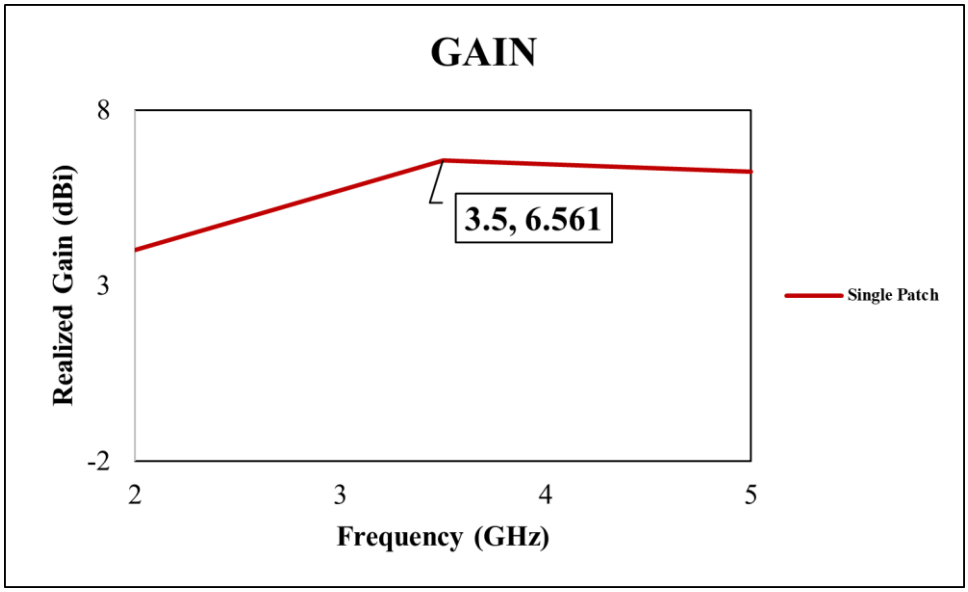

Figure 3. 30 Gain value of Single Circular Antenna.

The resulting value as shown in Figure 3.30 is 6.561 dB at the desired resonant frequency. The gain value has exceeded the specified specifications, namely gain >3 dBi. Thus, a single antenna design is said to have good performance when viewed from its gain value.

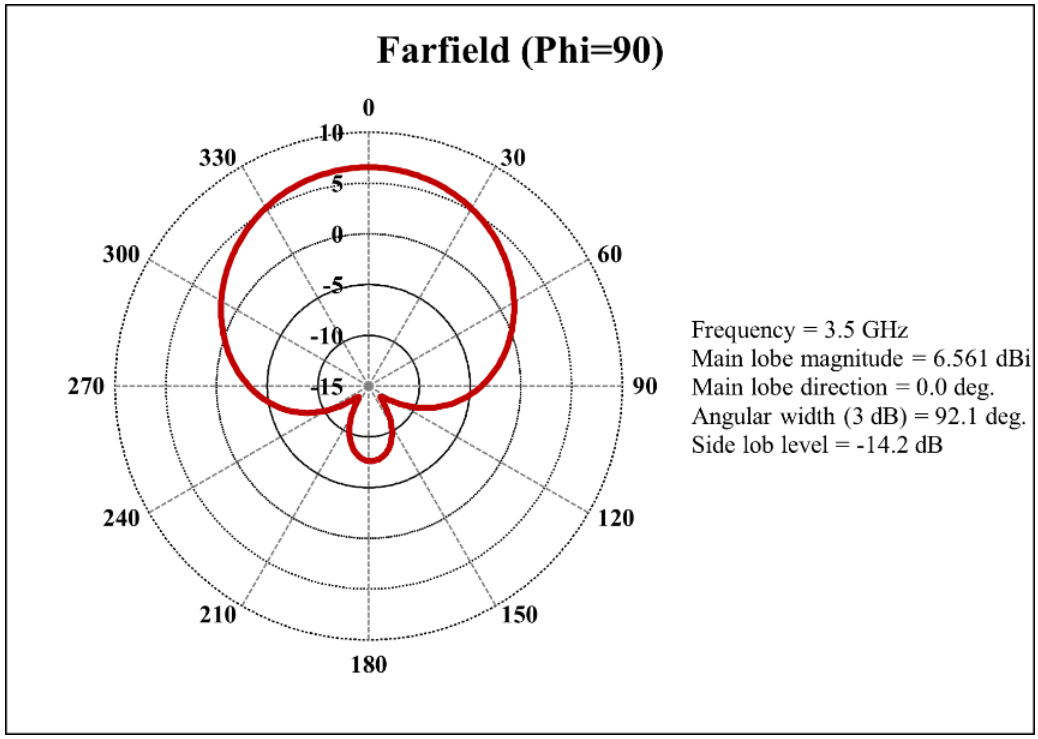

Figure 3. 31 Angular width of Single Circular Antenna.

Another characteristic that was tested and whose value was found out was the HPBW, in Figure 3.31 it is shown that the HPBW value obtained was 92.1°. The HPBW measured on this single antenna will then be used as a reference in designing MIMO antennas (both 2 elements, 4 elements, 16 elements, etc.) to then find out the pattern of changes in value.

The simulation results of Circular Slotted X Antenna are also indicated by three values including s-parameter, gain and HPBW. Figure 3.29 shows the s-parameter value of -31.99 dB which means that the antenna can work properly. Furthermore, the gain value in Figure 3.30 is 6.561 dBi and the HPBW value in Figure 3.31 is 92.1°

3.8.2 Simulation of Vertical 2 MIMO Antenna Elements

The simulation of the vertical 2 MIMO Circular Antenna configuration is intended as a comparison for calculating the vertical Array Factor with the following simulation.

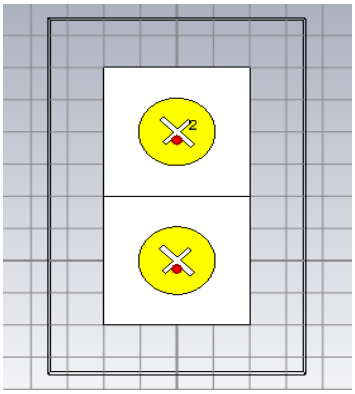

Figure 3. 32 Simulation of Vertical 2 MIMO Circular antenna Elements.

Based on the simulation results in Figure 3.32, the following results are obtained.

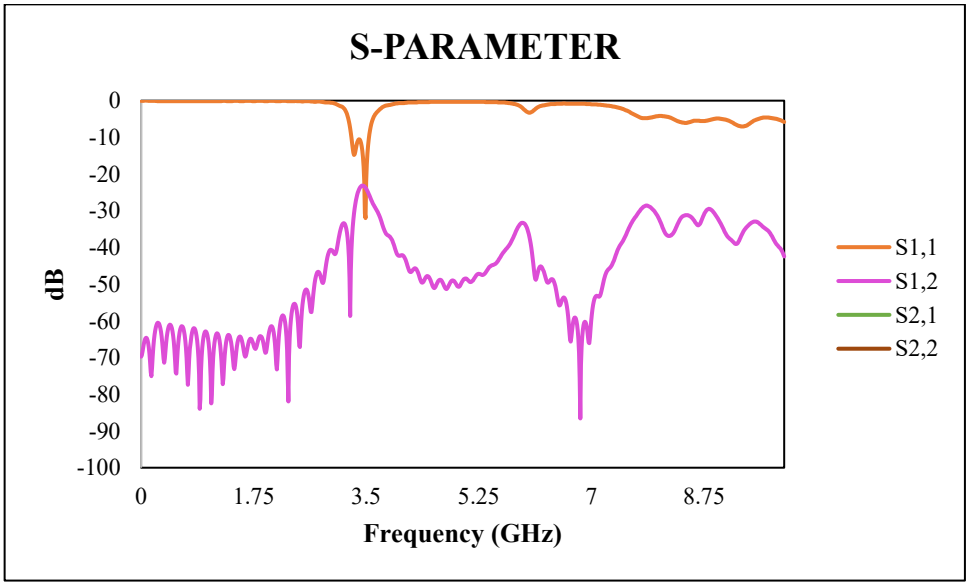

Figure 3. 33 S-parameter of Vertical 2 MIMO Circular Antenna Elements.

The s-parameter values generated on the vertical 2 MIMO antenna as shown in Figure 3.33 have values $S_{1,1}$, $S_{1,2}$, $S_{2,1}$, $S_{2,2}$ where the values $S_{1,1}$ and $S_{2,2}$ indicate the value of s-parameter for each element. antenna, while the $S_{1,2}$ and $S_{2,1}$ value indicate mutual coupling between adjacent antennas. The overall s-parameter value generated at the resonant frequency has a value <-10 dB so that the vertical 2 MIMO antenna design has good performance when viewed from the s-parameter value.

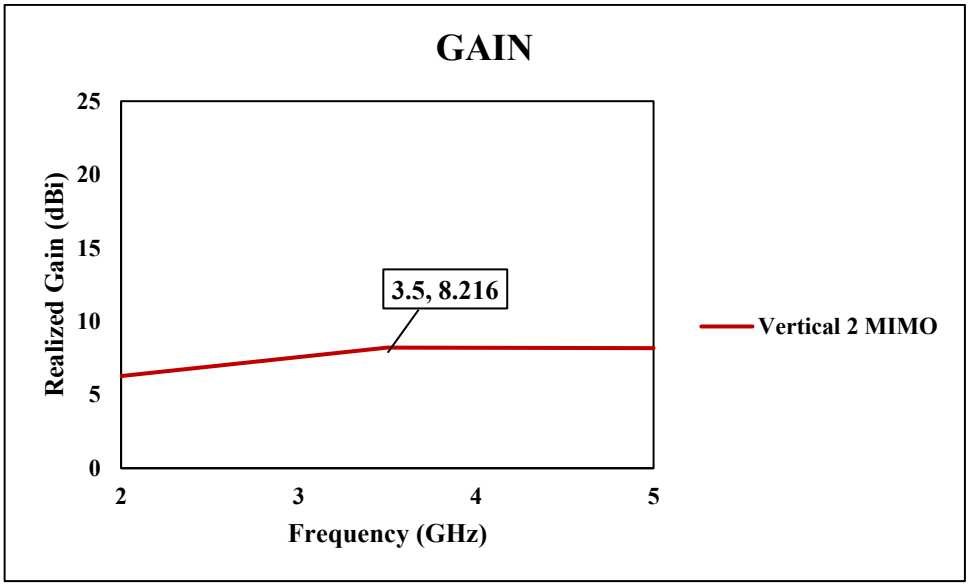

Figure 3. 34 Gain value of Vertical 2 MIMO Circular Antenna Elements.

The resulting gain as shown in Figure 3.34 is 8.216 dBi. This gain value is the gain value measured using the stacking antenna approach based on the MIMO configuration designed.

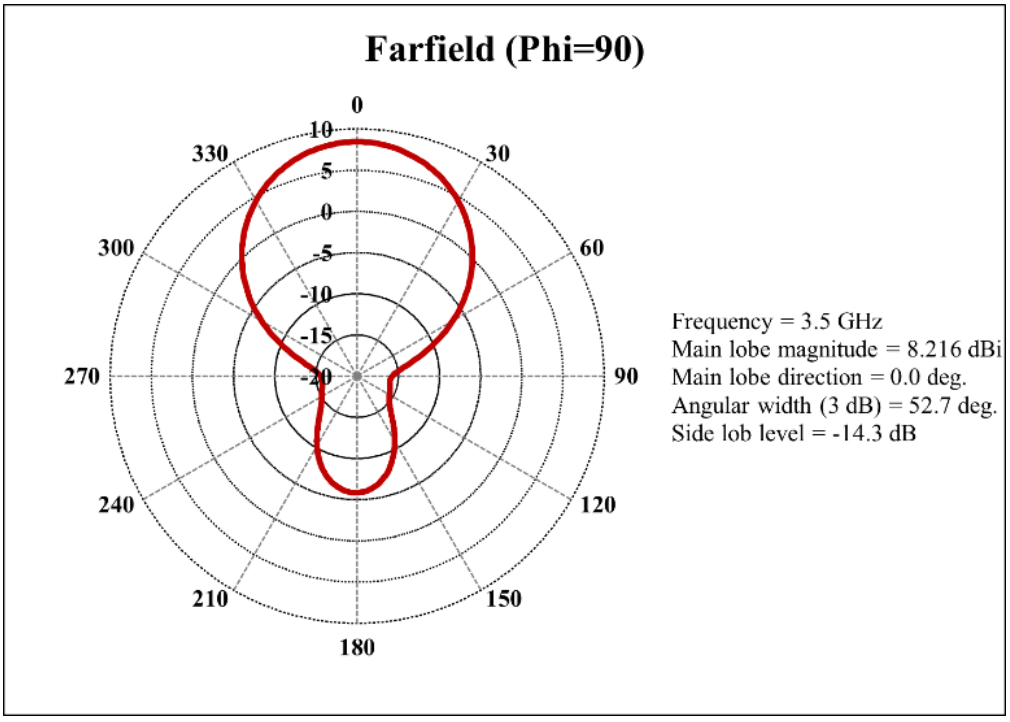

Figure 3. 35 Angular width of Vertical 2 MIMO Circular Antenna Elements.

The HPBW value produced in the vertical 2 MIMO Antenna design as shown in Figure 3.35 is 52.7 degrees. The HPBW value generated in this design will then

be compared with the single scheme HPBW value and as a reference for further MIMO configuration design.

The simulation results of vertical 2 MIMO Antenna are also indicated by three values including s-parameter, gain and HPBW. Figure 3.33 shows the s-parameter value of each antenna are $< -10\,dB$ which means that the antenna can work properly. Furthermore, the gain value in Figure 3.34 is 8.261 dBi and the HPBW value in Figure 3.35 is 52.7°.

3.8.3 Simulation of Horizontal 2 MIMO Antenna Elements

The simulation of the horizontal 2 MIMO Circular Antenna configuration is intended as a comparison for calculating the horizontal Array Factor with the following simulation.

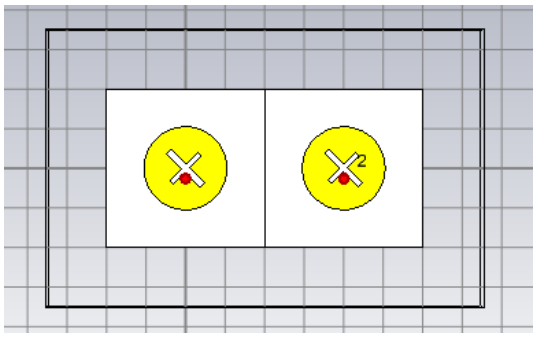

Figure 3. 36 Simulation of Horizontal 2 MIMO Circular Antenna Elements.

Based on the simulation results in Figure 3.36, the following results are obtained.

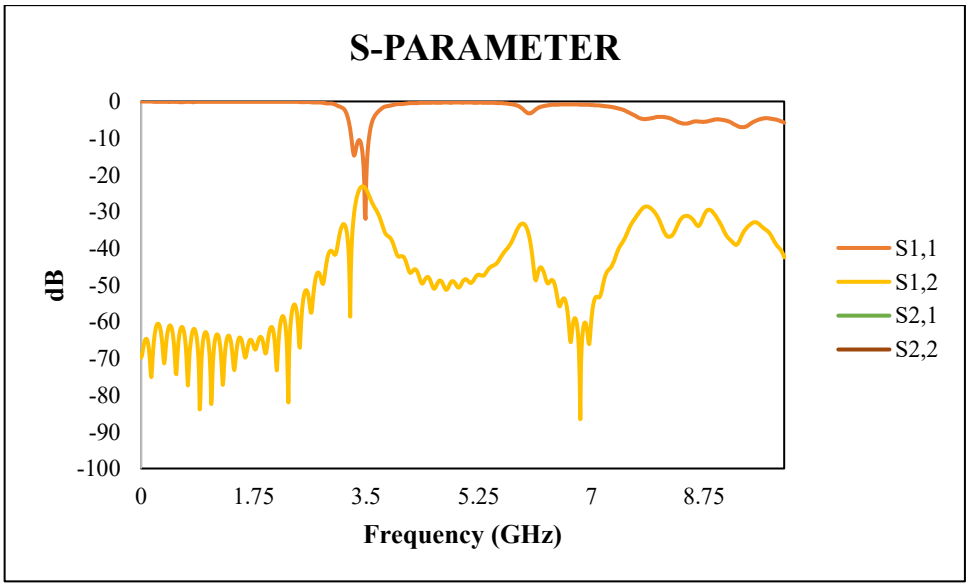

Figure 3. 37 S-parameter of Horizontal 2 MIMO Circular Antenna Elements.

The s-parameter values generated on the horizontal 2 MIMO antenna as shown in Figure 3.37 have values $S_{1,1}$, $S_{1,2}$, $S_{2,1}$, $S_{2,2}$ where the values $S_{1,1}$ and $S_{2,2}$ indicate the value of s-parameter for each element. antenna, while the $S_{1,2}$ and $S_{2,1}$ value indicate mutual coupling between adjacent antennas. The overall s-parameter value generated at the resonant frequency has a value <-10 dB so that the 2x1 MIMO antenna design has good performance when viewed from its s-parameter value.

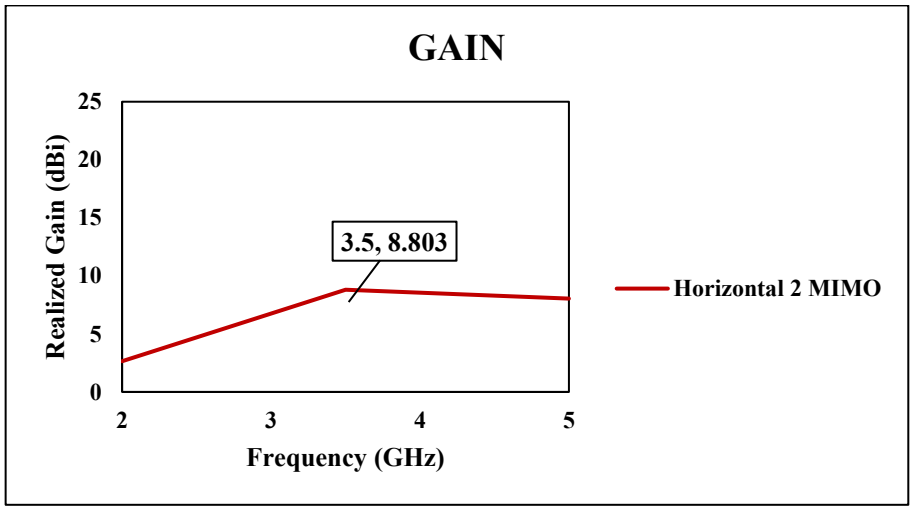

Figure 3. 38 Gain value of Horizontal 2 MIMO Circular Antenna Elements.

The resulting gain as shown in Figure 3.38 is 8.803 dBi. This gain value is the gain value measured using the array antenna approach based on the MIMO configuration designed.

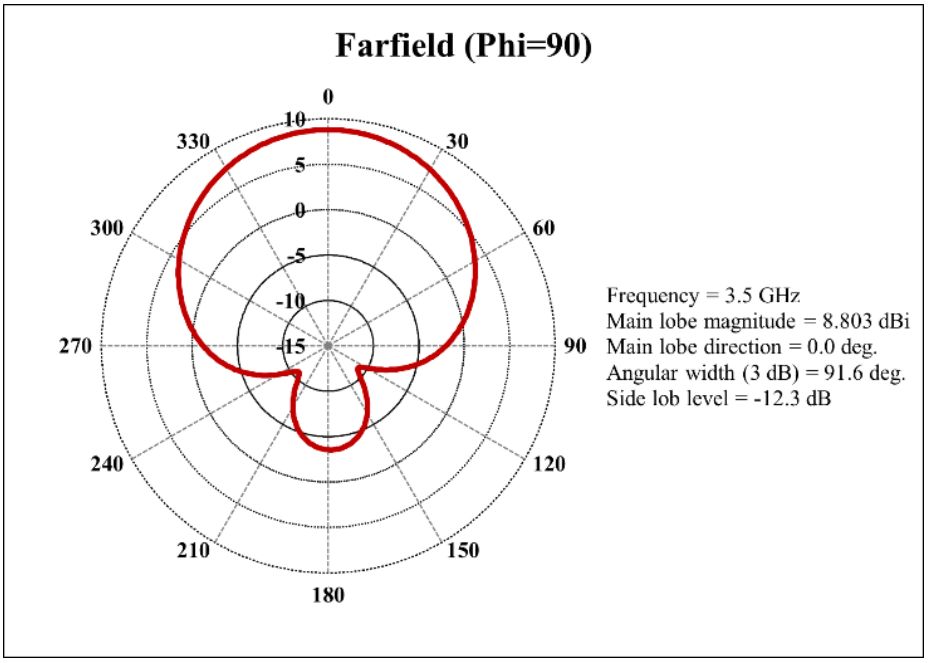

Figure 3. 39 Angular width of Horizontal 2 MIMO Circular Antenna Elements.

The HPBW value produced in the horizontal 2 MIMO Antenna design as shown in Figure 3.39 is 91.6 degrees. The HPBW value generated in this design will then be compared with the single scheme HPBW value and as a reference for further MIMO configuration design.

The simulation results of horizontal 2 MIMO Antenna are also indicated by three values including s-parameter, gain and HPBW. Figure 3.37 shows the s-parameter value of each antenna are $< -10\ dB$ which means that the antenna can work properly. Furthermore, the gain value in Figure 3.38 is 8.803 dBi and the HPBW value in Figure 3.39 is 91.6°.

3.8.4 Simulation of 4 MIMO Antenna Elements

The simulation is carried out for the 4 MIMO antenna configuration which refers to the optimization of a single antenna and as a comparison to the rectangular antenna simulation.

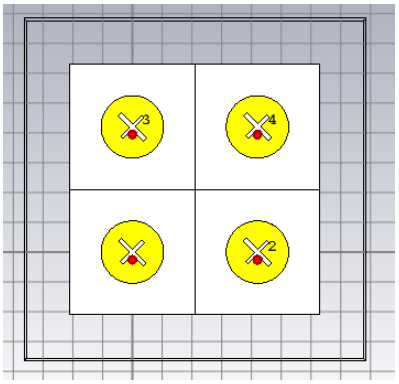

Figure 3. 40 Simulation of 4 MIMO Circular Antenna Elements.

Based on the simulation results in Figure 3.40, the following results obtained.

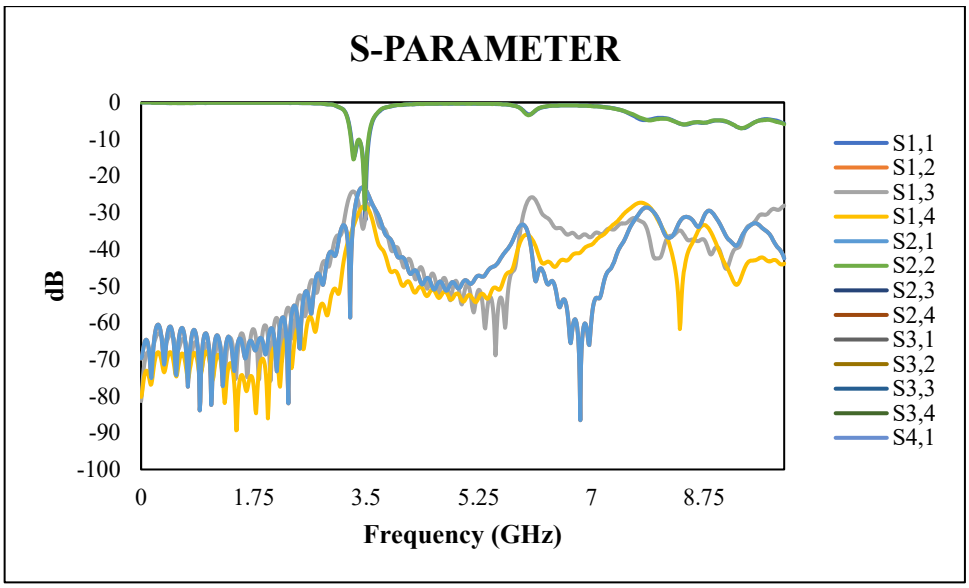

Figure 3. 41 S-parameter of 4 MIMO Circular Antenna Elements.

The s-parameter value generated on the 4 MIMO antenna as shown in Figure 3.41 has a value of $S_{1,1}$, $S_{1,2}$, …, $S_{4,3}$, $S_{4,4}$ where for the return value loss pattern $S_{N,N}$ ($S_{1,1}$, $S_{2,2}$, $S_{3,3}$, $S_{4,4}$) shows the value of s-parameter for each antenna element, while the value of s-parameter pattern $S_{N,M}$ (s-parameter other than the pattern $S_{N,N}$) shows mutual coupling between adjacent antennas. The overall s-parameter value generated at the resonant frequency has a value of <-10 dB so that the 4 MIMO antenna design has good performance when viewed from the s-parameter value.

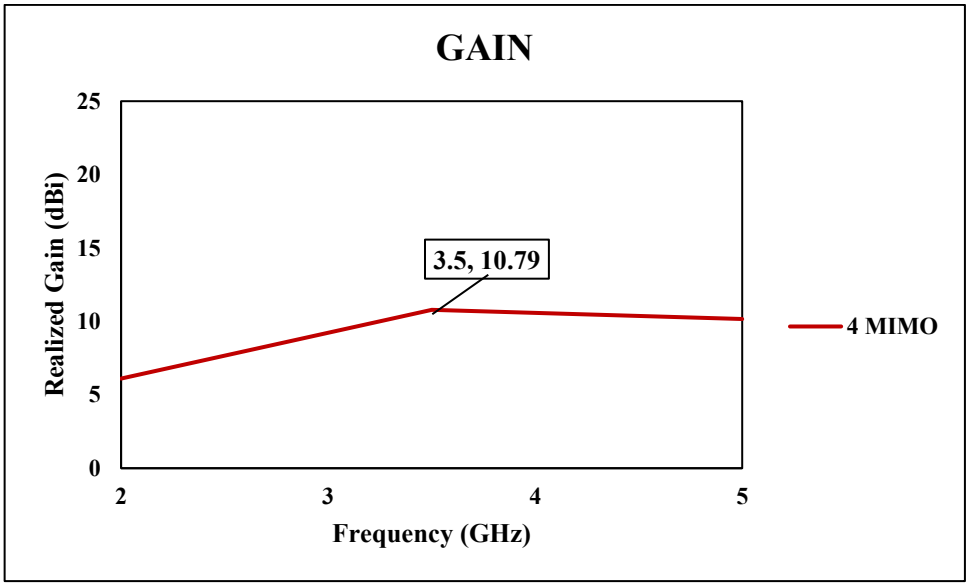

Figure 3. 42 Gain value of 4 MIMO Circular Antenna Elements.

The resulting gain as shown in Figure 3.42 is 10.79 dBi. This gain value is the gain value measured using the stacking antenna approach based on the MIMO configuration designed.

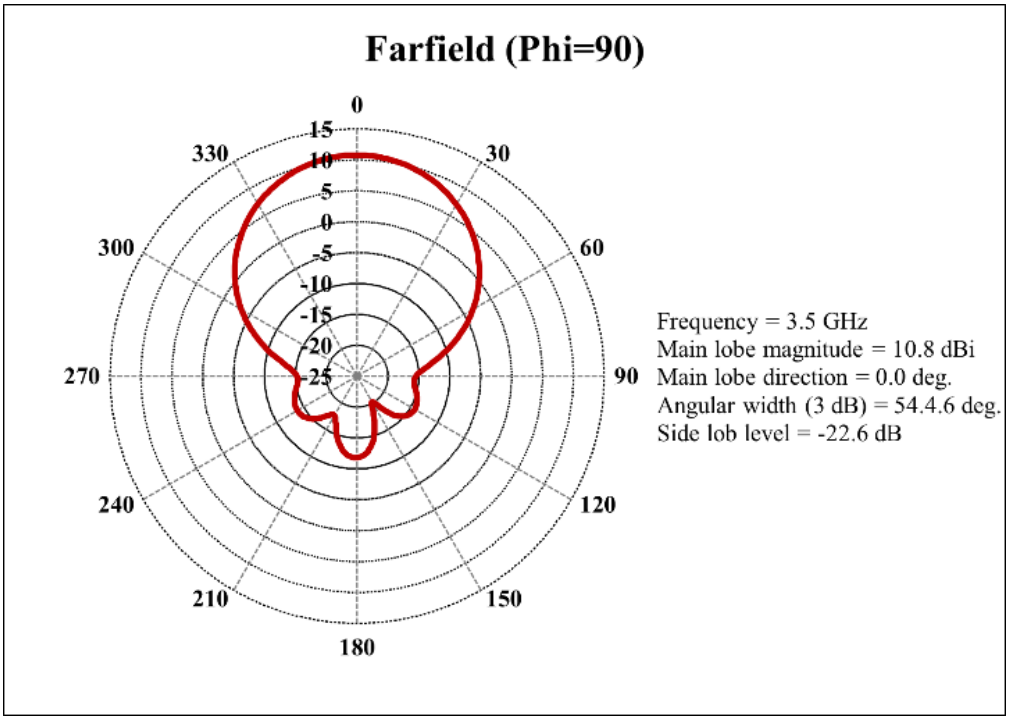

Figure 3. 43 Angular width of 4 MIMO Circular Antenna Elements.

The HPBW value generated in the 4 MIMO Antenna design as shown in Figure 3.43 is 54.46°. The HPBW value generated in this design will then be

compared with the HPBW value for a single scheme and as a reference for further MIMO configuration designs.

The simulation results of 4 MIMO Antenna are also indicated by three values including s-parameter, gain and HPBW. Figure 3.41 shows the s-parameter value of each antenna are $< -10\ dB$ which means that the antenna can work properly. Furthermore, the gain value in Figure 3.42 is 10.79 dBi and the HPBW value in Figure 3.43 is 54.6°.

3.8.5 Simulation of 16 MIMO Antenna

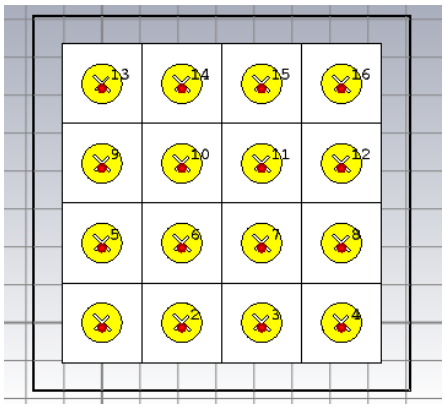

Figure 3. 44 Simulation of 16 MIMO Circular Antenna Elements.

Based on the simulation results in Figure 3.44, the following results are obtained.

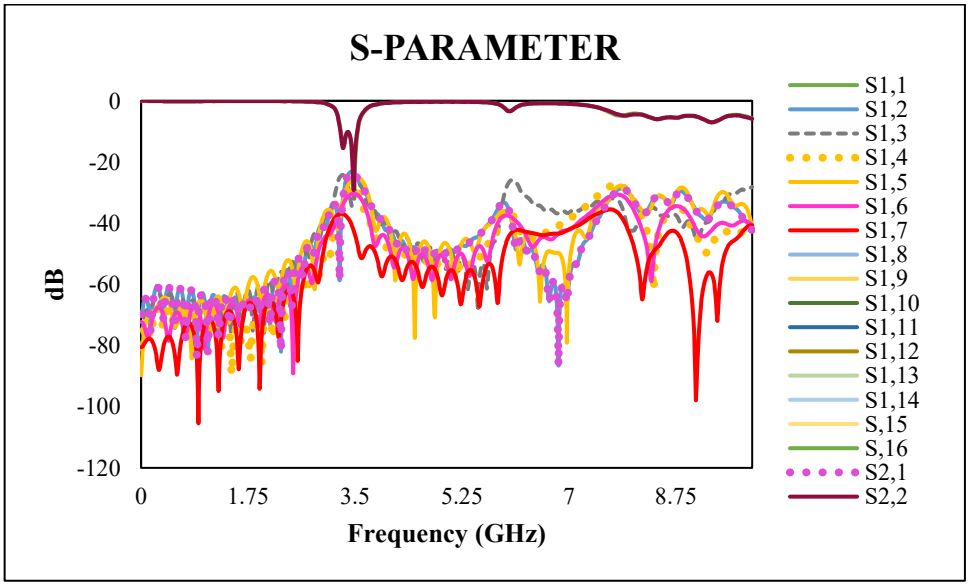

Figure 3. 45 S-parameter of 16 MIMO Circular Antenna Elements.

The s-parameter value generated on the 16 MIMO antenna as shown in Figure 3.45 has a s-parameter value where the $S_{N,N}$ patterned s-parameter value indicates the s-parameter value for each antenna element, while the $S_{N,M}$ patterned s-parameter value (s-parameter other than pattern $S_{N,N}$) shows mutual coupling between adjacent antennas. The overall s-parameter value generated at the resonant frequency has a value of <-10 dB so that the 16 MIMO antenna design has good performance from its s-parameter value.

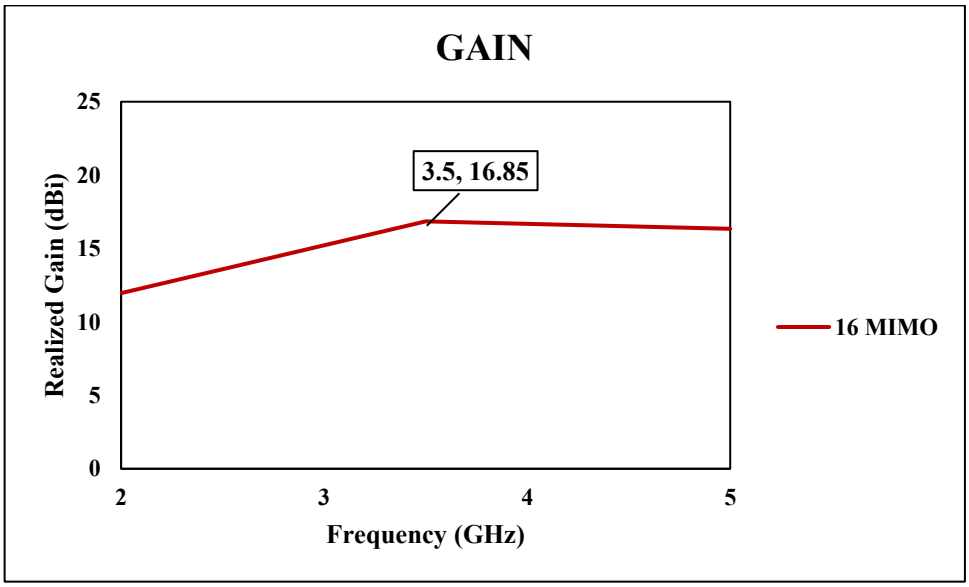

Figure 3. 46 Gain value of 16 MIMO Circular Antenna Elements.

The resulting gain as shown in Figure 3.46 is 16.85 dBi. This gain value is the gain value measured by the array antenna approach based on the MIMO configuration designed.

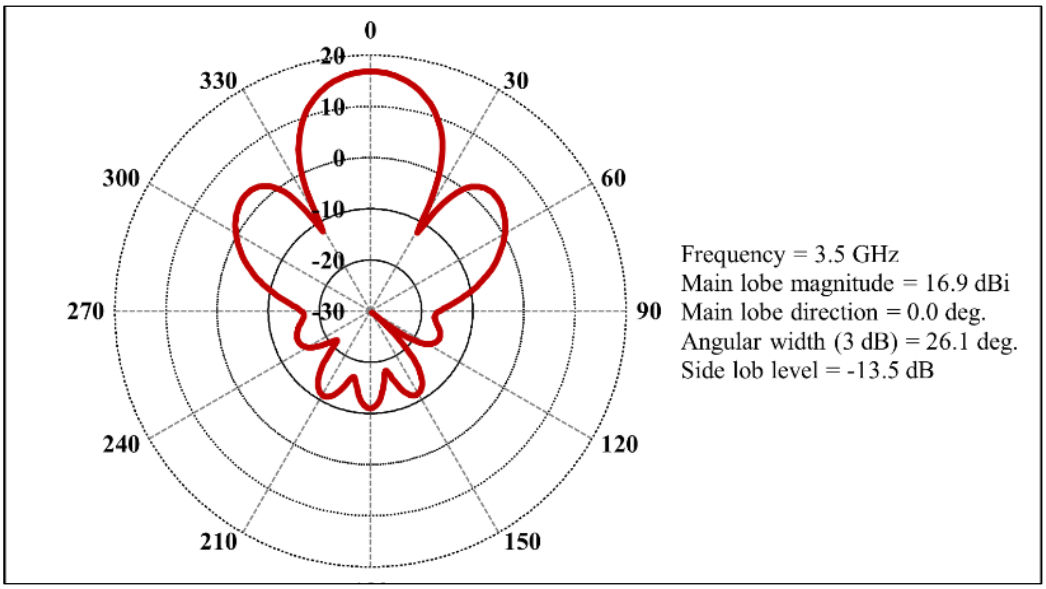

Figure 3. 47 Angular width of 16 MIMO Circular Antenna Elements.

The HPBW value produced in the 16 MIMO Antenna design as shown in Figure 3.47 is 26.1°. The HPBW value generated in this design will then be compared with the single scheme HPBW value and as a reference for further MIMO configuration design.

The simulation results of 16 MIMO Antenna are also indicated by three values including s-parameter, gain and HPBW. Figure 3.45 shows the s-parameter value of each antenna are $< -10\ dB$ which means that the antenna can work properly. Furthermore, the gain value in Figure 3.46 is 16.85 dBi and the HPBW value in Figure 3.47 is 26.1°.

3.8.6 Simulation of 64 MIMO Antenna Elements

The next step is the simulation on the MIMO Antenna 64 configuration as the final configuration which will be simulated and used as a reference for calculating the Array Factor. Antenna simulation can be seen in the Figure 3.48.

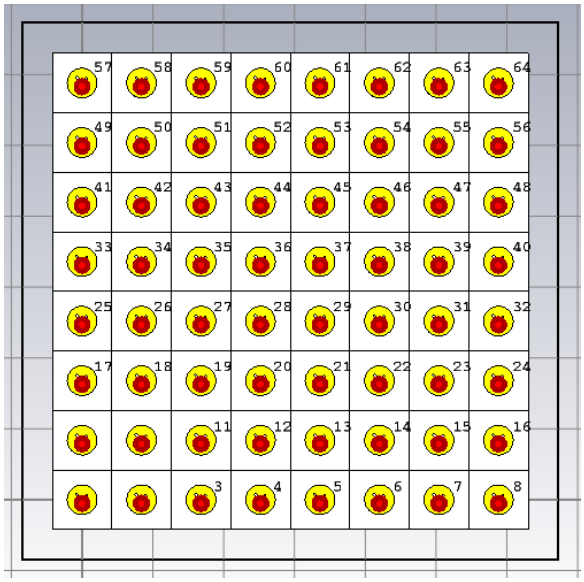

Figure 3. 48 Simulation of 64 MIMO Circular Antenna Elements.

Based on the simulation results in Figure 3.48, the following results are obtained.

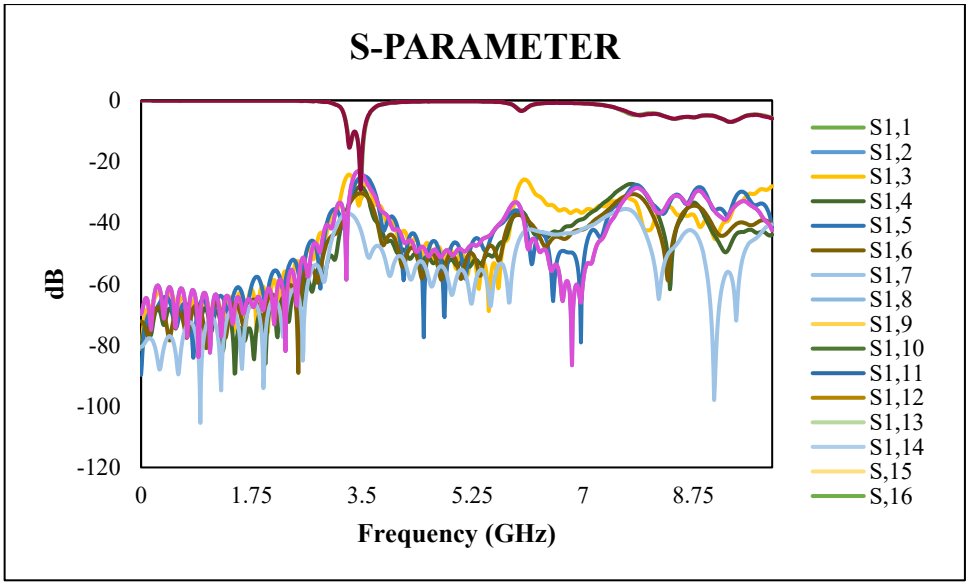

Figure 3. 49 S-parameter of 64 MIMO Circular Antenna Elements.

The s-parameter value generated on the 64 MIMO antenna as shown in Figure 3.49 has a s-parameter value where the $S_{N,N}$ patterned s-parameter value indicates the s-parameter value for each antenna element, while the $S_{N,M}$ patterned s-parameter value (s-parameter other than pattern $S_{N,N}$) shows mutual coupling between adjacent antennas. The overall s-parameter value generated at the resonant frequency has a value of <-10 dB so that the 64 MIMO antenna design has good performance when viewed from the s-parameter value.

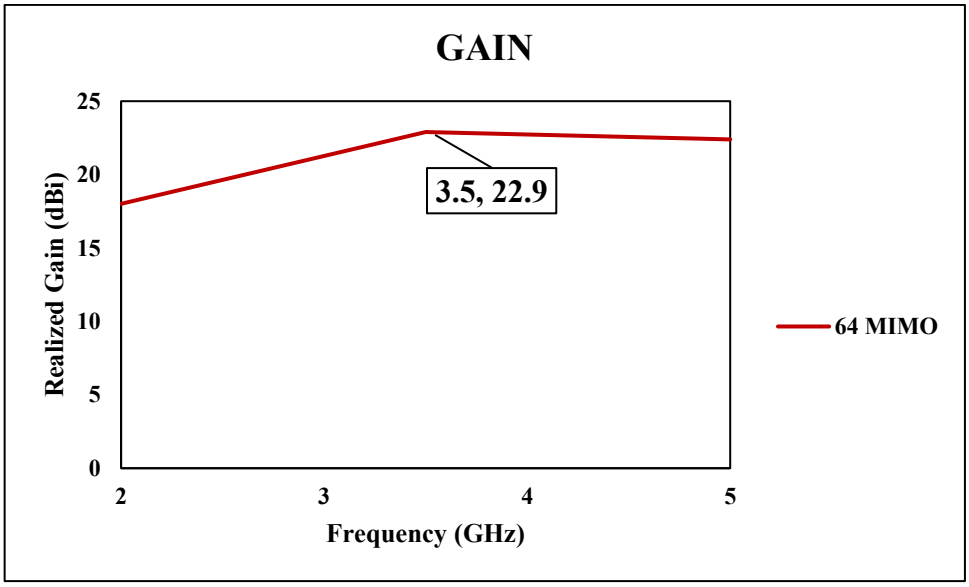

Figure 3. 50 Gain value of 64 MIMO Circular Antenna Elements.

The resulting gain as shown in Figure 3.50 is 22.9 dBi. This gain value is the gain value measured by the array antenna approach based on the MIMO configuration designed.

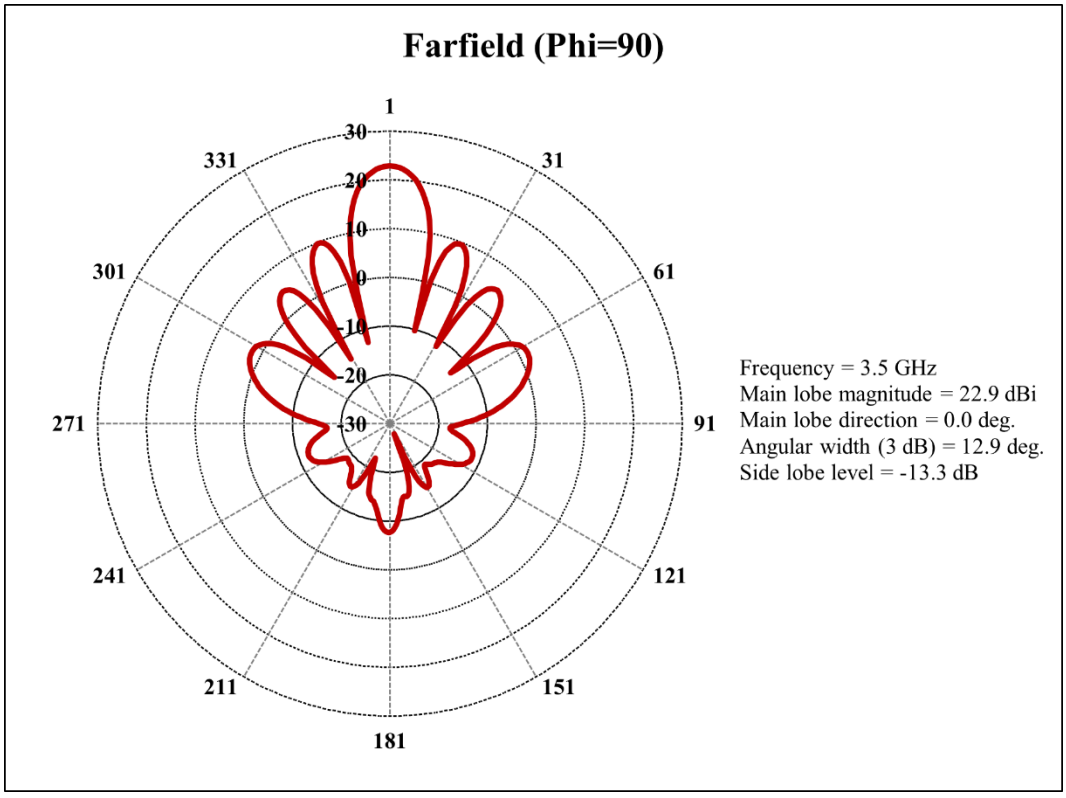

Figure 3. 51 Angular width of 64 MIMO Circular Antenna Elements.

The HPBW value produced in the 64 MIMO Antenna design as shown in Figure 3.51 is 12.9°. The HPBW value generated in this design will then be

compared with the single scheme HPBW value and as a reference for further MIMO configuration design.

The simulation results of 64 MIMO Antenna are also indicated by three values including s-parameter, gain and HPBW. Figure 3.49 shows the s-parameter value of each antenna are $< -10\ dB$ which means that the antenna can work properly. Furthermore, the gain value in Figure 3.50 is 22.9 dBi and the HPBW value in Figure 3.51 is 12.9°.

3.9 Field Gain Calculation of MIMO Configuration

The field gain calculation is performed to measure the resulting gain value on the MIMO configuration antenna. The first thing that needs to be done is measuring the gain value on a single antenna. After that, the calculation of the field gain for each configuration scheme is carried out.

Referring to the simulation results that have been carried out, the single antenna gain value for the rectangular patch shape is 6.41 dBi and the circular patch shape is 6.561 dBi.

3.9.1 Field Gain Calculation of Rectangular Patch Antenna

Based on equation (2.13), the field gain value for the MIMO configuration can be calculated to predict the value as follows.

1. Field Gain of 4 MIMO

$$G_F = \sqrt{n} \times G_S = \frac{10 \log n}{2} + G_S$$

$$G_F = \sqrt{4} \times 6.41 = \frac{10 \log 4}{2} + 6.41 = 9.41\ dBi$$

2. Field Gain of 16 MIMO

$$G_F = \sqrt{n} \times G_S = \frac{10 \log n}{2} + G_S$$

$$G_F = \sqrt{16} \times 6.41 = \frac{10 \log 16}{2} + 6.41 = 12.43\ dBi$$

3.9.2 Field Gain Calculation of Circular Patch Antenna

As with the rectangular patch, the field gain is calculated based on equation (2.13), the field gain value for the MIMO configuration can be calculated to predict the value as follows.

1. Field Gain of 4 MIMO

$$G_F = \sqrt{n} \times G_S = \frac{10 \log n}{2} + G_S$$

$$G_F = \sqrt{4} \times 6.561 = \frac{10 \log 4}{2} + 6.561 = 9.872\ dBi$$

2. Field Gain of 16 MIMO

$$G_F = \sqrt{n} \times G_S = \frac{10 \log n}{2} + G_S$$

$$G_F = \sqrt{16} \times 6.561 = \frac{10 \log 16}{2} + 6.561 = 12.581\ dBi$$

3.10 Summary of Simulation Result

Table 3. 4 Summary Table of Simulation Result.

MIMO Configurations (Elements)	Rectangular Antenna		Circular Antenna	
	HPBW	GAIN (dBi)	HPBW	GAIN (dBi)
1	95.1°	6.410	92.1°	6.561
2 elements	51.0°	8.006	52.7°	8.216
2 elements	93.9°	8.745	91.6°	8.803
4 elements	55.7°	10.400	54.4°	10.790
16 elements	26.6°	16.480	26.1°	16.850
64 elements	13.2°	22.71	12.9°	22.9

The following is a summary table contain the gain and angular width of rectangular antenna and circular antenna which shows the simulation results of the single patch, vertical 2 MIMO, horizontal 2 MIMO, 4 MIMO, 16 MIMO and 64 MIMO configurations.

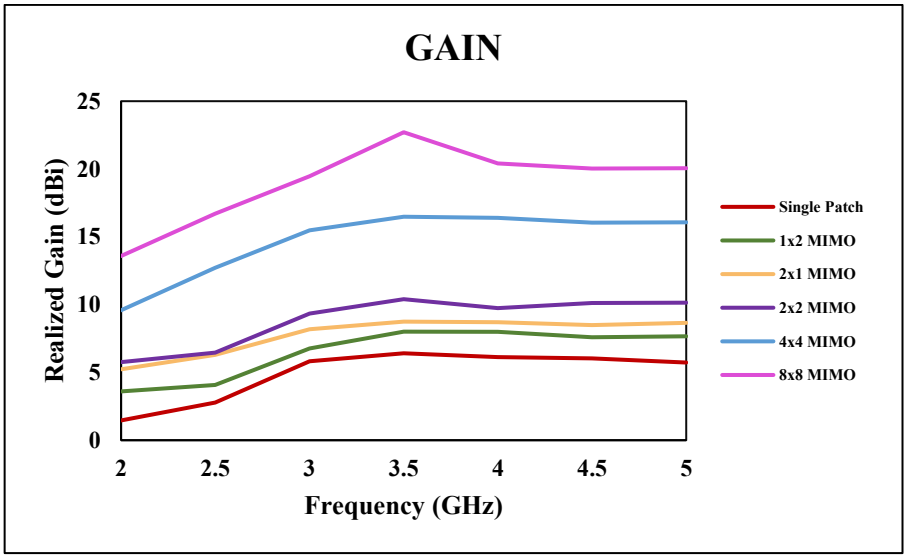

Figure 3. 52 Gain value increment of Rectangular Truncated Corner Antenna.

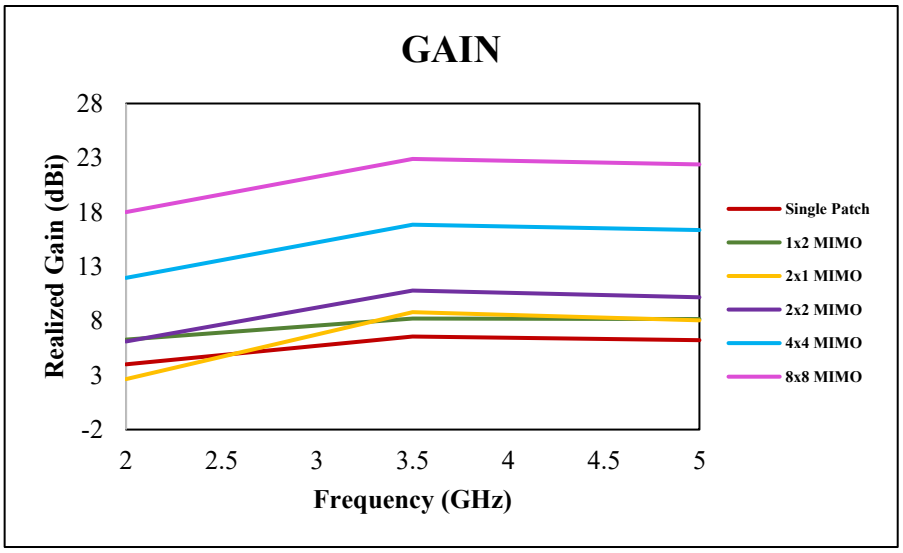

Figure 3. 53 Gain value increment of Circular Slotted X Antenna.

The graph of increasing the gain value based on the MIMO configuration is shown in Figure 3.52 for the gain value of the Rectangular Truncated Corner Antenna and Figure 5.53 for the gain value of the Circular Slotted X Antenna. The

two figures show the result that the gain value increases directly proportional to the number of MIMO configuration elements.

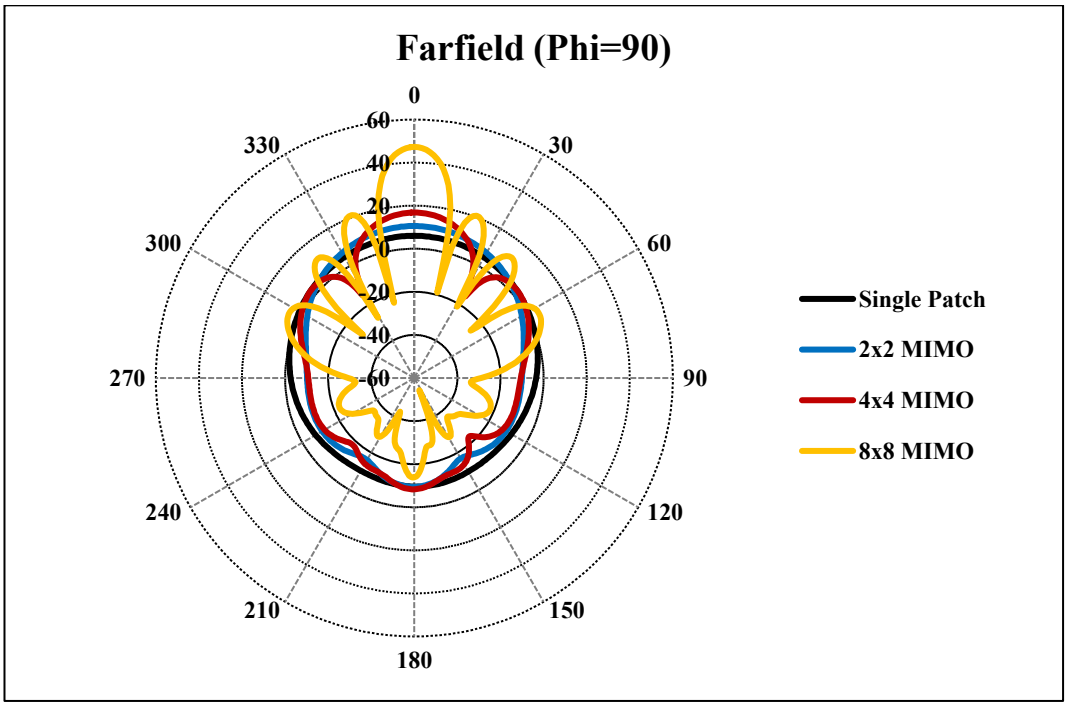

Figure 3. 54 Angular width decrement of Rectangular Truncated Corner Antenna.

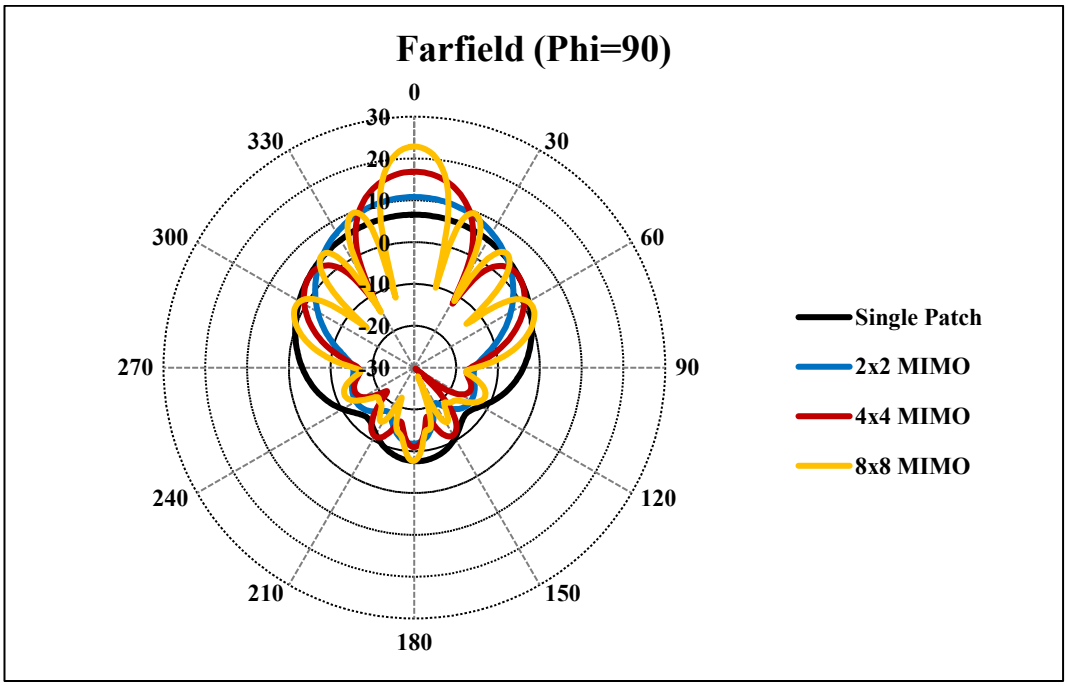

Figure 3. 55 Angular width decrement of Circular Slotted X Antenna.

The decrease of Angular width based on the MIMO configuration is shown in Figure 3.54 for the gain value of the Rectangular Truncated Corner Antenna and

Figure 3.55 for the gain value of the Circular Slotted X Antenna. The two figures show that the angular width is getting sharper, and the power is getting stronger inversely with the number of MIMO configuration elements. So, it can be concluded that a good angular width with strong power will be produced by designing a MIMO configuration with more elements.

IV. RESULT AND ANALYSIS

4.1 Antenna Realization

Antenna realization has been conducted following the design and simulation process in the CST Studio Suite Software, which produces results that are in line with the requirements.

4.2 Analysis

This section shows the results of the simulations that have been carried out on a rectangular antenna with a truncated corner and a circular antenna with an x-slot. MIMO configuration of 4 elements, 16 elements and 64 elements for each type of antenna is performed to find gain and HPBW values and analyse these values to then be used as a reference in predicting the achievement of values that can be generated on Massive MIMO Antennas (large number of elements).

4.2.1 Gain

The gain value analyzed is the gain value of the exponential pattern MIMO antenna configuration with the number of elements 1, 4 elements, 16 elements and 64 element for each type of antenna.

Table 4. 1 Increment Percentage of Gain Value.

MIMO Configurations (Element)	Rectangular Antenna with Truncated Corner		Circular Antenna with X Slot	
	GAIN (dBi)	Percentage of increase value	GAIN (dBi)	Percentage of increase value
1	6.410	100.00 %	6.561	100.00 %
4 elements	10.40	62.24 %	10.79	64.45 %
16 elements	16.48	58.46 %	16.85	56.16 %
64 elements	22.71	37.80%	22.9	35.91%

Based on Table 4.1, the increment of gain value obtained for each MIMO Antenna configuration for the two types of antennas and has the value that tends to be the same. Thus, the gain value for the Massive MIMO Antenna can be predicted by referring to the pattern of increasing values obtained. The gain value increases for each additional element which indicates that the more elements used, the greater

the gain value obtained. Thus, it can be predicted that if the number of MIMO configuration elements increases (with an exponential increase), then the resulting gain value will be higher, and this proves that increasing the number of MIMO configuration elements can significantly improve antenna performance.

The increase in gain value as the number of antenna elements increases is then searched for the pattern of increase in both rectangular antennas and circular antennas. The sample gain value of the simulation results is still lacking so that the number of samples is increased by predicting the gain value that can be generated in a large-scale MIMO antenna scheme until the number of antenna elements reach tens of thousands of elements.

For each different patch shape, a graph was plotted and analysed individually. The variables in the equations were then analysed to draw conclusions from the two resulting formula approximations. Each patch shape has its own enhancement pattern as follows.

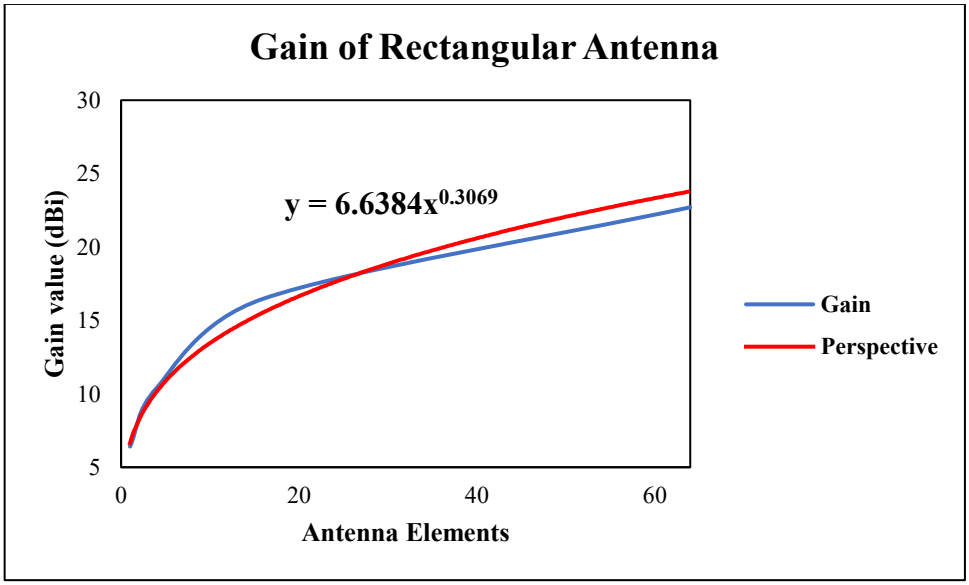

Figure 4. 1 Gain value increment of rectangular antenna.

In Figure 4.1, the gain value of the rectangular antenna is directly proportional to the number of antenna elements which then forms a curve and can be formulated with the formula $y = 6.6384x^{0.3069}$.

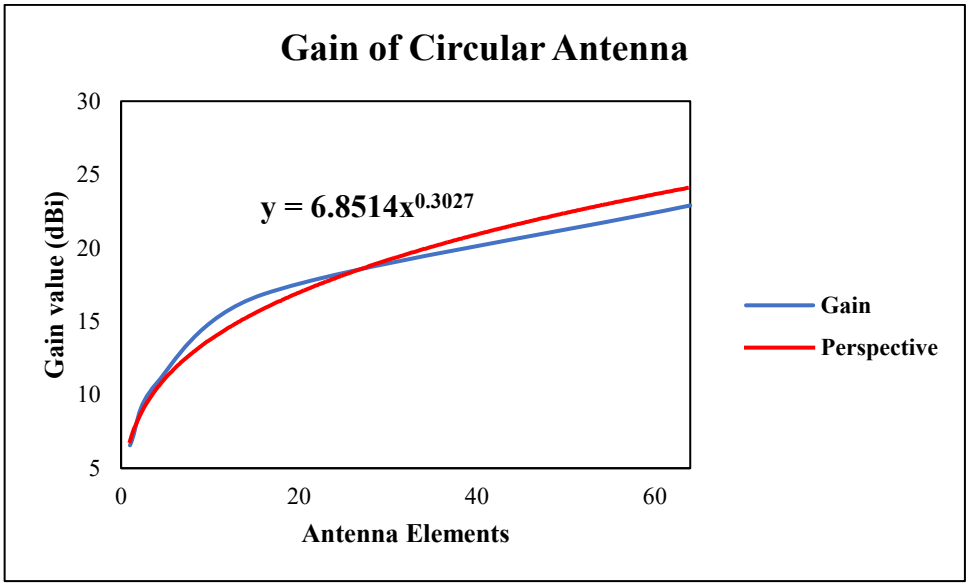

Figure 4. 2 Gain value increment of circular antenna.

Figure 4.2 demonstrates that, like the Rectangular Antenna, the gain value of the circular antenna is linearly proportional to the number of antenna elements, forming a curve that can be expressed using the formula $y = 6.8514x^{0.3027}$.

The gain (y) in the first equation rises at a pace determined by the exponent (0.3069). The gain increases exponentially according to the value of x. The gain (y) in the second equation likewise grows at a rate that is influenced by the exponent (0.3027). The variations coefficient a value (6.6384 and 6.8514), however, point to a variation in the gain's beginning value at the same x value. A typical exponential gain improvement trend may be seen in both equations. The gain achieved increases with the value of x (number of MIMO antenna elements).

The two equations each show the exponential relationship between gain (y) in dBi and the quantity of MIMO antenna elements (x). The second equation's bigger exponent implies that as the number of MIMO antenna elements rises, the gain does so more quickly than it did in the first equation. The gain that can be realized increases with increasing values of x. However, as the number of antenna elements rises, the rate of gain increase slows. The equation explains how a MIMO system's gain improvement might be affected by the number of antenna elements used. The two equations' varied coefficient values suggest that the initial gain value at the same number of antennas will vary slightly. The features of the antenna being

utilized, such as its frequency response, radiation pattern, and efficiency, also have an impact on the increase in gain with a given number of antenna elements.

It is crucial to remember that the gain in dBi represents a comparison to an ideal isotropic antenna, which emits light evenly in all directions. Based on the anticipated number of antenna elements, the equation can be used to calculate the gain of a MIMO system. For MIMO systems to work as intended, analysis of this gain pattern is crucial during design and optimization. The equation enables performance comparisons between MIMO systems with various numbers of antenna elements, enabling the choice of the number of antenna elements that best meets the requirements of a given application.

In this study, we present a methodology for deriving the antenna gain equation based on empirical data obtained from antenna measurements. The objective is to establish a mathematical relationship between antenna gain (y) and the number of antenna elements (x) through the power-law equation $(y = ax^b)$. This approach allows us to quantitatively express how antenna gain evolves with the increase in the number of elements.

1. Data Conversion: Given gain values in decibels (dBi), it is crucial to convert them to linear form using $y_{linear} = 10^{\frac{ydB}{10}}$. This conversion is necessary as the equation will be utilized in its linear form, not dB.
2. Equation Transformation: Taking the natural logarithm (ln) of both sides yields $\ln(y) = \ln ax^b$.
3. Exponent Separation: Exploiting logarithmic properties, we can separate the exponent: $\ln(y) = \ln(a) + \ln(x^b)$.
4. Exponent Rearrangement: Employing additional logarithmic properties, rearrange the equation to move the exponent b upfront: $\ln(y) = \ln(a) + b\ln(x)$..
5. System of Equations: Defining $\ln(y_1) = Y_1, \ln(y_2) = Y_2$, and so forth for the given data points, a system of linear equations is formed as $Y = \ln(a) + bX$, where $X = \ln(x)$.
6. Solution of the System: Solving this system of equations yields the values of $\ln(a)$and b.

7. Calculation of a: Upon obtaining $\ln(a)$ and b, a can be calculated by exponentiating $\ln(a)$, yielding $a = e^{\ln(a)}$.

The resulting values of a and b form the equation $y = ax^b$, enabling accurate prediction of antenna gain based on the number of antenna elements. This methodology offers insights into the relationship between gain and antenna size, allowing for optimized design and deployment in various applications.

This methodology bridges the gap between empirical data and mathematical modelling, providing a robust framework for antenna characterization and design optimization. It offers researchers and practitioners a systematic approach to derive an equation that characterizes the behaviour of antenna gain as the array size varies. This approach can be instrumental in guiding the development of efficient antenna systems tailored to specific requirements.

4.2.2 HPBW

Same with analysis of gain, the angular width analysed is the angular width of the exponential pattern MIMO antenna configuration with the number of elements 1, 4 elements, 16 elements and 64 elements.

Table 4. 2 Decrement Percentage of Angular Width.

MIMO Configurations (Element)	Rectangular Antenna with Truncated Corner		Circular Antenna with X Slot	
	HPBW	Percentage of decrease value	HPBW	Percentage of decrease value
1	95.1°	100.00 %	92.1°	100.00 %
4 elements	55.7°	41.43 %	54.4°	39.52 %
16 elements	26.6°	52.24 %	26.1°	52.24 %
64 elements	13.2°	50.37%	12.9°	51.50%

Based on Table 4.2, the decrement of angular width obtained for each MIMO Antenna configuration for the two types of antennas and has the value that tends to be the same. Thus, the gain value for the Massive MIMO Antenna can be predicted

by referring to the pattern of decrement values obtained. HPBW is getting sharper for each added element which shows that the more elements used, the HPBW angle will be sharper. Interest with the result of HPBW, we can predict that a MIMO configuration with a large number of elements (with an exponential increase) will produce a sharper angular width, and this proves that a MIMO configuration with a very large number of elements in an antenna will make the antenna performance very good.

The decrease in HPBW as the number of antenna elements increases is then searched for the pattern of increase in both rectangular and circular antennas. Like the gain value analysis, the HPBW angle analysis is also predicted by finding the formulas as in the chart.

The predicted values are expected to result in values up to the minimum angle and have positive values. If the predicted values yield a negative minimum value, the prediction for that value is stopped until a positive minimum value is obtained. The predicted values up to the positive minimum are then plotted on a graph to generate a curve, from which conclusions can be drawn in the form of a formula. The resulting formula can then be used to calculate the scalability of Massive MIMO antennas with a very large number of elements and to avoid anomalies in predicting values for large-scale configurations.

For each different patch shape, a graph is plotted and analysed individually. The variables in the equations are then analysed to draw conclusions from the two resulting formula approximations. Each patch shape has its own decrease pattern as shown in Figure 4.3.

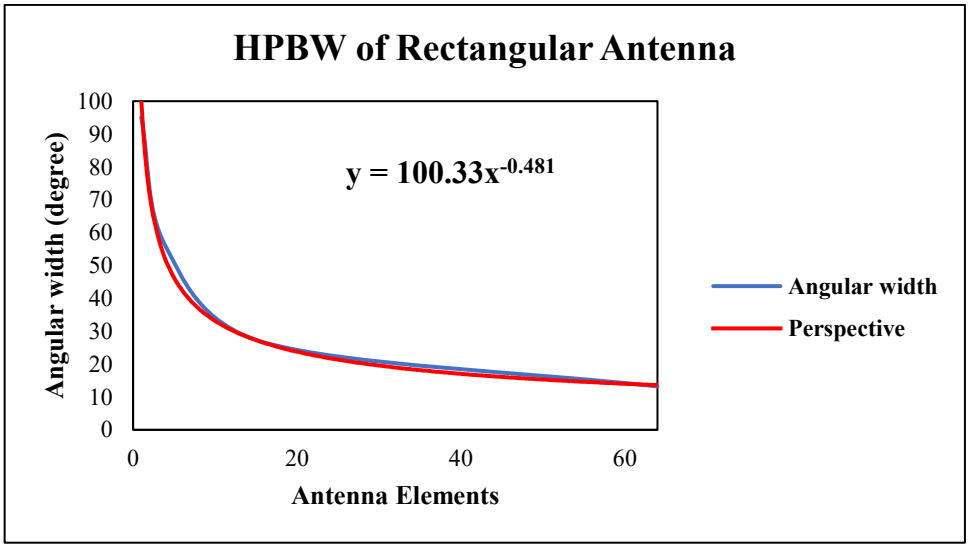

Figure 4. 3 Angular width decrement of rectangular antenna.

In Figure 4.3, the HPBW angle of the rectangular antenna is inversely proportional to the increase in the number of antenna elements which then forms a curve and can be formulated by the formula $y = 100.33x^{-0.481}$

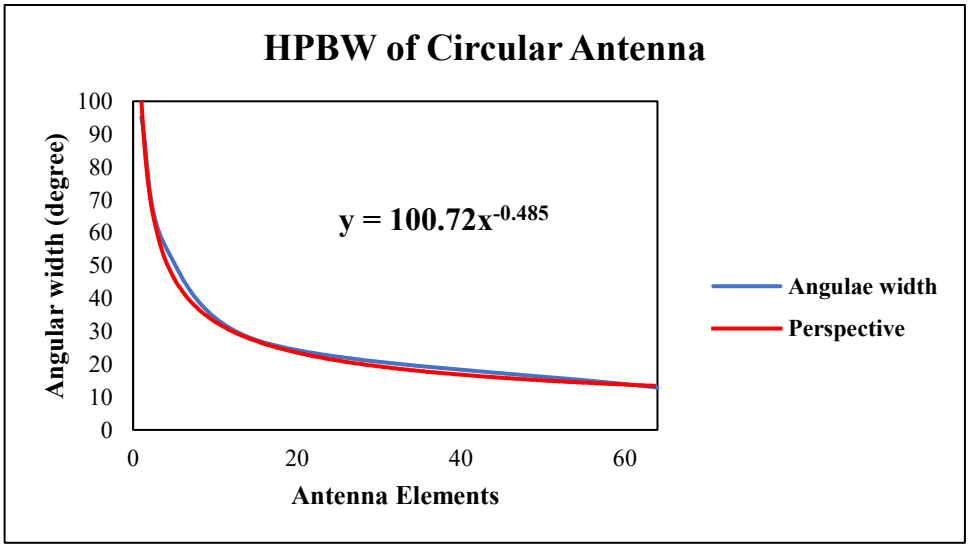

Figure 4. 4 Angular width decrement of circular antenna.

The gain value of the circular antenna, similar to the rectangular antenna, is shown in Figure 4.4 to be directly proportional to the number of antenna elements. This relationship results in a curve that may be described by the following formula $y = 100.72x^{-0.485}$

In both equations, the HPBW angle (y) decreases with the natural logarithm of the x value (number of MIMO antenna elements). The higher the value of x, the

smaller the HPBW angle. The difference in the coefficient and constant values in the two equations shows the difference in the rate of decrease of the HPBW angle at the same x value. Both equations show a slow pattern of decreasing HPBW angle as the value of x (number of MIMO antenna elements) increases, indicating that the HPBW angle decreases more slowly as the number of MIMO antenna elements used increases. The HPBW angle is measured in degrees.

Across a range of x values (number of MIMO antenna elements), various values of the coefficients and constants in the equations might cause variations in the degree of gain increase or HPBW angle drop in both analyses. Additionally, it should be noted that the relative measurements of gain (measured in dBi) and HPBW angle (measured in degrees) both provide information on the radiation pattern and focus of MIMO antennas with various element counts.

The equation describes the logarithmic relationship between the number of MIMO antenna elements (x) and the HPBW angle (y) in degrees. The natural logarithm (ln) is used to describe the pattern of decreasing HPBW angle with increasing number of antenna elements. The HPBW angle indicates how wide the antenna radiation pattern is at the point where the radiated power drops to half of its peak. The second equation shows a slower decrease in HPBW angle compared to the first equation, due to the difference in the coefficient values (100.33 and -100.72). The larger the value of x (number of MIMO antenna elements), the smaller the HPBW angle, indicating an increase in the sharpness of the radiation pattern. The slower decrease in HPBW angle in the second equation indicates that increasing the number of antenna elements provides less benefit in narrowing the radiation pattern compared to the first equation. The difference in constants in the two equations indicates the difference in HPBW angle at the same number of antenna elements. It is important to note that the radiation pattern of a MIMO antenna is also affected by the antenna design, such as shape, frequency bandwidth, and desired radiation pattern.

The equation can be used to estimate the HPBW angle of the MIMO system based on the planned number of antenna elements. Analysis of the HPBW angle drop pattern is important in MIMO system design to ensure signal directionality and antenna interference reduction. Using these equations, further analysis can be

done to compare the performance of MIMO systems with different numbers of antenna elements. This information is important in selecting the optimal number of antenna elements to achieve the desired radiation pattern, limit antenna interference, and maximize overall system efficiency.

Given the values of Half Power Beamwidth (HPBW) for different numbers of antenna elements (N):

- $N_1 = 1\ for\ \theta_1$
- $N_2 = 4\ for\ \theta_2$
- $N_3 = 16\ for\ \theta_3$
- $N_4 = 64\ for\ \theta_4$

We want to obtain the equation $y = f(x)$, where y is the HPBW value and x is the number of antenna elements.

First, we'll convert the angle values from degrees to radians (y in radians):

Angle in radians = Angle in degrees $\times \frac{\pi}{180}$

Next, we'll establish the relationship between y and x. Let's write the general equation $y = f(x)$ in the form $y = kx^n$, where k and n are the constants, we need to find.

Using the first data (N_1):

$$y_1 = kx^n{}_1$$

Angle 1 in radians = $k \times 1^n$

Angle 1 in radians = k

Using the second data (N_2):

$$y_2 = kx^n{}_2$$

Angle 2 in radians = $k \times 4^n$

Angle 2 in radians = $k \times 2^{2n}$

Using the third data (N_3):

$$y_3 = kx^n{}_3$$

Angle 3 in radians = $k \times 16^n$

Angle 3 in radians = $k \times 2^{4n}$

Using the fourth data (N_4):

$$y_4 = kx^n{}_4$$

Angle 4 in radians = $k \times 64^n$

Angle 4 in radians = $k \times 2^{6n}$

From here, we can set up a system of equations as follows:

Angle 2 in radians = $k \times 2^{2n}$

Angle 3 in radians = $k \times 2^{4n}$

Angle 4 in radians = $k \times 2^{6n}$

Comparing this with the general equation $y = kx^n$, we can see that n is the exponent of 2.

In other words, $n = 2$.

Now that we know $n = 2$, we can find the value of k using the first data (N_1):

Angle 1 in radians = k

k = Angle in radians

$$k = \theta_1 \times \frac{\pi}{180}$$

Hence, the resulting equation $y = f(x)$ is:

$$y = \left(\theta_1 \times \frac{\pi}{180}\right) x^2$$

In summary, the derived equation $y = \left(\theta_1 \times \frac{\pi}{180}\right) x^2$ establishes a connection between the Half Power Beamwidth (HPBW) y and the number of antenna

elements x, based on the provided angle data and angular conversion principles. The analysis confirms a quadratic relationship $(n = 2)$ between HPBW and the element count, aligned with the observed data.

V. CONCLUSIONS

5.1 Conclusions

MIMO configuration research was carried out on two types of antennas, namely Rectangular Truncated Corner Patch Antenna and Circular Slotted X Patch Antenna with RHCP and LHCP. Both types of antennas were simulated with exponential MIMO configurations of 1, 4 elements, 16 elements and 64 element. Right hand circular polarization (RHCP) and left hand circular polarization (LHCP) have a significant impact on the s-parameter between adjacent elements in a MIMO antenna system, thereby ensuring efficient inter-element performance. When RHCP and LHCP are used in MIMO antennas, they provide a diversity effect that helps mitigate multipath fading and improve the system's capacity and reliability. By employing orthogonal polarizations, the cross-polarization interference between adjacent elements is minimized, resulting in reduced interference and improved signal quality. This polarization diversity enhances the isolation between antennas and minimizes the impact of mutual coupling, thereby maintaining the desired performance of closely spaced antenna elements.

The increase in gain and decrease in half-power beamwidth (HPBW) for each MIMO configuration scheme and patch type were also analyzed. The gain increases with the addition of each MIMO antenna element due to the phenomenon of antenna array gain. When multiple antennas are combined in a MIMO configuration, their individual signals combine constructively, resulting in a stronger overall signal in the desired direction. This constructive interference leads to an increased gain, allowing for improved signal strength and coverage. On the other hand, the decrease in half-power beamwidth (HPBW) occurs because as more antenna elements are added, the antenna array becomes more focused and directive. The narrower beamwidth concentrates the transmitted or received energy into a smaller angular region, providing better spatial resolution and increased directivity. Consequently, the HPBW decreases, resulting in a narrower beam and improved signal concentration towards the desired target or receiver.

In this study, two equations were derived to depict the pattern of antenna gain improvement based on the number of MIMO antenna elements. In the case of rectangular antennas, the equation $y = 6.6384x^{0.3069}$ shows that the gain increases

exponentially with the addition of elements. However, for circular antennas, the equation $y = 6.8514x^{0.3027}$ indicates that the gain also increases exponentially but at a slightly lower growth rate. Therefore, adding antenna elements in the MIMO configuration for rectangular antennas can result in a greater gain compared to circular antennas. Nonetheless, both configurations exhibit a significant increase in gain with the addition of elements, indicating that the utilization of MIMO and the addition of antenna elements can effectively enhance system performance and capacity.

There is also a decrease in HPBW value from the given equations, it can be observed that the pattern of decreasing HPBW angle for the rectangular shape $y = 100.33x^{-0.481}$ has a negative exponent, while for the circular shape $y = 100.72x^{-0.485}$ it has a positive exponent. This indicates that as the number of MIMO antenna elements (x) increases, the HPBW angle for rectangular antennas will become smaller, whereas the HPBW angle for circular antennas will become larger. This implies that with the addition of MIMO antenna elements, the rectangular antenna provides a narrower and more directional beamwidth, while the circular antenna offers a wider beamwidth. This analysis allows for the selection of an appropriate antenna based on the application's needs, depending on the desired focus or wider coverage in the MIMO antenna system.

The derived equations in gain depict the improvement based on the number of MIMO antenna elements for both rectangular and circular configurations. It is observed that rectangular antennas exhibit a higher exponential growth rate in gain compared to circular antennas. Additionally, the angular width explains the decrease in half-power beamwidth (HPBW) based on the equations provided. The negative exponent in the rectangular antenna equation signifies a reduction in the HPBW angle with the addition of elements, whereas the positive exponent in the circular antenna equation indicates an increase in HPBW angle. This implies that rectangular antennas offer a narrower and more directional beamwidth, while circular antennas provide a wider coverage. Therefore, the analysis reveals the relationship between the gain improvement and beamwidth characteristics, guiding the selection of suitable antennas based on specific application requirements in a MIMO antenna system.

5.2 Recommendations

Based on the conclusion, the following recommendations are suggested for further research and development:

1. Investigate Other Antenna Configurations: Explore additional antenna configurations, apart from rectangular and circular antennas, to evaluate their impact on MIMO performance. This can include different shapes, sizes, or designs that may provide unique advantages in terms of gain improvement and beamwidth characteristics.
2. Experimental Validation: Conduct experimental validation to verify the simulation results obtained in this study. Real-world measurements and testing can provide valuable insights into the practical performance of MIMO antenna systems, considering factors such as environmental conditions, interference, and practical implementation challenges.
3. Optimization of Polarization Diversity: Further investigate the optimization of polarization diversity techniques, specifically focusing on the implementation of Right-Hand Circular Polarization (RHCP) and Left-Hand Circular Polarization (LHCP). Evaluate their effectiveness in mitigating multipath fading, reducing interference, and improving signal quality in different MIMO scenarios.
4. Comparative Analysis: Perform a comparative analysis of various MIMO configurations and patch types, considering factors such as gain improvement, beamwidth characteristics, signal quality, and system capacity. This analysis can aid in selecting the most suitable configuration for specific applications or environments.
5. Practical Considerations: Consider practical considerations, such as cost, size, power consumption, and implementation complexity, when designing and deploying MIMO antenna systems. Investigate techniques to optimize these factors while maintaining performance and reliability.
6. Application-Specific Studies: Conduct studies focusing on specific applications, such as wireless communication, radar, or satellite systems, to explore the impact of MIMO configurations on their performance. This can

involve analysing the effects of varying antenna elements, different frequencies, or channel conditions on system performance.

BIBLIOGRAPHY

[1] H. Yuan, C. Wang, Y. Li, N. Liu, and G. Cui, "The design of array antennas used for Massive MIMO system in the fifth generation mobile communication," *ISAPE 2016 - Proc. 11th Int. Symp. Antennas, Propag. EM Theory*, pp. 75–78, 2017, doi: 10.1109/ISAPE.2016.7833881.

[2] H. L. Chu, G. Mishra, and S. K. Sharma, "Dual Polarized Wideband Vivaldi 4x4 Subarray Antenna Aperture for 5G Massive MIMO Panels with Simultaneous Multiple Beams," *Proc. - ANTEM 2018 2018 18th Int. Symp. Antenna Technol. Appl. Electromagn.*, vol. 2018-Augus, pp. 1–2, 2018, doi: 10.1109/ANTEM.2018.8572871.

[3] S. A. Khwandah, J. P. Cosmas, P. I. Lazaridis, Z. D. Zaharis, and I. P. Chochliouros, "Massive MIMO Systems for 5G Communications," *Wirel. Pers. Commun.*, vol. 120, no. 3, pp. 2101–2115, 2021, doi: 10.1007/s11277-021-08550-9.

[4] N. H. M. Adnan, I. M. Rafiqul, and A. H. M. Z. Alam, "Massive MIMO for Fifth Generation (5G): Opportunities and Challenges," *Proc. - 6th Int. Conf. Comput. Commun. Eng. Innov. Technol. to Serve Humanit. ICCCE 2016*, pp. 47–52, 2016, doi: 10.1109/ICCCE.2016.23.

[5] H. Zhai, J. Zhang, Y. Zang, Q. Gao, and C. Liang, "An LTE Base-Station Magnetoelectric Dipole Antenna with Anti-Interference Characteristics and Its MIMO System Application," *IEEE Antennas Wirel. Propag. Lett.*, vol. 14, pp. 906–909, 2015, doi: 10.1109/LAWP.2014.2384519.

[6] S. Biswas, K. Singh, O. Taghizadeh, and T. Ratnarajah, "Coexistence of MIMO Radar and FD MIMO cellular systems with QoS considerations," *IEEE Trans. Wirel. Commun.*, vol. 17, no. 11, pp. 7281–7294, 2018, doi: 10.1109/TWC.2018.2866044.

[7] S. S. Jehangir and M. S. Sharawi, "A Miniaturized UWB Bi-Planar Yagi-Like Antenna," *2017 IEEE Antennas Propag. Soc. Int. Symp. Proc.*, vol. 2017-Janua, pp. 501–502, 2017, doi: 10.1109/APUSNCURSINRSM.2017.8072293.

[8] MC. A. Balanis, *Antenna Theory*. Hoboken, NJ: Wiley, 2016.

[9] Y. Li, C. Y. D. Sim, Y. Luo, and G. Yang, "12-Port 5G Massive MIMO Antenna Array in Sub-6GHz Mobile Handset for LTE Bands 42/43/46 Applications," *IEEE Access*, vol. 6, pp. 344–354, 2017, doi: 10.1109/ACCESS.2017.2763161.

[10] E. L. Bengtsson, F. Rusek, S. Malkowsky, F. Tufvesson, P. C. Karlsson, and O. Edfors, "A Simulation Framework for Multiple-Antenna Terminals in 5G Massive MIMO Systems," *IEEE Access*, vol. 5, pp. 26819–26831, 2017, doi: 10.1109/ACCESS.2017.2775210.

[11] Y. Zhang and Y. Li, "A Dimension-Reduction Multibeam Antenna Scheme

with Dual Integrated Butler Matrix Networks for Low-Complex Massive MIMO Systems," *IEEE Antennas Wirel. Propag. Lett.*, vol. 19, no. 11, pp. 1938–1942, 2020, doi: 10.1109/LAWP.2020.3001565.

[12] A. Elsakka *et al.*, "A mm-Wave Phased-Array Fed Torus Reflector Antenna With ±30° Scan Range for Massive-MIMO Base-Station Applications," *IEEE Trans. Antennas Propag.*, vol. 70, no. 5, pp. 3398–3410, 2022, doi: 10.1109/TAP.2021.3138450.

[13] J. N. Sahalos, "Design of Shared Aperture Radar Arrays with Low Sidelobe Level of the Two-Way Array Factor," *IEEE Trans. Antennas Propag.*, vol. 68, no. 7, pp. 5415–5420, 2020, doi: 10.1109/TAP.2020.2981735.

[14] B. Molaei and A. A. Kishk, "Non-Reciprocity View of the MIMO Antenna Arrays in Transmitting and Receiving Modes Using the Maximized Unique Receiving Pattern Theory Resulted by Angle-Wise Array Factor," *IEEE Access*, vol. 8, pp. 100280–100287, 2020, doi: 10.1109/ACCESS.2020.2998439.

[15] F. Yang, S. Yang, W. Long, Y. Chen, S. Qu, and J. Hu, "A novel 3-d-nufft method for the efficient calculation of the array factor of conformal arrays," *IEEE Trans. Antennas Propag.*, vol. 69, no. 10, pp. 7047–7052, 2021, doi: 10.1109/TAP.2021.3076204.

[16] W. M. Abdel-Wahab, Y. Wang, H. Al-Saedi, H. A. Mohamed, and S. Safavi-Naeini, "A Broadband RHCP/LHCP SIW-Integrated Patch Array Antenna for MM-Wave Applications," *2018 IEEE Antennas Propag. Soc. Int. Symp. Usn. Natl. Radio Sci. Meet. APSURSI 2018 - Proc.*, no. 1, pp. 1741–1742, 2018, doi: 10.1109/APUSNCURSINRSM.2018.8608532.

[17] L. N. A. Bamogho, J. J. Laurin, and M. A. Moharram, "Design of a Flexible Broadband RHCP/LHCP Polarizer Unit-Cell," *Proc. - ANTEM 2018 2018 18th Int. Symp. Antenna Technol. Appl. Electromagn.*, vol. 2018-Augus, pp. 1–2, 2018, doi: 10.1109/ANTEM.2018.8572935.

[18] S. C. Pavone, M. Casaletti, and M. Albani, "Automatic design of a RHCP linear slot array in substrate integrated waveguide," *IET Conf. Publ.*, vol. 2018, no. CP741, pp. 3–5, 2018, doi: 10.1049/cp.2018.1115.

[19] D. F. Mona, E. S. Sakomura, D. C. Nascimento, and D. B. Ferreira, "Mechanical tension effects on cylindrical truncated-corner microstrip antennas," *2019 IEEE Int. Symp. Antennas Propag. Usn. Radio Sci. Meet. APSURSI 2019 - Proc.*, pp. 1929–1930, 2019, doi: 10.1109/APUSNCURSINRSM.2019.8888522.

[20] R. Fikri, D. Kumiawan, and Iskandar, "Design Truncated Corner Rectangular Patch Antenna with Multiple Slot Used in High Altitude Platform Station," *Proceeding 2019 5th Int. Conf. Wirel. Telemat. ICWT 2019*, pp. 2–5, 2019, doi: 10.1109/ICWT47785.2019.8978262.

[21] F. Armin, A. Noer, Kamirul, and S. Prasetya, "Modification of 2.2 GHz S-Band Rectangular Patch Microstrip Antenna using Truncated Corner Method

for Satellite Applications," *2020 3rd Int. Semin. Res. Inf. Technol. Intell. Syst. ISRITI 2020*, pp. 284–288, 2020, doi: 10.1109/ISRITI51436.2020.9315475.

[22] H. M. El Misilmani, M. Al-Husseini, K. Y. Kabalan, and A. El-Hajj, "Compact circularly polarized multiband antennas for RFID applications," *Int. J. Antennas Propag.*, vol. 2014, 2014, doi: 10.1155/2014/783602.

[23] S. Salsabila, H. H. Ryanu, L. O. Nur, and U. Telkom, "Wearable Antenna Jenis Mikrostrip Dengan Struktur Electromagnetic Band Gap Untuk Komunikasi Wireless Pada Tubuh," no. November 2021, pp. 267–276.

[24] R. TAFAZOLLI, *Wiley 5G Ref: Security*. S.l.: WILEY-BLACKWELL, 2021.

[25] H. B. P. Ltd, "n78 (3500 MHz)," *HBR Radiofrequency Technologies*. https://halberdbastion.com/technology/cellular/5g-nr/5g-frequency-bands/n78-3500-mhz.

[26] X. Gao, O. Edfors, F. Rusek, and F. Tufvesson, "Massive MIMO Performance Evaluation Based on Measured Propagation Data," *IEEE Trans. Wirel. Commun.*, vol. 14, no. 7, pp. 3899–3911, 2015, doi: 10.1109/TWC.2015.2414413.

[27] T. Kebede, Y. Wondie, J. Steinbrunn, H. B. Kassa, and K. T. Kornegay, "Precoding and Beamforming Techniques in mmWave-Massive MIMO: Performance Assessment," *IEEE Access*, vol. 10, pp. 16365–16387, 2022, doi: 10.1109/ACCESS.2022.3149301.

[28] D. M. Dobkin, *RF Engineering for Wireless Networks: Hardware, Antennas, and Propagation*. Amsterdam: Elsevier/Newnes, 2005.

[29] C. A. Balanis, *Antenna Theory Analysis and Design*, 4th ed. 2016.

[30] F. Taher et al., "Design and analysis of circular polarized two-port MIMO antennas with various antenna element orientations," MDPI, https://www.mdpi.com/2072-666X/14/2/380 (accessed Aug. 22, 2023).

[31] N. Blaunstein and C. Christodoulou, "Radio Propagation and Adaptive Antennas for Wireless Communication Links," *Radio Propag. Adapt. Antennas Wirel. Commun. Links*, pp. 34–53, 2006, doi: 10.1002/0470069996.

[32] A. Askarian and K. Wu, "Miniaturized Dual-Band Slot Antenna with Self-Scalable Pattern for Array Applications," *2020 IEEE Int. Symp. Antennas Propag. North Am. Radio Sci. Meet. IEEECONF 2020 - Proc.*, pp. 1943–1944, 2020, doi: 10.1109/IEEECONF35879.2020.9329855.

[33] H. Q. Ngo, *Massive MIMO: Fundamentals and System Designs*, no. 1642. 2015.

APENDIX

Journal / Conference Status

No	Title	Journal/Proceeding	Index	Status
1	Massive MIMO Antenna Scalability of A Simple Rectangular Truncated Patch Antenna	ISAP 2023	International Conference	Accepted
2	Scalable Modular Massive MIMO Antenna of Rectangular Truncated Corner Patch Antenna and Circular Slotted X Patch Antenna for 5G Antenna Communication	INFOTEL	SINTA 2	Accepted
3	Scalability of MIMO Antennas: Assessing Gain and HPBW for Different Antenna Element Configurations	JURNAL REKAYASA ELEKTRIKA (JRE)	SINTA 2	IN REVIEW

- ISAP 2023

Dear Dr. Bambang Nugroho,

We are pleased to inform you that the submitted paper #1570916424 ('Massive Mimo Antenna Scalability of A Simple Rectangular Truncated Patch Antenna') has been ACCEPTED for presentation at the 2023 IEEE International Symposium On Antennas And Propagation (ISAP). You are hereby invited to participate and present the paper at ISAP 2023 that will be held from 30th October to 2nd November 2023 in Kuala Lumpur, Malaysia. This notification email serves as our formal acceptance of your paper as well as an invitation to present your work at 2023 IEEE International Symposium On Antennas And Propagation (ISAP).

The decision resulted from a peer-review process by the ISAP 2023 Technical Program Committee that comprises more than 500 reviewers worldwide. You are required to read reviewer comments and make necessary corrections where appropriate, as suggested for the Final Manuscript submission. Your paper may still be rejected if this is not respected. Reviewers' comments are included at the end of this notification email or can be found at https://edas.info/showPaper.php?m=1570916424.

At least one of the authors is required to PRE-REGISTER, pay the REGISTRATION FEE, designate a PRESENTER and complete the online IEEE Copyright form in EDAS, before uploading the FINAL MANUSCRIPT. The deadline for the Final Manuscript submission is SEPTEMBER 15, 2023. Information about the registration procedures, fees, and instructions for final manuscript preparation and submission is available at the ISAP 2023 website https://isap2023.apmttemc.org/.

We would like to take this opportunity to thank you for choosing ISAP 2023 to present your research results and look forward to see you during the conference.

Best Regards,

Mohamad Kamal A Rahim - General Chair

- INFOTEL

[INFOTEL] Editor Decision

2023-08-11 03:42 AM

Salwa Salsabila:

Letter of Acceptance (LoA)

==========

On behalf of the Editor, we are pleased to inform that your submission to JURNAL INFOTEL, "Scalable Modular Massive MIMO Antenna of Rectangular Truncated Corner Patch Antenna and Circular Slotted X Patch Antenna for 5G Antenna Communication" **is Accepted**

- JRE

Home > User > Author > **Active Submissions**

Active Submissions

ACTIVE ARCHIVE

ID	MM-DD SUBMIT	SEC	AUTHORS	TITLE	STATUS
33177	07-17	TELE	Nur	SCALABILITY OF MIMO ANTENNAS: ASSESSING GAIN AND HPBW FOR...	IN REVIEW

1. Data cst rec
    a. Rl 1 elemen

Frequency / GHz	S2,2 (13)/abs,dB	Frequency / GHz	S2,2 (13)/abs,dB	Frequency / GHz	S2,2 (13)/abs,dB	Frequency / GHz	S2,2 (13)/abs,dB
0	-0.005753249	2.49	-0.43254716	4.9899998	-0.83152112	7.4899998	-4.7645497
0.01	-0.005891358	2.5	-0.44613047	5	-0.83480058	7.5	-4.7836331
0.02	-0.006308338	2.51	-0.46008351	5.0100002	-0.83929997	7.5100002	-4.8075169
0.029999999	-0.007001358	2.52	-0.47428093	5.02	-0.8449002	7.52	-4.8353736
0.039999999	-0.007971295	2.53	-0.48859539	5.0300002	-0.85147457	7.5300002	-4.8662929
0.050000001	-0.009216729	2.54	-0.50290301	5.04	-0.85889619	7.54	-4.8992843
0.059999999	-0.010736254	2.55	-0.51709705	5.0500002	-0.8670455	7.5500002	-4.9332905
0.07	-0.012527917	2.5599999	-0.53108293	5.0599999	-0.87581353	7.5599999	-4.9671916
0.079999998	-0.014588725	2.5699999	-0.54479648	5.0700002	-0.88510438	7.5700002	-4.9998272
0.090000004	-0.016915638	2.5799999	-0.55820107	5.0799999	-0.89484394	7.5799999	-5.0300169
0.1	-0.019505056	2.5899999	-0.57129676	5.0900002	-0.90497863	7.5900002	-5.056582
0.11	-0.02235062	2.5999999	-0.58412149	5.0999999	-0.91547473	7.5999999	-5.0783768
0.12	-0.025446389	2.6099999	-0.59675755	5.1100001	-0.92632424	7.6100001	-5.0943228
0.13	-0.02878562	2.6199999	-0.60932647	5.1199999	-0.9375394	7.6199999	-5.1034389
0.14	-0.032356563	2.6300001	-0.62199522	5.1300001	-0.94915014	7.6300001	-5.1048765
0.15000001	-0.036151457	2.6400001	-0.63496735	5.1399999	-0.96120559	7.6399999	-5.0979466
0.16	-0.040157049	2.6500001	-0.648483	5.1500001	-0.97376714	7.6500001	-5.0821445
0.17	-0.044359422	2.6600001	-0.66281441	5.1599998	-0.98690567	7.6599998	-5.0571684
0.18000001	-0.048743784	2.6700001	-0.67825698	5.1700001	-1.0006974	7.6700001	-5.0229274
0.19	-0.053292491	2.6800001	-0.69512226	5.1799998	-1.0152196	7.6799998	-4.9795396
0.2	-0.057988911	2.6900001	-0.7137312	5.1900001	-1.0305457	7.6900001	-4.9273212
0.20999999	-0.062812135	2.7	-0.73440541	5.1999998	-1.0467459	7.6999998	-4.8667683
0.22	-0.067740916	2.71	-0.75745471	5.21	-1.063877	7.71	-4.7985338
0.23	-0.072754538	2.72	-0.78317252	5.2199998	-1.081987	7.7199998	-4.7233892
0.23999999	-0.077829456	2.73	-0.81182396	5.23	-1.1011084	7.73	-4.6421991
0.25	-0.082940946	2.74	-0.84363979	5.2399998	-1.1212608	7.7399998	-4.555879
0.25999999	-0.088066869	2.75	-0.87880302	5.25	-1.1424489	7.75	-4.465371
0.27000001	-0.093183333	2.76	-0.91745077	5.2600002	-1.1646629	7.7600002	-4.3716076
0.28	-0.098265933	2.77	-0.95965943	5.27	-1.1878837	7.77	-4.2754855
0.28999999	-0.10329119	2.78	-1.0054449	5.2800002	-1.2120799	7.7800002	-4.1778534
0.30000001	-0.10823784	2.79	-1.0547548	5.29	-1.2372126	7.79	-4.0794839
0.31	-0.11308471	2.8	-1.1074671	5.3000002	-1.2632423	7.8000002	-3.981074
0.31999999	-0.11781222	2.8099999	-1.1633904	5.3099999	-1.2901274	7.8099999	-3.88323
0.33000001	-0.12240303	2.8199999	-1.2222608	5.3200002	-1.3178284	7.8200002	-3.7864723
0.34	-0.12684154	2.8299999	-1.2837481	5.3299999	-1.3463153	7.8299999	-3.6912305
0.34999999	-0.13111363	2.8399999	-1.3474556	5.3400002	-1.3755637	7.8400002	-3.5978502
0.36000001	-0.13521014	2.8499999	-1.4129295	5.3499999	-1.4055661	7.8499999	-3.5065969
0.37	-0.1391217	2.8599999	-1.4796665	5.3600001	-1.4363271	7.8600001	-3.417667
0.38	-0.14284253	2.8699999	-1.5471231	5.3699999	-1.4678692	7.8699999	-3.33119
0.38999999	-0.14637115	2.8800001	-1.6147325	5.3800001	-1.5002291	7.8800001	-3.2472452
0.40000001	-0.14970541	2.8900001	-1.6819141	5.3899999	-1.5334643	7.8899999	-3.1658654
0.41	-0.15284989	2.9000001	-1.748095	5.4000001	-1.5676449	7.9000001	-3.0870473
0.41999999	-0.15580716	2.9100001	-1.8127285	5.4099998	-1.6028571	7.9099998	-3.0107614
0.43000001	-0.15858488	2.9200001	-1.875309	5.4200001	-1.6392001	7.9200001	-2.9369594
0.44	-0.16119095	2.9300001	-1.935392	5.4299998	-1.6767798	7.9299998	-2.8655819
0.44999999	-0.16363718	2.9400001	-1.9926157	5.4400001	-1.7157121	7.9400001	-2.7965627
0.46000001	-0.16593275	2.95	-2.0467139	5.4499998	-1.7561113	7.9499998	-2.7298361
0.47	-0.16809105	2.96	-2.0975265	5.46	-1.7980951	7.96	-2.6653425
0.47999999	-0.17012286	2.97	-2.1450151	5.4699998	-1.8417725	7.9699998	-2.6030252
0.49000001	-0.17204385	2.98	-2.1892636	5.48	-1.8872456	7.98	-2.5428384
0.5	-0.17386272	2.99	-2.2304847	5.4899998	-1.9346062	7.9899998	-2.4847433
0.50999999	-0.17559377	3	-2.2690091	5.5	-1.9839301	8	-2.4287106
0.51999998	-0.17724483	3.01	-2.305289	5.5100002	-2.0352785	8.0100002	-2.3747185
0.52999997	-0.1788248	3.02	-2.3398801	5.52	-2.0886927	8.0200005	-2.322748
0.54000002	-0.18034271	3.03	-2.3734294	5.5300002	-2.1441961	8.0299997	-2.2727866
0.55000001	-0.18180156	3.04	-2.4066633	5.54	-2.2017922	8.04	-2.2248193
0.56	-0.18320612	3.05	-2.4403696	5.5500002	-2.2614667	8.0500002	-2.1788277
0.56999999	-0.18455593	3.0599999	-2.4753819	5.5599999	-2.3231855	8.0600004	-2.134791
0.57999998	-0.18585079	3.0699999	-2.5125645	5.5700002	-2.3868969	8.0699997	-2.0926784
0.58999997	-0.18708688	3.0799999	-2.5527982	5.5799999	-2.452537	8.0799999	-2.0524506
0.60000002	-0.18826092	3.0899999	-2.5969709	5.5900002	-2.5200272	8.0900002	-2.0140566
0.61000001	-0.18936488	3.0999999	-2.6459645	5.5999999	-2.5892782	8.1000004	-1.9774328

0.62	-0.19039166	3.1099999	-2.7006488	5.6100001	-2.6601908	8.1099997	-1.9425042
0.63	-0.19133133	3.1199999	-2.7618792	5.6199999	-2.7326615	8.1199999	-1.9091829
0.63999999	-0.19217551	3.1300001	-2.8304906	5.6300001	-2.80658	8.1300001	-1.877373
0.64999998	-0.19291468	3.1400001	-2.9073023	5.6399999	-2.8818323	8.1400003	-1.8469676
0.66000003	-0.19353851	3.1500001	-2.9931127	5.6500001	-2.9583	8.1499996	-1.8178539
0.67000002	-0.19403928	3.1600001	-3.0887137	5.6599998	-3.0358632	8.1599998	-1.7899164
0.68000001	-0.19440964	3.1700001	-3.194886	5.6700001	-3.1143929	8.1700001	-1.7630392
0.69	-0.19464169	3.1800001	-3.3124155	5.6799998	-3.1937566	8.1800003	-1.7371092
0.69999999	-0.19473329	3.1900001	-3.4420991	5.6900001	-3.2738058	8.1899996	-1.712021
0.70999998	-0.19468142	3.2	-3.5847519	5.6999998	-3.3543841	8.1999998	-1.6876777
0.72000003	-0.19448682	3.21	-3.7412278	5.71	-3.4353107	8.21	-1.6639955
0.73000002	-0.19415208	3.22	-3.9124286	5.7199998	-3.5163839	8.2200003	-1.6409057
0.74000001	-0.19368228	3.23	-4.0993192	5.73	-3.597371	8.2299995	-1.6183559
0.75	-0.19308637	3.24	-4.3029499	5.7399998	-3.678008	8.2399998	-1.5963119
0.75999999	-0.19237423	3.25	-4.5244712	5.75	-3.7579884	8.25	-1.5747563
0.76999998	-0.19155885	3.26	-4.765164	5.7600002	-3.8369636	8.2600002	-1.5536909
0.77999997	-0.19065436	3.27	-5.0264654	5.77	-3.9145394	8.2700005	-1.5331324
0.79000002	-0.18967702	3.28	-5.3100002	5.7800002	-3.9902763	8.2799997	-1.5131119
0.80000001	-0.18864351	3.29	-5.6176201	5.79	-4.0636863	8.29	-1.4936715
0.81	-0.187572	3.3	-5.9514592	5.8000002	-4.1342431	8.3000002	-1.4748649
0.81999999	-0.18648024	3.3099999	-6.3139845	5.8099999	-4.20138	8.3100004	-1.4567445
0.82999998	-0.18538469	3.3199999	-6.7080821	5.8200002	-4.2645065	8.3199997	-1.4393693
0.83999997	-0.18430211	3.3299999	-7.13715	5.8299999	-4.3230169	8.3299999	-1.4227928
0.85000002	-0.18324638	3.3399999	-7.6052301	5.8400002	-4.3763065	8.3400002	-1.407065
0.86000001	-0.18223056	3.3499999	-8.1171802	5.8499999	-4.4237854	8.3500004	-1.3922235
0.87	-0.18126403	3.3599999	-8.6789066	5.8600001	-4.4649023	8.3599997	-1.3782976
0.88	-0.18035409	3.3699999	-9.2976936	5.8699999	-4.4991597	8.3699999	-1.3653014
0.88999999	-0.17950537	3.3800001	-9.982663	5.8800001	-4.5261379	8.3800001	-1.3532334
0.89999998	-0.17871766	3.3900001	-10.745451	5.8899999	-4.5455055	8.3900003	-1.3420769
0.91000003	-0.17798963	3.4000001	-11.60122	5.9000001	-4.5570423	8.3999996	-1.3318006
0.92000002	-0.17731527	3.4100001	-12.570219	5.9099998	-4.5606441	8.4099998	-1.3223574
0.93000001	-0.17668679	3.4200001	-13.680318	5.9200001	-4.5563352	8.4200001	-1.3136882
0.94	-0.17609224	3.4300001	-14.971214	5.9299998	-4.5442621	8.4300003	-1.3057255
0.94999999	-0.17551828	3.4400001	-16.501797	5.9400001	-4.5246995	8.4399996	-1.2983926
0.95999998	-0.17495138	3.45	-18.363313	5.9499998	-4.4980315	8.4499998	-1.2916118
0.97000003	-0.17437481	3.46	-20.701578	5.96	-4.4647442	8.46	-1.2853049
0.98000002	-0.17377187	3.47	-23.730967	5.9699998	-4.4254065	8.4700003	-1.2793977
0.99000001	-0.17312763	3.48	-27.431359	5.98	-4.3806509	8.4799995	-1.2738271
1	-0.17242557	3.49	-29.021596	5.9899998	-4.3311531	8.4899998	-1.2685377
1.01	-0.1716526	3.5	-25.872445	6	-4.2776082	8.5	-1.2634922
1.02	-0.17079764	3.51	-22.363305	6.0100002	-4.2207153	8.5100002	-1.2586713
1.03	-0.16985093	3.52	-19.634725	6.02	-4.1611555	8.5200005	-1.2540733
1.04	-0.16880757	3.53	-17.504148	6.0300002	-4.0995775	8.5299997	-1.2497192
1.05	-0.16766513	3.54	-15.782961	6.04	-4.0365836	8.54	-1.2456482
1.0599999	-0.1664268	3.55	-14.351188	6.0500002	-3.9727212	8.5500002	-1.2419204
1.0700001	-0.16509589	3.5599999	-13.133145	6.0599999	-3.9084757	8.5600004	-1.2386127
1.08	-0.16368194	3.5699999	-12.079142	6.0700002	-3.8442652	8.5699997	-1.235819
1.09	-0.16219849	3.5799999	-11.155111	6.0799999	-3.7804409	8.5799999	-1.2336436
1.1	-0.16066112	3.5899999	-10.336779	6.0900002	-3.7172875	8.5900002	-1.2321994
1.11	-0.15908743	3.5999999	-9.6062643	6.0999999	-3.6550245	8.6000004	-1.2316037
1.12	-0.15749714	3.6099999	-8.9500125	6.1100001	-3.5938162	8.6099997	-1.231974
1.13	-0.15591252	3.6199999	-8.3574874	6.1199999	-3.5337732	8.6199999	-1.2334256
1.14	-0.15435396	3.6300001	-7.8203141	6.1300001	-3.4749604	8.6300001	-1.2360628
1.15	-0.15284474	3.6400001	-7.331706	6.1399999	-3.4174087	8.6400003	-1.2399825
1.16	-0.15140423	3.6500001	-6.8860607	6.1500001	-3.3611176	8.6499996	-1.2452643
1.17	-0.1500499	3.6600001	-6.4786796	6.1599998	-3.3060651	8.6599998	-1.2519755
1.1799999	-0.14879928	3.6700001	-6.1055607	6.1700001	-3.252219	8.6700001	-1.2601623
1.1900001	-0.14766326	3.6800001	-5.7632475	6.1799998	-3.1995357	8.6800003	-1.2698593
1.2	-0.14665044	3.6900001	-5.4487169	6.1900001	-3.1479782	8.6899996	-1.2810794
1.21	-0.14576556	3.7	-5.1592979	6.1999998	-3.0975076	8.6999998	-1.2938253
1.22	-0.14500777	3.71	-4.8926029	6.21	-3.0481	8.71	-1.3080836
1.23	-0.14437205	3.72	-4.646482	6.2199998	-2.9997387	8.7200003	-1.3238335
1.24	-0.14384987	3.73	-4.4189865	6.23	-2.9524227	8.7299995	-1.3410513

1.25	-0.14342744	3.74	-4.2083419	6.2399998	-2.9061646	8.7399998	-1.3597094
1.26	-0.14308793	3.75	-4.0129254	6.25	-2.8609907	8.75	-1.3797864
1.27	-0.14281068	3.76	-3.8312504	6.2600002	-2.8169352	8.7600002	-1.4012698
1.28	-0.14257349	3.77	-3.66196	6.27	-2.7740452	8.7700005	-1.4241596
1.29	-0.14235327	3.78	-3.5038144	6.2800002	-2.7323695	8.7799997	-1.4484746
1.3	-0.14212523	3.79	-3.3556897	6.29	-2.6919616	8.79	-1.4742529
1.3099999	-0.14186652	3.8	-3.2165685	6.3000002	-2.6528705	8.8000002	-1.5015584
1.3200001	-0.14155385	3.8099999	-3.0855442	6.3099999	-2.6151419	8.8100004	-1.5304788
1.33	-0.14116917	3.8199999	-2.9618114	6.3200002	-2.5788112	8.8199997	-1.5611284
1.34	-0.14069569	3.8299999	-2.8446667	6.3299999	-2.5439034	8.8299999	-1.5936434
1.35	-0.14012124	3.8399999	-2.733502	6.3400002	-2.5104289	8.8400002	-1.628185
1.36	-0.13943856	3.8499999	-2.6278055	6.3499999	-2.4783823	8.8500004	-1.6649308
1.37	-0.13864507	3.8599999	-2.527147	6.3600001	-2.4477425	8.8599997	-1.7040724
1.38	-0.13774542	3.8699999	-2.4311813	6.3699999	-2.418474	8.8699999	-1.7458083
1.39	-0.13674734	3.8800001	-2.3396321	6.3800001	-2.390526	8.8800001	-1.7903363
1.4	-0.13566468	3.8900001	-2.2522858	6.3899999	-2.3638347	8.8900003	-1.8378442
1.41	-0.13451584	3.9000001	-2.1689838	6.4000001	-2.3383262	8.8999996	-1.8885053
1.42	-0.13332425	3.9100001	-2.0896108	6.4099998	-2.3139226	8.9099998	-1.9424629
1.4299999	-0.13211547	3.9200001	-2.0140828	6.4200001	-2.2905418	8.9200001	-1.9998263
1.4400001	-0.13091802	3.9300001	-1.9423397	6.4299998	-2.2681034	8.9300003	-2.0606562
1.45	-0.12976087	3.9400001	-1.8743349	6.4400001	-2.2465362	8.9399996	-2.1249583
1.46	-0.12867327	3.95	-1.8100226	6.4499998	-2.225776	8.9499998	-2.1926732
1.47	-0.12768455	3.96	-1.7493548	6.46	-2.2057761	8.96	-2.2636683
1.48	-0.12682005	3.97	-1.6922719	6.4699998	-2.1865071	8.9700003	-2.3377312
1.49	-0.12610202	3.98	-1.6386946	6.48	-2.1679596	8.9799995	-2.4145602
1.5	-0.12554924	3.99	-1.588524	6.4899998	-2.1501496	8.9899998	-2.4937645
1.51	-0.12517431	4	-1.5416341	6.5	-2.1331152	9	-2.5748603
1.52	-0.12498402	4.0100002	-1.4978728	6.5100002	-2.1169204	9.0100002	-2.6572693
1.53	-0.12497895	4.02	-1.4570651	6.52	-2.1016511	9.0200005	-2.7403234
1.54	-0.1251542	4.0300002	-1.4190082	6.5300002	-2.0874169	9.0299997	-2.8232719
1.55	-0.12549655	4.04	-1.383479	6.54	-2.0743438	9.04	-2.9052903
1.5599999	-0.1259894	4.0500002	-1.3502378	6.5500002	-2.0625753	9.0500002	-2.9854951
1.5700001	-0.12660879	4.0599999	-1.3190308	6.5599999	-2.0522653	9.0600004	-3.0629646
1.58	-0.12732683	4.0700002	-1.2896014	6.5700002	-2.0435766	9.0699997	-3.1367539
1.59	-0.12811288	4.0799999	-1.2616926	6.5799999	-2.0366719	9.0799999	-3.2059306
1.6	-0.12893352	4.0900002	-1.2350552	6.5900002	-2.0317139	9.0900002	-3.2695933
1.61	-0.12975574	4.0999999	-1.2094561	6.5999999	-2.0288581	9.1000004	-3.326905
1.62	-0.13054453	4.1100001	-1.1846816	6.6100001	-2.0282514	9.1099997	-3.37712
1.63	-0.13127041	4.1199999	-1.1605462	6.6199999	-2.0300266	9.1199999	-3.4196142
1.64	-0.13190543	4.1300001	-1.1368975	6.6300001	-2.0343001	9.1300001	-3.4539023
1.65	-0.13242832	4.1399999	-1.1136177	6.6399999	-2.0411721	9.1400003	-3.4796574
1.66	-0.13282067	4.1500001	-1.0906292	6.6500001	-2.0507245	9.1499996	-3.4967234
1.67	-0.13307265	4.1599998	-1.0678908	6.6599998	-2.0630227	9.1599998	-3.5051145
1.6799999	-0.13318283	4.1700001	-1.0454018	6.6700001	-2.0781131	9.1700001	-3.5050116
1.6900001	-0.13315541	4.1799998	-1.0231957	6.6799998	-2.0960298	9.1800003	-3.4967499
1.7	-0.13300522	4.1900001	-1.0013367	6.6900001	-2.1167961	9.1899996	-3.4808013
1.71	-0.13275054	4.1999998	-0.97991939	6.6999998	-2.1404291	9.1999998	-3.4577509
1.72	-0.13242065	4.21	-0.95905462	6.71	-2.1669413	9.21	-3.4282691
1.73	-0.13204782	4.2199998	-0.93886944	6.7199998	-2.1963512	9.2200003	-3.393084
1.74	-0.13166925	4.23	-0.91949514	6.73	-2.2286833	9.2299995	-3.352956
1.75	-0.13132652	4.2399998	-0.9010649	6.7399998	-2.2639789	9.2399998	-3.3086521
1.76	-0.13106243	4.25	-0.88369938	6.75	-2.3022972	9.25	-3.2609204
1.77	-0.13091714	4.2600002	-0.86750625	6.7600002	-2.3437232	9.2600002	-3.2104788
1.78	-0.13093346	4.27	-0.85257333	6.77	-2.3883713	9.2700005	-3.1579923
1.79	-0.13114543	4.2800002	-0.83896092	6.7800002	-2.4363892	9.2799997	-3.1040666
1.8	-0.13158526	4.29	-0.82670056	6.79	-2.4879596	9.29	-3.0492413
1.8099999	-0.13227768	4.3000002	-0.81579038	6.8000002	-2.5433045	9.3000002	-2.9939882
1.8200001	-0.13323975	4.3099999	-0.8061992	6.8099999	-2.6026812	9.3100004	-2.9387091
1.83	-0.13447878	4.3200002	-0.79786057	6.8200002	-2.6663887	9.3199997	-2.8837407
1.84	-0.13599521	4.3299999	-0.79067985	6.8299999	-2.7347538	9.3299999	-2.8293578
1.85	-0.13777631	4.3400002	-0.78453463	6.8400002	-2.8081386	9.3400002	-2.7757825
1.86	-0.1398052	4.3499999	-0.77928134	6.8499999	-2.8869284	9.3500004	-2.723187
1.87	-0.14205202	4.3600001	-0.77475939	6.8600001	-2.9715289	9.3599997	-2.6717028

1.88	-0.14448253
1.89	-0.14705572
1.9	-0.14972591
1.91	-0.15244451
1.92	-0.15516331
1.9299999	-0.15783492
1.9400001	-0.1604171
1.95	-0.16287237
1.96	-0.1651716
1.97	-0.16729486
1.98	-0.16923216
1.99	-0.1709858
2	-0.17256895
2.01	-0.1740057
2.02	-0.1753318
2.03	-0.17659263
2.04	-0.17784071
2.05	-0.17913454
2.0599999	-0.18053775
2.0699999	-0.18211268
2.0799999	-0.18392294
2.0899999	-0.18602412
2.0999999	-0.18846994
2.1099999	-0.19130075
2.1199999	-0.19454995
2.1300001	-0.19823408
2.1400001	-0.20236025
2.1500001	-0.20691844
2.1600001	-0.21188547
2.1700001	-0.21722532
2.1800001	-0.2228879
2.1900001	-0.22881533
2.2	-0.23493832
2.21	-0.24118514
2.22	-0.24747983
2.23	-0.25374834
2.24	-0.25992065
2.25	-0.26593585
2.26	-0.2717415
2.27	-0.27730215
2.28	-0.28259502
2.29	-0.28761844
2.3	-0.29238681
2.3099999	-0.29693545
2.3199999	-0.30131718
2.3299999	-0.30560115
2.3399999	-0.30987298
2.3499999	-0.31422722
2.3599999	-0.31876895
2.3699999	-0.32360853
2.3800001	-0.32885144
2.3900001	-0.33460435
2.4000001	-0.34096178
2.4100001	-0.34800816
2.4200001	-0.3558077
2.4300001	-0.36440827
2.4400001	-0.37383442
2.45	-0.38408694
2.46	-0.39514335
2.47	-0.40695556
2.48	-0.41945342

4.3699999	-0.77080088
4.3800001	-0.76723275
4.3899999	-0.76388881
4.4000001	-0.76061841
4.4099998	-0.7572871
4.4200001	-0.75379004
4.4299998	-0.75005485
4.4400001	-0.74604649
4.4499998	-0.74176635
4.46	-0.73726034
4.4699998	-0.73261039
4.48	-0.72793678
4.4899998	-0.72339183
4.5	-0.71915554
4.5100002	-0.71542493
4.52	-0.71241091
4.5300002	-0.71032657
4.54	-0.70937842
4.5500002	-0.7097579
4.5599999	-0.71163338
4.5700002	-0.71514191
4.5799999	-0.72038204
4.5900002	-0.72740897
4.5999999	-0.73622905
4.6100001	-0.74679712
4.6199999	-0.75901504
4.6300001	-0.77273461
4.6399999	-0.7877537
4.6500001	-0.80382658
4.6599998	-0.8206673
4.6700001	-0.83795346
4.6799998	-0.85534264
4.6900001	-0.87247308
4.6999998	-0.88898276
4.71	-0.90451669
4.7199998	-0.91874008
4.73	-0.93134895
4.7399998	-0.9420805
4.75	-0.95072459
4.7600002	-0.95712757
4.77	-0.96120275
4.7800002	-0.96292577
4.79	-0.96234253
4.8000002	-0.95956064
4.8099999	-0.95474924
4.8200002	-0.94812914
4.8299999	-0.93996311
4.8400002	-0.93055054
4.8499999	-0.9202112
4.8600001	-0.90927704
4.8699999	-0.8980829
4.8800001	-0.88695225
4.8899999	-0.87618948
4.9000001	-0.86607557
4.9099998	-0.85685557
4.9200001	-0.8487368
4.9299998	-0.84188789
4.9400001	-0.83643238
4.9499998	-0.83245274
4.96	-0.82998674
4.9699998	-0.82903816
4.98	-0.8295704

6.8699999	-3.062353
6.8800001	-3.1598209
6.8899999	-3.2643406
6.9000001	-3.376303
6.9099998	-3.4960667
6.9200001	-3.6239475
6.9299998	-3.7601973
6.9400001	-3.9049965
6.9499998	-4.0584297
6.96	-4.2204665
6.9699998	-4.3909441
6.98	-4.5695391
6.9899998	-4.7557407
7	-4.9488297
7.0100002	-5.1478437
7.02	-5.3515497
7.0300002	-5.5584215
7.04	-5.7666174
7.0500002	-5.9739699
7.0599999	-6.1779855
7.0700002	-6.3758752
7.0799999	-6.5645986
7.0900002	-6.7409476
7.0999999	-6.9016596
7.1100001	-7.0435638
7.1199999	-7.1637509
7.1300001	-7.2597516
7.1399999	-7.3297061
7.1500001	-7.3724982
7.1599998	-7.3878401
7.1700001	-7.3762886
7.1799998	-7.3391975
7.1900001	-7.2786037
7.1999998	-7.1970774
7.21	-7.0975456
7.2199998	-6.983121
7.23	-6.8569435
7.2399998	-6.7220571
7.25	-6.5813107
7.2600002	-6.4373012
7.27	-6.2923356
7.2800002	-6.1484259
7.29	-6.0072904
7.3000002	-5.8703742
7.3099999	-5.7388724
7.3200002	-5.6137591
7.3299999	-5.4958113
7.3400002	-5.3856408
7.3499999	-5.2837106
7.3600001	-5.1903646
7.3699999	-5.1058393
7.3800001	-5.0302821
7.3899999	-4.9637604
7.4000001	-4.9062722
7.4099998	-4.857752
7.4200001	-4.8180723
7.4299998	-4.7870479
7.4400001	-4.7644345
7.4499998	-4.7499275
7.46	-4.7431578
7.4699998	-4.7436895
7.48	-4.7510154

9.3699999	-2.6214325
9.3800001	-2.5724506
9.3900003	-2.5248117
9.3999996	-2.4785595
9.4099998	-2.433729
9.4200001	-2.390349
9.4300003	-2.3484444
9.4399996	-2.308043
9.4499998	-2.2691663
9.46	-2.2318374
9.4700003	-2.1960741
9.4799995	-2.1618905
9.4899998	-2.1292919
9.5	-2.0982736
9.5100002	-2.068821
9.5200005	-2.0409034
9.5299997	-2.0144743
9.54	-1.9894728
9.5500002	-1.9658198
9.5600004	-1.9434219
9.5699997	-1.9221714
9.5799999	-1.9019485
9.5900002	-1.882624
9.6000004	-1.8640648
9.6099997	-1.8461367
9.6199999	-1.8287089
9.6300001	-1.8116572
9.6400003	-1.7948726
9.6499996	-1.778261
9.6599998	-1.7617472
9.6700001	-1.7452804
9.6800003	-1.7288326
9.6899996	-1.7124019
9.6999998	-1.6960085
9.71	-1.6796989
9.7200003	-1.6635373
9.7299995	-1.6476059
9.7399998	-1.6320006
9.75	-1.6168231
9.7600002	-1.6021789
9.7700005	-1.5881713
9.7799997	-1.5748963
9.79	-1.5624387
9.8000002	-1.5508639
9.8100004	-1.5402222
9.8199997	-1.5305381
9.8299999	-1.5218137
9.8400002	-1.5140292
9.8500004	-1.5071388
9.8599997	-1.5010782
9.8699999	-1.4957622
9.8800001	-1.4910933
9.8900003	-1.4869606
9.8999996	-1.4832519
9.9099998	-1.4798511
9.9200001	-1.4766483
9.9300003	-1.4735461
9.9399996	-1.4704579
9.9499998	-1.4673189
9.96	-1.4640861
9.9700003	-1.4607392
9.9799995	-1.4572826
9.9899998	-1.4537464

			10	-1.4501807

b. Rl 4 elemen

c. Rl 16 elemen

d. Hpbw 1 elemen

Theta [deg.]	Phi [deg.]	Abs(Dir.)[dBi]	Abs(Theta)[dBi]	Phase(Theta)[deg.]	Abs(Phi)[dBi]	Phase(Phi)[deg.]	Ax.Ratio[dB]
0	90	6.04E+00	-8.85E-01	23.67	5.06E+00	346.401	1.17E+01
1	90	6.04E+00	-9.03E-01	23.518	5.06E+00	346.407	1.18E+01
2	90	6.03E+00	-9.23E-01	23.364	5.05E+00	346.41	1.18E+01
3	90	6.02E+00	-9.46E-01	23.209	5.05E+00	346.41	1.18E+01
4	90	6.01E+00	-9.72E-01	23.052	5.04E+00	346.408	1.19E+01
5	90	5.99E+00	-1.00E+00	22.894	5.02E+00	346.402	1.19E+01
6	90	5.97E+00	-1.03E+00	22.735	5.01E+00	346.395	1.20E+01
7	90	5.95E+00	-1.07E+00	22.574	4.99E+00	346.384	1.20E+01
8	90	5.93E+00	-1.11E+00	22.412	4.97E+00	346.37	1.21E+01
9	90	5.90E+00	-1.15E+00	22.248	4.95E+00	346.354	1.21E+01
10	90	5.87E+00	-1.19E+00	22.083	4.92E+00	346.335	1.22E+01
11	90	5.84E+00	-1.23E+00	21.917	4.89E+00	346.313	1.22E+01
12	90	5.80E+00	-1.28E+00	21.749	4.86E+00	346.288	1.23E+01
13	90	5.77E+00	-1.34E+00	21.58	4.82E+00	346.26	1.23E+01
14	90	5.72E+00	-1.39E+00	21.41	4.79E+00	346.23	1.24E+01
15	90	5.68E+00	-1.45E+00	21.239	4.75E+00	346.196	1.24E+01
16	90	5.63E+00	-1.51E+00	21.066	4.70E+00	346.159	1.24E+01
17	90	5.58E+00	-1.57E+00	20.892	4.66E+00	346.12	1.25E+01
18	90	5.53E+00	-1.64E+00	20.717	4.61E+00	346.077	1.25E+01
19	90	5.48E+00	-1.70E+00	20.54	4.56E+00	346.031	1.26E+01
20	90	5.42E+00	-1.78E+00	20.363	4.50E+00	345.982	1.26E+01
21	90	5.36E+00	-1.85E+00	20.183	4.45E+00	345.93	1.27E+01
22	90	5.30E+00	-1.93E+00	20.003	4.39E+00	345.874	1.27E+01
23	90	5.23E+00	-2.01E+00	19.822	4.32E+00	345.815	1.28E+01
24	90	5.16E+00	-2.09E+00	19.639	4.26E+00	345.753	1.28E+01
25	90	5.09E+00	-2.18E+00	19.455	4.19E+00	345.688	1.28E+01
26	90	5.02E+00	-2.26E+00	19.269	4.12E+00	345.619	1.29E+01
27	90	4.95E+00	-2.36E+00	19.083	4.05E+00	345.546	1.29E+01
28	90	4.87E+00	-2.45E+00	18.895	3.98E+00	345.47	1.30E+01
29	90	4.79E+00	-2.55E+00	18.706	3.90E+00	345.39	1.30E+01
30	90	4.70E+00	-2.64E+00	18.515	3.82E+00	345.307	1.30E+01
31	90	4.62E+00	-2.75E+00	18.324	3.74E+00	345.22	1.31E+01
32	90	4.53E+00	-2.85E+00	18.131	3.65E+00	345.129	1.31E+01
33	90	4.44E+00	-2.96E+00	17.937	3.57E+00	345.034	1.32E+01
34	90	4.35E+00	-3.07E+00	17.741	3.48E+00	344.935	1.32E+01
35	90	4.25E+00	-3.18E+00	17.544	3.39E+00	344.833	1.32E+01
36	90	4.15E+00	-3.30E+00	17.346	3.29E+00	344.726	1.33E+01
37	90	4.05E+00	-3.41E+00	17.146	3.20E+00	344.615	1.33E+01
38	90	3.95E+00	-3.54E+00	16.945	3.10E+00	344.5	1.34E+01
39	90	3.85E+00	-3.66E+00	16.743	3.00E+00	344.381	1.34E+01
40	90	3.74E+00	-3.79E+00	16.54	2.90E+00	344.258	1.34E+01
41	90	3.63E+00	-3.91E+00	16.334	2.79E+00	344.13	1.35E+01
42	90	3.52E+00	-4.04E+00	16.128	2.69E+00	343.998	1.35E+01
43	90	3.41E+00	-4.18E+00	15.92	2.58E+00	343.862	1.36E+01
44	90	3.30E+00	-4.31E+00	15.711	2.47E+00	343.721	1.36E+01
45	90	3.18E+00	-4.45E+00	15.5	2.36E+00	343.575	1.36E+01
46	90	3.06E+00	-4.60E+00	15.287	2.24E+00	343.425	1.37E+01
47	90	2.94E+00	-4.74E+00	15.074	2.13E+00	343.271	1.37E+01
48	90	2.82E+00	-4.89E+00	14.858	2.01E+00	343.111	1.37E+01
49	90	2.69E+00	-5.04E+00	14.641	1.89E+00	342.947	1.38E+01
50	90	2.57E+00	-5.19E+00	14.422	1.77E+00	342.778	1.38E+01
51	90	2.44E+00	-5.34E+00	14.201	1.65E+00	342.605	1.38E+01

52	90	2.31E+00	-5.50E+00	13.979	1.52E+00	342.427	1.39E+01
53	90	2.18E+00	-5.66E+00	13.755	1.40E+00	342.243	1.39E+01
54	90	2.05E+00	-5.82E+00	13.529	1.27E+00	342.055	1.39E+01
55	90	1.91E+00	-5.99E+00	13.301	1.14E+00	341.863	1.40E+01
56	90	1.78E+00	-6.15E+00	13.071	1.01E+00	341.665	1.40E+01
57	90	1.64E+00	-6.32E+00	12.838	8.82E-01	341.463	1.41E+01
58	90	1.50E+00	-6.49E+00	12.604	7.50E-01	341.255	1.41E+01
59	90	1.36E+00	-6.67E+00	12.367	6.16E-01	341.043	1.41E+01
60	90	1.22E+00	-6.85E+00	12.128	4.81E-01	340.826	1.42E+01
61	90	1.08E+00	-7.03E+00	11.886	3.45E-01	340.605	1.42E+01
62	90	9.31E-01	-7.21E+00	11.642	2.08E-01	340.379	1.42E+01
63	90	7.86E-01	-7.40E+00	11.394	6.98E-02	340.148	1.43E+01
64	90	6.39E-01	-7.59E+00	11.144	-6.94E-02	339.913	1.43E+01
65	90	4.91E-01	-7.78E+00	10.891	-2.10E-01	339.673	1.44E+01
66	90	3.42E-01	-7.97E+00	10.634	-3.51E-01	339.429	1.44E+01
67	90	1.92E-01	-8.17E+00	10.373	-4.93E-01	339.18	1.45E+01
68	90	4.10E-02	-8.37E+00	10.108	-6.35E-01	338.927	1.45E+01
69	90	-1.11E-01	-8.57E+00	9.839	-7.79E-01	338.67	1.46E+01
70	90	-2.64E-01	-8.78E+00	9.566	-9.23E-01	338.41	1.46E+01
71	90	-4.18E-01	-8.99E+00	9.288	-1.07E+00	338.145	1.47E+01
72	90	-5.73E-01	-9.20E+00	9.005	-1.21E+00	337.877	1.47E+01
73	90	-7.28E-01	-9.42E+00	8.716	-1.36E+00	337.606	1.48E+01
74	90	-8.84E-01	-9.64E+00	8.421	-1.51E+00	337.331	1.48E+01
75	90	-1.04E+00	-9.86E+00	8.12	-1.65E+00	337.053	1.49E+01
76	90	-1.20E+00	-1.01E+01	7.811	-1.80E+00	336.773	1.50E+01
77	90	-1.36E+00	-1.03E+01	7.495	-1.95E+00	336.49	1.50E+01
78	90	-1.52E+00	-1.06E+01	7.17	-2.10E+00	336.205	1.51E+01
79	90	-1.68E+00	-1.08E+01	6.837	-2.24E+00	335.918	1.52E+01
80	90	-1.84E+00	-1.10E+01	6.493	-2.39E+00	335.629	1.53E+01
81	90	-2.00E+00	-1.13E+01	6.139	-2.54E+00	335.34	1.54E+01
82	90	-2.16E+00	-1.15E+01	5.773	-2.69E+00	335.049	1.55E+01
83	90	-2.32E+00	-1.18E+01	5.395	-2.84E+00	334.758	1.56E+01
84	90	-2.48E+00	-1.20E+01	5.002	-2.99E+00	334.466	1.57E+01
85	90	-2.64E+00	-1.23E+01	4.594	-3.14E+00	334.175	1.59E+01
86	90	-2.80E+00	-1.26E+01	4.169	-3.28E+00	333.885	1.60E+01
87	90	-2.96E+00	-1.29E+01	3.725	-3.43E+00	333.596	1.61E+01
88	90	-3.12E+00	-1.31E+01	3.262	-3.58E+00	333.308	1.63E+01
89	90	-3.29E+00	-1.34E+01	2.775	-3.73E+00	333.023	1.65E+01
90	90	-3.45E+00	-1.37E+01	2.265	-3.88E+00	332.74	1.67E+01
91	90	-3.61E+00	-1.40E+01	1.726	-4.02E+00	332.461	1.69E+01
92	90	-3.77E+00	-1.43E+01	1.158	-4.17E+00	332.185	1.71E+01
93	90	-3.93E+00	-1.46E+01	0.557	-4.32E+00	331.914	1.73E+01
94	90	-4.09E+00	-1.50E+01	359.918	-4.47E+00	331.648	1.76E+01
95	90	-4.26E+00	-1.53E+01	359.238	-4.61E+00	331.388	1.79E+01
96	90	-4.42E+00	-1.56E+01	358.513	-4.76E+00	331.134	1.82E+01
97	90	-4.58E+00	-1.60E+01	357.737	-4.90E+00	330.886	1.85E+01
98	90	-4.74E+00	-1.63E+01	356.904	-5.05E+00	330.647	1.89E+01
99	90	-4.90E+00	-1.67E+01	356.007	-5.19E+00	330.416	1.93E+01
100	90	-5.05E+00	-1.71E+01	355.039	-5.34E+00	330.194	1.97E+01
101	90	-5.21E+00	-1.74E+01	353.991	-5.48E+00	329.981	2.02E+01
102	90	-5.37E+00	-1.78E+01	352.853	-5.62E+00	329.779	2.08E+01
103	90	-5.53E+00	-1.82E+01	351.614	-5.77E+00	329.589	2.14E+01
104	90	-5.68E+00	-1.87E+01	350.26	-5.91E+00	329.411	2.21E+01
105	90	-5.84E+00	-1.91E+01	348.777	-6.05E+00	329.245	2.29E+01
106	90	-5.99E+00	-1.95E+01	347.148	-6.19E+00	329.093	2.39E+01
107	90	-6.14E+00	-2.00E+01	345.354	-6.33E+00	328.956	2.50E+01
108	90	-6.30E+00	-2.04E+01	343.373	-6.47E+00	328.833	2.63E+01
109	90	-6.45E+00	-2.09E+01	341.181	-6.61E+00	328.727	2.79E+01
110	90	-6.60E+00	-2.14E+01	338.752	-6.74E+00	328.637	3.00E+01
111	90	-6.74E+00	-2.18E+01	336.058	-6.88E+00	328.565	3.29E+01
112	90	-6.89E+00	-2.23E+01	333.069	-7.02E+00	328.512	3.75E+01
113	90	-7.03E+00	-2.28E+01	329.757	-7.15E+00	328.477	4.00E+01
114	90	-7.17E+00	-2.32E+01	326.098	-7.28E+00	328.463	4.00E+01

115	90	-7.31E+00	-2.36E+01	322.073	-7.42E+00	328.469	3.55E+01
116	90	-7.45E+00	-2.40E+01	317.677	-7.55E+00	328.496	3.12E+01
117	90	-7.59E+00	-2.44E+01	312.921	-7.68E+00	328.543	2.83E+01
118	90	-7.72E+00	-2.47E+01	307.845	-7.81E+00	328.615	2.60E+01
119	90	-7.85E+00	-2.49E+01	302.509	-7.94E+00	328.71	2.42E+01
120	90	-7.98E+00	-2.50E+01	297.002	-8.06E+00	328.829	2.26E+01
121	90	-8.10E+00	-2.50E+01	291.43	-8.19E+00	328.973	2.13E+01
122	90	-8.22E+00	-2.50E+01	285.91	-8.31E+00	329.141	2.01E+01
123	90	-8.34E+00	-2.49E+01	280.552	-8.44E+00	329.334	1.90E+01
124	90	-8.45E+00	-2.47E+01	275.447	-8.56E+00	329.553	1.80E+01
125	90	-8.56E+00	-2.44E+01	270.665	-8.68E+00	329.798	1.71E+01
126	90	-8.67E+00	-2.41E+01	266.247	-8.80E+00	330.07	1.63E+01
127	90	-8.77E+00	-2.38E+01	262.209	-8.91E+00	330.367	1.55E+01
128	90	-8.87E+00	-2.34E+01	258.551	-9.03E+00	330.691	1.48E+01
129	90	-8.96E+00	-2.30E+01	255.255	-9.14E+00	331.041	1.42E+01
130	90	-9.05E+00	-2.26E+01	252.299	-9.25E+00	331.418	1.36E+01
131	90	-9.14E+00	-2.22E+01	249.655	-9.35E+00	331.821	1.30E+01
132	90	-9.21E+00	-2.18E+01	247.293	-9.46E+00	332.249	1.24E+01
133	90	-9.29E+00	-2.15E+01	245.185	-9.56E+00	332.702	1.19E+01
134	90	-9.36E+00	-2.11E+01	243.304	-9.66E+00	333.18	1.14E+01
135	90	-9.42E+00	-2.07E+01	241.626	-9.76E+00	333.682	1.10E+01
136	90	-9.48E+00	-2.04E+01	240.128	-9.85E+00	334.207	1.05E+01
137	90	-9.53E+00	-2.00E+01	238.791	-9.94E+00	334.755	1.01E+01
138	90	-9.58E+00	-1.97E+01	237.598	-1.00E+01	335.323	9.76E+00
139	90	-9.62E+00	-1.94E+01	236.534	-1.01E+01	335.911	9.41E+00
140	90	-9.66E+00	-1.91E+01	235.584	-1.02E+01	336.518	9.08E+00
141	90	-9.69E+00	-1.88E+01	234.738	-1.03E+01	337.142	8.78E+00
142	90	-9.72E+00	-1.85E+01	233.986	-1.03E+01	337.781	8.50E+00
143	90	-9.75E+00	-1.82E+01	233.317	-1.04E+01	338.434	8.24E+00
144	90	-9.77E+00	-1.80E+01	232.725	-1.05E+01	339.1	8.01E+00
145	90	-9.78E+00	-1.77E+01	232.202	-1.05E+01	339.775	7.79E+00
146	90	-9.79E+00	-1.75E+01	231.742	-1.06E+01	340.459	7.60E+00
147	90	-9.80E+00	-1.73E+01	231.341	-1.07E+01	341.149	7.43E+00
148	90	-9.80E+00	-1.71E+01	230.993	-1.07E+01	341.844	7.27E+00
149	90	-9.80E+00	-1.69E+01	230.695	-1.08E+01	342.54	7.13E+00
150	90	-9.79E+00	-1.67E+01	230.442	-1.08E+01	343.237	7.02E+00
151	90	-9.79E+00	-1.65E+01	230.232	-1.08E+01	343.931	6.91E+00
152	90	-9.78E+00	-1.63E+01	230.061	-1.09E+01	344.621	6.82E+00
153	90	-9.77E+00	-1.62E+01	229.928	-1.09E+01	345.305	6.75E+00
154	90	-9.75E+00	-1.60E+01	229.829	-1.09E+01	345.981	6.69E+00
155	90	-9.74E+00	-1.59E+01	229.764	-1.10E+01	346.646	6.64E+00
156	90	-9.72E+00	-1.58E+01	229.729	-1.10E+01	347.298	6.60E+00
157	90	-9.71E+00	-1.56E+01	229.725	-1.10E+01	347.937	6.57E+00
158	90	-9.69E+00	-1.55E+01	229.749	-1.10E+01	348.559	6.55E+00
159	90	-9.67E+00	-1.54E+01	229.8	-1.10E+01	349.163	6.53E+00
160	90	-9.65E+00	-1.53E+01	229.877	-1.10E+01	349.748	6.52E+00
161	90	-9.63E+00	-1.52E+01	229.98	-1.10E+01	350.311	6.51E+00
162	90	-9.62E+00	-1.51E+01	230.108	-1.11E+01	350.852	6.51E+00
163	90	-9.60E+00	-1.51E+01	230.26	-1.11E+01	351.369	6.50E+00
164	90	-9.58E+00	-1.50E+01	230.435	-1.11E+01	351.86	6.50E+00
165	90	-9.57E+00	-1.49E+01	230.634	-1.11E+01	352.325	6.50E+00
166	90	-9.56E+00	-1.49E+01	230.856	-1.11E+01	352.763	6.50E+00
167	90	-9.54E+00	-1.48E+01	231.101	-1.11E+01	353.172	6.49E+00
168	90	-9.53E+00	-1.48E+01	231.369	-1.11E+01	353.552	6.49E+00
169	90	-9.52E+00	-1.48E+01	231.66	-1.11E+01	353.902	6.48E+00
170	90	-9.52E+00	-1.48E+01	231.974	-1.11E+01	354.22	6.47E+00
171	90	-9.51E+00	-1.47E+01	232.311	-1.11E+01	354.508	6.46E+00
172	90	-9.51E+00	-1.47E+01	232.672	-1.11E+01	354.763	6.44E+00
173	90	-9.51E+00	-1.47E+01	233.058	-1.11E+01	354.986	6.42E+00
174	90	-9.51E+00	-1.48E+01	233.468	-1.11E+01	355.175	6.39E+00
175	90	-9.52E+00	-1.48E+01	233.904	-1.11E+01	355.332	6.37E+00
176	90	-9.53E+00	-1.48E+01	234.367	-1.11E+01	355.455	6.34E+00
177	90	-9.54E+00	-1.48E+01	234.856	-1.11E+01	355.544	6.30E+00

178	90	-9.55E+00	-1.49E+01	235.374	-1.11E+01	355.599	6.26E+00
179	90	-9.56E+00	-1.49E+01	235.921	-1.11E+01	355.62	6.22E+00
180	90	-9.58E+00	-1.50E+01	236.499	-1.11E+01	355.607	6.18E+00
179	270	-9.60E+00	-1.51E+01	57.109	-1.11E+01	175.56	6.14E+00
178	270	-9.63E+00	-1.51E+01	57.754	-1.11E+01	175.479	6.10E+00
177	270	-9.65E+00	-1.52E+01	58.434	-1.11E+01	175.364	6.06E+00
176	270	-9.68E+00	-1.53E+01	59.152	-1.11E+01	175.215	6.02E+00
175	270	-9.71E+00	-1.54E+01	59.911	-1.11E+01	175.032	5.98E+00
174	270	-9.74E+00	-1.55E+01	60.712	-1.11E+01	174.816	5.94E+00
173	270	-9.77E+00	-1.57E+01	61.558	-1.11E+01	174.567	5.91E+00
172	270	-9.80E+00	-1.58E+01	62.453	-1.11E+01	174.285	5.89E+00
171	270	-9.84E+00	-1.59E+01	63.4	-1.11E+01	173.971	5.88E+00
170	270	-9.88E+00	-1.61E+01	64.402	-1.11E+01	173.625	5.88E+00
169	270	-9.91E+00	-1.62E+01	65.464	-1.11E+01	173.249	5.89E+00
168	270	-9.95E+00	-1.64E+01	66.59	-1.11E+01	172.842	5.91E+00
167	270	-9.99E+00	-1.65E+01	67.785	-1.11E+01	172.405	5.95E+00
166	270	-1.00E+01	-1.67E+01	69.054	-1.11E+01	171.94	6.01E+00
165	270	-1.01E+01	-1.69E+01	70.403	-1.11E+01	171.446	6.09E+00
164	270	-1.01E+01	-1.71E+01	71.837	-1.11E+01	170.927	6.19E+00
163	270	-1.01E+01	-1.73E+01	73.364	-1.11E+01	170.381	6.32E+00
162	270	-1.02E+01	-1.75E+01	74.992	-1.11E+01	169.812	6.47E+00
161	270	-1.02E+01	-1.77E+01	76.726	-1.11E+01	169.219	6.65E+00
160	270	-1.02E+01	-1.79E+01	78.576	-1.10E+01	168.606	6.86E+00
159	270	-1.03E+01	-1.81E+01	80.549	-1.10E+01	167.972	7.11E+00
158	270	-1.03E+01	-1.83E+01	82.654	-1.10E+01	167.32	7.38E+00
157	270	-1.03E+01	-1.86E+01	84.899	-1.10E+01	166.652	7.69E+00
156	270	-1.03E+01	-1.88E+01	87.292	-1.10E+01	165.969	8.04E+00
155	270	-1.03E+01	-1.90E+01	89.84	-1.10E+01	165.273	8.43E+00
154	270	-1.03E+01	-1.92E+01	92.549	-1.09E+01	164.566	8.86E+00
153	270	-1.03E+01	-1.94E+01	95.421	-1.09E+01	163.851	9.33E+00
152	270	-1.03E+01	-1.96E+01	98.46	-1.09E+01	163.13	9.85E+00
151	270	-1.03E+01	-1.98E+01	101.662	-1.08E+01	162.404	1.04E+01
150	270	-1.03E+01	-1.99E+01	105.021	-1.08E+01	161.676	1.11E+01
149	270	-1.03E+01	-2.01E+01	108.527	-1.07E+01	160.947	1.17E+01
148	270	-1.02E+01	-2.02E+01	112.164	-1.07E+01	160.221	1.25E+01
147	270	-1.02E+01	-2.02E+01	115.91	-1.06E+01	159.499	1.33E+01
146	270	-1.01E+01	-2.03E+01	119.74	-1.06E+01	158.783	1.43E+01
145	270	-1.01E+01	-2.03E+01	123.624	-1.05E+01	158.075	1.53E+01
144	270	-1.00E+01	-2.03E+01	127.529	-1.05E+01	157.378	1.65E+01
143	270	-9.96E+00	-2.02E+01	131.422	-1.04E+01	156.693	1.79E+01
142	270	-9.89E+00	-2.01E+01	135.269	-1.03E+01	156.022	1.96E+01
141	270	-9.81E+00	-2.00E+01	139.041	-1.03E+01	155.367	2.16E+01
140	270	-9.72E+00	-1.98E+01	142.71	-1.02E+01	154.729	2.41E+01
139	270	-9.63E+00	-1.96E+01	146.254	-1.01E+01	154.11	2.77E+01
138	270	-9.53E+00	-1.94E+01	149.655	-1.00E+01	153.511	3.38E+01
137	270	-9.43E+00	-1.91E+01	152.902	-9.92E+00	152.934	4.00E+01
136	270	-9.32E+00	-1.89E+01	155.987	-9.83E+00	152.379	3.41E+01
135	270	-9.20E+00	-1.86E+01	158.908	-9.73E+00	151.848	2.81E+01
134	270	-9.08E+00	-1.83E+01	161.664	-9.63E+00	151.342	2.47E+01
133	270	-8.96E+00	-1.80E+01	164.26	-9.54E+00	150.86	2.23E+01
132	270	-8.83E+00	-1.77E+01	166.699	-9.43E+00	150.405	2.05E+01
131	270	-8.70E+00	-1.74E+01	168.99	-9.33E+00	149.976	1.90E+01
130	270	-8.57E+00	-1.71E+01	171.14	-9.22E+00	149.573	1.78E+01
129	270	-8.44E+00	-1.68E+01	173.157	-9.11E+00	149.198	1.67E+01
128	270	-8.30E+00	-1.65E+01	175.048	-9.00E+00	148.85	1.58E+01
127	270	-8.16E+00	-1.62E+01	176.824	-8.89E+00	148.529	1.50E+01
126	270	-8.01E+00	-1.60E+01	178.491	-8.77E+00	148.235	1.43E+01
125	270	-7.87E+00	-1.57E+01	180.057	-8.66E+00	147.968	1.37E+01
124	270	-7.72E+00	-1.54E+01	181.53	-8.54E+00	147.729	1.32E+01
123	270	-7.57E+00	-1.51E+01	182.916	-8.42E+00	147.515	1.27E+01
122	270	-7.42E+00	-1.48E+01	184.222	-8.30E+00	147.328	1.22E+01
121	270	-7.27E+00	-1.46E+01	185.454	-8.17E+00	147.167	1.18E+01
120	270	-7.12E+00	-1.43E+01	186.617	-8.05E+00	147.032	1.14E+01

119	270	-6.97E+00	-1.40E+01	187.716	-7.93E+00	146.921	1.11E+01
118	270	-6.82E+00	-1.38E+01	188.756	-7.80E+00	146.835	1.07E+01
117	270	-6.67E+00	-1.35E+01	189.74	-7.67E+00	146.772	1.04E+01
116	270	-6.52E+00	-1.33E+01	190.674	-7.54E+00	146.734	1.02E+01
115	270	-6.36E+00	-1.30E+01	191.559	-7.41E+00	146.717	9.92E+00
114	270	-6.21E+00	-1.28E+01	192.4	-7.28E+00	146.721	9.70E+00
113	270	-6.06E+00	-1.26E+01	193.2	-7.15E+00	146.747	9.49E+00
112	270	-5.90E+00	-1.24E+01	193.961	-7.02E+00	146.792	9.30E+00
111	270	-5.75E+00	-1.21E+01	194.685	-6.88E+00	146.857	9.12E+00
110	270	-5.60E+00	-1.19E+01	195.376	-6.75E+00	146.941	8.96E+00
109	270	-5.44E+00	-1.17E+01	196.034	-6.62E+00	147.043	8.81E+00
108	270	-5.29E+00	-1.15E+01	196.663	-6.48E+00	147.162	8.67E+00
107	270	-5.14E+00	-1.13E+01	197.263	-6.34E+00	147.297	8.55E+00
106	270	-4.99E+00	-1.11E+01	197.836	-6.21E+00	147.447	8.43E+00
105	270	-4.83E+00	-1.09E+01	198.384	-6.07E+00	147.612	8.33E+00
104	270	-4.68E+00	-1.07E+01	198.908	-5.93E+00	147.792	8.24E+00
103	270	-4.53E+00	-1.05E+01	199.409	-5.79E+00	147.984	8.15E+00
102	270	-4.38E+00	-1.03E+01	199.889	-5.65E+00	148.189	8.08E+00
101	270	-4.23E+00	-1.02E+01	200.348	-5.51E+00	148.405	8.01E+00
100	270	-4.08E+00	-9.97E+00	200.788	-5.37E+00	148.632	7.95E+00
99	270	-3.93E+00	-9.80E+00	201.209	-5.23E+00	148.869	7.89E+00
98	270	-3.78E+00	-9.62E+00	201.613	-5.08E+00	149.115	7.85E+00
97	270	-3.62E+00	-9.45E+00	202	-4.94E+00	149.37	7.81E+00
96	270	-3.47E+00	-9.28E+00	202.37	-4.80E+00	149.632	7.77E+00
95	270	-3.32E+00	-9.11E+00	202.725	-4.65E+00	149.902	7.74E+00
94	270	-3.17E+00	-8.95E+00	203.065	-4.51E+00	150.179	7.72E+00
93	270	-3.02E+00	-8.79E+00	203.391	-4.36E+00	150.461	7.70E+00
92	270	-2.88E+00	-8.63E+00	203.703	-4.22E+00	150.748	7.69E+00
91	270	-2.73E+00	-8.47E+00	204.001	-4.07E+00	151.04	7.68E+00
90	270	-2.58E+00	-8.31E+00	204.287	-3.93E+00	151.336	7.67E+00
89	270	-2.43E+00	-8.16E+00	204.561	-3.78E+00	151.635	7.67E+00
88	270	-2.28E+00	-8.01E+00	204.823	-3.63E+00	151.937	7.67E+00
87	270	-2.13E+00	-7.85E+00	205.073	-3.49E+00	152.241	7.68E+00
86	270	-1.98E+00	-7.71E+00	205.312	-3.34E+00	152.547	7.69E+00
85	270	-1.84E+00	-7.56E+00	205.54	-3.19E+00	152.855	7.70E+00
84	270	-1.69E+00	-7.41E+00	205.758	-3.04E+00	153.163	7.72E+00
83	270	-1.54E+00	-7.27E+00	205.965	-2.90E+00	153.471	7.74E+00
82	270	-1.40E+00	-7.12E+00	206.163	-2.75E+00	153.779	7.76E+00
81	270	-1.25E+00	-6.98E+00	206.351	-2.60E+00	154.087	7.78E+00
80	270	-1.10E+00	-6.84E+00	206.53	-2.45E+00	154.394	7.81E+00
79	270	-9.59E-01	-6.70E+00	206.7	-2.31E+00	154.7	7.84E+00
78	270	-8.14E-01	-6.57E+00	206.861	-2.16E+00	155.004	7.87E+00
77	270	-6.70E-01	-6.43E+00	207.014	-2.01E+00	155.306	7.90E+00
76	270	-5.26E-01	-6.29E+00	207.158	-1.86E+00	155.606	7.93E+00
75	270	-3.83E-01	-6.16E+00	207.294	-1.72E+00	155.904	7.97E+00
74	270	-2.40E-01	-6.03E+00	207.422	-1.57E+00	156.199	8.00E+00
73	270	-9.76E-02	-5.90E+00	207.542	-1.42E+00	156.491	8.04E+00
72	270	4.39E-02	-5.77E+00	207.655	-1.28E+00	156.779	8.08E+00
71	270	1.85E-01	-5.64E+00	207.76	-1.13E+00	157.064	8.12E+00
70	270	3.25E-01	-5.51E+00	207.859	-9.88E-01	157.346	8.17E+00
69	270	4.64E-01	-5.38E+00	207.95	-8.44E-01	157.624	8.21E+00
68	270	6.03E-01	-5.26E+00	208.034	-7.01E-01	157.897	8.25E+00
67	270	7.41E-01	-5.14E+00	208.112	-5.58E-01	158.167	8.30E+00
66	270	8.78E-01	-5.01E+00	208.183	-4.16E-01	158.432	8.35E+00
65	270	1.01E+00	-4.89E+00	208.248	-2.75E-01	158.693	8.39E+00
64	270	1.15E+00	-4.77E+00	208.306	-1.34E-01	158.95	8.44E+00
63	270	1.28E+00	-4.65E+00	208.358	5.23E-03	159.201	8.49E+00
62	270	1.42E+00	-4.54E+00	208.405	1.44E-01	159.449	8.54E+00
61	270	1.55E+00	-4.42E+00	208.445	2.81E-01	159.691	8.59E+00
60	270	1.68E+00	-4.31E+00	208.48	4.18E-01	159.929	8.64E+00
59	270	1.81E+00	-4.19E+00	208.509	5.53E-01	160.163	8.69E+00
58	270	1.94E+00	-4.08E+00	208.532	6.87E-01	160.391	8.74E+00
57	270	2.07E+00	-3.97E+00	208.551	8.20E-01	160.614	8.79E+00

56	270	2.19E+00	-3.86E+00	208.564	9.52E-01	160.833	8.84E+00
55	270	2.32E+00	-3.75E+00	208.572	1.08E+00	161.046	8.89E+00
54	270	2.44E+00	-3.65E+00	208.575	1.21E+00	161.255	8.94E+00
53	270	2.56E+00	-3.54E+00	208.573	1.34E+00	161.459	9.00E+00
52	270	2.68E+00	-3.44E+00	208.566	1.47E+00	161.658	9.05E+00
51	270	2.80E+00	-3.34E+00	208.554	1.59E+00	161.852	9.10E+00
50	270	2.92E+00	-3.24E+00	208.538	1.71E+00	162.041	9.15E+00
49	270	3.04E+00	-3.14E+00	208.518	1.84E+00	162.226	9.21E+00
48	270	3.15E+00	-3.04E+00	208.493	1.95E+00	162.405	9.26E+00
47	270	3.26E+00	-2.95E+00	208.464	2.07E+00	162.58	9.31E+00
46	270	3.37E+00	-2.85E+00	208.43	2.19E+00	162.75	9.37E+00
45	270	3.48E+00	-2.76E+00	208.393	2.30E+00	162.916	9.42E+00
44	270	3.59E+00	-2.67E+00	208.351	2.42E+00	163.077	9.47E+00
43	270	3.70E+00	-2.58E+00	208.306	2.53E+00	163.233	9.52E+00
42	270	3.80E+00	-2.49E+00	208.257	2.64E+00	163.385	9.58E+00
41	270	3.90E+00	-2.41E+00	208.204	2.74E+00	163.532	9.63E+00
40	270	4.00E+00	-2.33E+00	208.147	2.85E+00	163.675	9.68E+00
39	270	4.10E+00	-2.25E+00	208.087	2.95E+00	163.813	9.74E+00
38	270	4.19E+00	-2.17E+00	208.023	3.05E+00	163.948	9.79E+00
37	270	4.29E+00	-2.09E+00	207.956	3.15E+00	164.077	9.84E+00
36	270	4.38E+00	-2.02E+00	207.886	3.25E+00	164.203	9.89E+00
35	270	4.47E+00	-1.94E+00	207.812	3.34E+00	164.325	9.95E+00
34	270	4.56E+00	-1.87E+00	207.735	3.44E+00	164.442	1.00E+01
33	270	4.64E+00	-1.80E+00	207.655	3.53E+00	164.556	1.01E+01
32	270	4.73E+00	-1.74E+00	207.572	3.61E+00	164.665	1.01E+01
31	270	4.81E+00	-1.67E+00	207.486	3.70E+00	164.771	1.02E+01
30	270	4.88E+00	-1.61E+00	207.398	3.78E+00	164.873	1.02E+01
29	270	4.96E+00	-1.55E+00	207.306	3.86E+00	164.971	1.03E+01
28	270	5.03E+00	-1.49E+00	207.212	3.94E+00	165.065	1.03E+01
27	270	5.11E+00	-1.43E+00	207.114	4.02E+00	165.156	1.04E+01
26	270	5.17E+00	-1.38E+00	207.015	4.09E+00	165.243	1.04E+01
25	270	5.24E+00	-1.33E+00	206.913	4.16E+00	165.327	1.05E+01
24	270	5.31E+00	-1.28E+00	206.808	4.23E+00	165.407	1.05E+01
23	270	5.37E+00	-1.24E+00	206.7	4.30E+00	165.484	1.06E+01
22	270	5.43E+00	-1.19E+00	206.591	4.36E+00	165.557	1.06E+01
21	270	5.48E+00	-1.15E+00	206.479	4.42E+00	165.627	1.07E+01
20	270	5.54E+00	-1.11E+00	206.365	4.48E+00	165.694	1.07E+01
19	270	5.59E+00	-1.08E+00	206.248	4.53E+00	165.758	1.08E+01
18	270	5.64E+00	-1.04E+00	206.13	4.58E+00	165.818	1.08E+01
17	270	5.68E+00	-1.01E+00	206.009	4.63E+00	165.875	1.09E+01
16	270	5.72E+00	-9.81E-01	205.886	4.68E+00	165.929	1.09E+01
15	270	5.77E+00	-9.55E-01	205.761	4.73E+00	165.981	1.10E+01
14	270	5.80E+00	-9.32E-01	205.634	4.77E+00	166.029	1.10E+01
13	270	5.84E+00	-9.11E-01	205.505	4.81E+00	166.074	1.11E+01
12	270	5.87E+00	-8.92E-01	205.375	4.84E+00	166.116	1.11E+01
11	270	5.90E+00	-8.77E-01	205.242	4.88E+00	166.155	1.12E+01
10	270	5.93E+00	-8.64E-01	205.107	4.91E+00	166.191	1.12E+01
9	270	5.95E+00	-8.54E-01	204.971	4.93E+00	166.225	1.13E+01
8	270	5.97E+00	-8.46E-01	204.833	4.96E+00	166.256	1.13E+01
7	270	5.99E+00	-8.41E-01	204.694	4.98E+00	166.283	1.14E+01
6	270	6.01E+00	-8.39E-01	204.552	5.00E+00	166.308	1.14E+01
5	270	6.02E+00	-8.40E-01	204.409	5.02E+00	166.331	1.15E+01
4	270	6.03E+00	-8.44E-01	204.265	5.03E+00	166.35	1.15E+01
3	270	6.04E+00	-8.50E-01	204.118	5.04E+00	166.367	1.16E+01
2	270	6.04E+00	-8.59E-01	203.971	5.05E+00	166.381	1.16E+01
1	270	6.04E+00	-8.71E-01	203.821	5.05E+00	166.392	1.17E+01

e. Hpbw 4 elemen

f. Hpbw 16 elemen

2. Data cst cir

a. Rl 1 elemen

Frequency / GHz	S2,2 (13)/abs,dB	Frequency / GHz	S2,2 (13)/abs,dB	Frequency / GHz	S2,2 (13)/abs,dB	Frequency / GHz	S2,2 (13)/abs,dB
0	-0.005753249	2.49	-0.43254716	4.9899998	-0.83152112	7.4899998	-4.7645497
0.01	-0.005891358	2.5	-0.44613047	5	-0.83480058	7.5	-4.7836331
0.02	-0.006308338	2.51	-0.46008351	5.0100002	-0.83929997	7.5100002	-4.8075169
0.029999999	-0.007001358	2.52	-0.47428093	5.02	-0.8449002	7.52	-4.8353736
0.039999999	-0.007971295	2.53	-0.48859539	5.0300002	-0.85147457	7.5300002	-4.8662929
0.050000001	-0.009216729	2.54	-0.50290301	5.04	-0.85889619	7.54	-4.8992843
0.059999999	-0.010736254	2.55	-0.51709705	5.0500002	-0.8670455	7.5500002	-4.9332905
0.07	-0.012527917	2.5599999	-0.53108293	5.0599999	-0.87581353	7.5599999	-4.9671916
0.079999998	-0.014588725	2.5699999	-0.54479648	5.0700002	-0.88510438	7.5700002	-4.9998272
0.090000004	-0.016915638	2.5799999	-0.55820107	5.0799999	-0.89484394	7.5799999	-5.0300169
0.1	-0.019505056	2.5899999	-0.57129676	5.0900002	-0.90497863	7.5900002	-5.056582
0.11	-0.02235062	2.5999999	-0.58412149	5.0999999	-0.91547473	7.5999999	-5.0783768
0.12	-0.025446389	2.6099999	-0.59675755	5.1100001	-0.92632424	7.6100001	-5.0943228
0.13	-0.02878562	2.6199999	-0.60932647	5.1199999	-0.9375394	7.6199999	-5.1034389
0.14	-0.032356563	2.6300001	-0.62199522	5.1300001	-0.94915014	7.6300001	-5.1048765
0.15000001	-0.036151457	2.6400001	-0.63496735	5.1399999	-0.96120559	7.6399999	-5.0979466
0.16	-0.040157049	2.6500001	-0.648483	5.1500001	-0.97376714	7.6500001	-5.0821445
0.17	-0.044359422	2.6600001	-0.66281441	5.1599998	-0.98690567	7.6599998	-5.0571684
0.18000001	-0.048743784	2.6700001	-0.67825698	5.1700001	-1.0006974	7.6700001	-5.0229274
0.19	-0.053292491	2.6800001	-0.69512226	5.1799998	-1.0152196	7.6799998	-4.9795396
0.2	-0.057988911	2.6900001	-0.7137312	5.1900001	-1.0305457	7.6900001	-4.9273212
0.20999999	-0.062812135	2.7	-0.73440541	5.1999998	-1.0467459	7.6999998	-4.8667683
0.22	-0.067740916	2.71	-0.75745471	5.21	-1.063877	7.71	-4.7985338
0.23	-0.072754538	2.72	-0.78317252	5.2199998	-1.081987	7.7199998	-4.7233892
0.23999999	-0.077829456	2.73	-0.81182396	5.23	-1.1011084	7.73	-4.6421991
0.25	-0.082940946	2.74	-0.84363979	5.2399998	-1.1212608	7.7399998	-4.555879
0.25999999	-0.088066869	2.75	-0.87880302	5.25	-1.1424489	7.75	-4.465371
0.27000001	-0.093183333	2.76	-0.91745077	5.2600002	-1.1646629	7.7600002	-4.3716076
0.28	-0.098265933	2.77	-0.95965943	5.27	-1.1878837	7.77	-4.2754855
0.28999999	-0.10329119	2.78	-1.0054449	5.2800002	-1.2120799	7.7800002	-4.1778534
0.30000001	-0.10823784	2.79	-1.0547548	5.29	-1.2372126	7.79	-4.0794839
0.31	-0.11308471	2.8	-1.1074671	5.3000002	-1.2632423	7.8000002	-3.981074
0.31999999	-0.11781222	2.8099999	-1.1633904	5.3099999	-1.2901274	7.8099999	-3.88323
0.33000001	-0.12240303	2.8199999	-1.2222608	5.3200002	-1.3178284	7.8200002	-3.7864723
0.34	-0.12684154	2.8299999	-1.2837481	5.3299999	-1.3463153	7.8299999	-3.6912305
0.34999999	-0.13111363	2.8399999	-1.3474556	5.3400002	-1.3755637	7.8400002	-3.5978502
0.36000001	-0.13521014	2.8499999	-1.4129295	5.3499999	-1.4055661	7.8499999	-3.5065969
0.37	-0.1391217	2.8599999	-1.4796665	5.3600001	-1.4363271	7.8600001	-3.417667
0.38	-0.14284253	2.8699999	-1.5471231	5.3699999	-1.4678692	7.8699999	-3.33119
0.38999999	-0.14637115	2.8800001	-1.6147325	5.3800001	-1.5002291	7.8800001	-3.2472452
0.40000001	-0.14970541	2.8900001	-1.6819141	5.3899999	-1.5334643	7.8899999	-3.1658654
0.41	-0.15284989	2.9000001	-1.748095	5.4000001	-1.5676449	7.9000001	-3.0870473
0.41999999	-0.15580716	2.9100001	-1.8127285	5.4099998	-1.6028571	7.9099998	-3.0107614
0.43000001	-0.15858488	2.9200001	-1.875309	5.4200001	-1.6392001	7.9200001	-2.9369594
0.44	-0.16119095	2.9300001	-1.935392	5.4299998	-1.6767798	7.9299998	-2.8655819
0.44999999	-0.16363718	2.9400001	-1.9926157	5.4400001	-1.7157121	7.9400001	-2.7965627
0.46000001	-0.16593275	2.95	-2.0467139	5.4499998	-1.7561113	7.9499998	-2.7298361
0.47	-0.16809105	2.96	-2.0975265	5.46	-1.7980951	7.96	-2.6653425
0.47999999	-0.17012286	2.97	-2.1450151	5.4699998	-1.8417725	7.9699998	-2.6030252
0.49000001	-0.17204385	2.98	-2.1892636	5.48	-1.8872456	7.98	-2.5428384
0.5	-0.17386272	2.99	-2.2304847	5.4899998	-1.9346062	7.9899998	-2.4847433
0.50999999	-0.17559377	3	-2.2690091	5.5	-1.9839301	8	-2.4287106
0.51999998	-0.17724483	3.01	-2.305289	5.5100002	-2.0352785	8.0100002	-2.3747185
0.52999997	-0.1788248	3.02	-2.3398801	5.52	-2.0886927	8.0200005	-2.322748
0.54000002	-0.18034271	3.03	-2.3734294	5.5300002	-2.1441961	8.0299997	-2.2727866
0.55000001	-0.18180156	3.04	-2.4066633	5.54	-2.2017922	8.04	-2.2248193
0.56	-0.18320612	3.05	-2.4403696	5.5500002	-2.2614667	8.0500002	-2.1788277
0.56999999	-0.18455593	3.0599999	-2.4753819	5.5599999	-2.3231855	8.0600004	-2.134791
0.57999998	-0.18585079	3.0699999	-2.5125645	5.5700002	-2.3868969	8.0699997	-2.0926784
0.58999997	-0.18708688	3.0799999	-2.5527982	5.5799999	-2.452537	8.0799999	-2.0524506

0.60000002	-0.18826092	3.0899999	-2.5969709	5.5900002	-2.5200272	8.0900002	-2.0140566
0.61000001	-0.18936488	3.0999999	-2.6459645	5.5999999	-2.5892782	8.1000004	-1.9774328
0.62	-0.19039166	3.1099999	-2.7006488	5.6100001	-2.6601908	8.1099997	-1.9425042
0.63	-0.19133133	3.1199999	-2.7618792	5.6199999	-2.7326615	8.1199999	-1.9091829
0.63999999	-0.19217551	3.1300001	-2.8304906	5.6300001	-2.80658	8.1300001	-1.877373
0.64999998	-0.19291468	3.1400001	-2.9073023	5.6399999	-2.8818323	8.1400003	-1.8469676
0.66000003	-0.19353851	3.1500001	-2.9931127	5.6500001	-2.9583	8.1499996	-1.8178539
0.67000002	-0.19403928	3.1600001	-3.0887137	5.6599998	-3.0358632	8.1599998	-1.7899164
0.68000001	-0.19440964	3.1700001	-3.194886	5.6700001	-3.1143929	8.1700001	-1.7630392
0.69	-0.19464169	3.1800001	-3.3124155	5.6799998	-3.1937566	8.1800003	-1.7371092
0.69999999	-0.19473329	3.1900001	-3.4420991	5.6900001	-3.2738058	8.1899996	-1.712021
0.70999998	-0.19468142	3.2	-3.5847519	5.6999998	-3.3543841	8.1999998	-1.6876777
0.72000003	-0.19448682	3.21	-3.7412278	5.71	-3.4353107	8.21	-1.6639955
0.73000002	-0.19415208	3.22	-3.9124286	5.7199998	-3.5163839	8.2200003	-1.6409057
0.74000001	-0.19368228	3.23	-4.0993192	5.73	-3.597371	8.2299995	-1.6183559
0.75	-0.19308637	3.24	-4.3029499	5.7399998	-3.678008	8.2399998	-1.5963119
0.75999999	-0.19237423	3.25	-4.5244712	5.75	-3.7579884	8.25	-1.5747563
0.76999998	-0.19155885	3.26	-4.765164	5.7600002	-3.8369636	8.2600002	-1.5536909
0.77999997	-0.19065436	3.27	-5.0264654	5.77	-3.9145394	8.2700005	-1.5331324
0.79000002	-0.18967702	3.28	-5.3100002	5.7800002	-3.9902763	8.2799997	-1.5131119
0.80000001	-0.18864351	3.29	-5.6176201	5.79	-4.0636863	8.29	-1.4936715
0.81	-0.187572	3.3	-5.9514592	5.8000002	-4.1342431	8.3000002	-1.4748649
0.81999999	-0.18648024	3.3099999	-6.3139845	5.8099999	-4.20138	8.3100004	-1.4567445
0.82999998	-0.18538469	3.3199999	-6.7080821	5.8200002	-4.2645065	8.3199997	-1.4393693
0.83999997	-0.18430211	3.3299999	-7.13715	5.8299999	-4.3230169	8.3299999	-1.4227928
0.85000002	-0.18324638	3.3399999	-7.6052301	5.8400002	-4.3763065	8.3400002	-1.407065
0.86000001	-0.18223056	3.3499999	-8.1171802	5.8499999	-4.4237854	8.3500004	-1.3922235
0.87	-0.18126403	3.3599999	-8.6789066	5.8600001	-4.4649023	8.3599997	-1.3782976
0.88	-0.18035409	3.3699999	-9.2976936	5.8699999	-4.4991597	8.3699999	-1.3653014
0.88999999	-0.17950537	3.3800001	-9.982663	5.8800001	-4.5261379	8.3800001	-1.3532334
0.89999998	-0.17871766	3.3900001	-10.745451	5.8899999	-4.5455055	8.3900003	-1.3420769
0.91000003	-0.17798963	3.4000001	-11.60122	5.9000001	-4.5570423	8.3999996	-1.3318006
0.92000002	-0.17731527	3.4100001	-12.570219	5.9099998	-4.5606441	8.4099998	-1.3223574
0.93000001	-0.17668679	3.4200001	-13.680318	5.9200001	-4.5563352	8.4200001	-1.3136882
0.94	-0.17609224	3.4300001	-14.971214	5.9299998	-4.5442621	8.4300003	-1.3057255
0.94999999	-0.17551828	3.4400001	-16.501797	5.9400001	-4.5246995	8.4399996	-1.2983926
0.95999998	-0.17495138	3.45	-18.363313	5.9499998	-4.4980315	8.4499998	-1.2916118
0.97000003	-0.17437481	3.46	-20.701578	5.96	-4.4647442	8.46	-1.2853049
0.98000002	-0.17377187	3.47	-23.730967	5.9699998	-4.4254065	8.4700003	-1.2793977
0.99000001	-0.17312763	3.48	-27.431359	5.98	-4.3806509	8.4799995	-1.2738271
1	-0.17242557	3.49	-29.021596	5.9899998	-4.3311531	8.4899998	-1.2685377
1.01	-0.1716526	3.5	-25.872445	6	-4.2776082	8.5	-1.2634922
1.02	-0.17079764	3.51	-22.363305	6.0100002	-4.2207153	8.5100002	-1.2586713
1.03	-0.16985093	3.52	-19.634725	6.02	-4.1611555	8.5200005	-1.2540733
1.04	-0.16880757	3.53	-17.504148	6.0300002	-4.0995775	8.5299997	-1.2497192
1.05	-0.16766513	3.54	-15.782961	6.04	-4.0365836	8.54	-1.2456482
1.0599999	-0.1664268	3.55	-14.351188	6.0500002	-3.9727212	8.5500002	-1.2419204
1.0700001	-0.16509589	3.5599999	-13.133145	6.0599999	-3.9084757	8.5600004	-1.2386127
1.08	-0.16368194	3.5699999	-12.079142	6.0700002	-3.8442652	8.5699997	-1.235819
1.09	-0.16219849	3.5799999	-11.155111	6.0799999	-3.7804409	8.5799999	-1.2336436
1.1	-0.16066112	3.5899999	-10.336779	6.0900002	-3.7172875	8.5900002	-1.2321994
1.11	-0.15908743	3.5999999	-9.6062643	6.0999999	-3.6550245	8.6000004	-1.2316037
1.12	-0.15749714	3.6099999	-8.9500125	6.1100001	-3.5938162	8.6099997	-1.231974
1.13	-0.15591252	3.6199999	-8.3574874	6.1199999	-3.5337732	8.6199999	-1.2334256
1.14	-0.15435396	3.6300001	-7.8203141	6.1300001	-3.4749604	8.6300001	-1.2360628
1.15	-0.15284474	3.6400001	-7.331706	6.1399999	-3.4174087	8.6400003	-1.2399825
1.16	-0.15140423	3.6500001	-6.8860607	6.1500001	-3.3611176	8.6499996	-1.2452643
1.17	-0.1500499	3.6600001	-6.4786796	6.1599998	-3.3060651	8.6599998	-1.2519755
1.1799999	-0.14879928	3.6700001	-6.1055607	6.1700001	-3.252219	8.6700001	-1.2601623
1.1900001	-0.14766326	3.6800001	-5.7632475	6.1799998	-3.1995357	8.6800003	-1.2698593
1.2	-0.14665044	3.6900001	-5.4487169	6.1900001	-3.1479782	8.6899996	-1.2810794
1.21	-0.14576556	3.7	-5.1592979	6.1999998	-3.0975076	8.6999998	-1.2938253
1.22	-0.14500777	3.71	-4.8926029	6.21	-3.0481	8.71	-1.3080836

1.23	-0.14437205	3.72	-4.646482	6.2199998	-2.9997387	8.7200003	-1.3238335
1.24	-0.14384987	3.73	-4.4189865	6.23	-2.9524227	8.7299995	-1.3410513
1.25	-0.14342744	3.74	-4.2083419	6.2399998	-2.9061646	8.7399998	-1.3597094
1.26	-0.14308793	3.75	-4.0129254	6.25	-2.8609907	8.75	-1.3797864
1.27	-0.14281068	3.76	-3.8312504	6.2600002	-2.8169352	8.7600002	-1.4012698
1.28	-0.14257349	3.77	-3.66196	6.27	-2.7740452	8.7700005	-1.4241596
1.29	-0.14235327	3.78	-3.5038144	6.2800002	-2.7323695	8.7799997	-1.4484746
1.3	-0.14212523	3.79	-3.3556897	6.29	-2.6919616	8.79	-1.4742529
1.3099999	-0.14186652	3.8	-3.2165685	6.3000002	-2.6528705	8.8000002	-1.5015584
1.3200001	-0.14155385	3.8099999	-3.0855442	6.3099999	-2.6151419	8.8100004	-1.5304788
1.33	-0.14116917	3.8199999	-2.9618114	6.3200002	-2.5788112	8.8199997	-1.5611284
1.34	-0.14069569	3.8299999	-2.8446667	6.3299999	-2.5439034	8.8299999	-1.5936434
1.35	-0.14012124	3.8399999	-2.733502	6.3400002	-2.5104289	8.8400002	-1.628185
1.36	-0.13943856	3.8499999	-2.6278055	6.3499999	-2.4783823	8.8500004	-1.6649308
1.37	-0.13864507	3.8599999	-2.527147	6.3600001	-2.4477425	8.8599997	-1.7040724
1.38	-0.13774542	3.8699999	-2.4311813	6.3699999	-2.418474	8.8699999	-1.7458083
1.39	-0.13674734	3.8800001	-2.3396321	6.3800001	-2.390526	8.8800001	-1.7903363
1.4	-0.13566468	3.8900001	-2.2522858	6.3899999	-2.3638347	8.8900003	-1.8378442
1.41	-0.13451584	3.9000001	-2.1689838	6.4000001	-2.3383262	8.8999996	-1.8885053
1.42	-0.13332425	3.9100001	-2.0896108	6.4099998	-2.3139226	8.9099998	-1.9424629
1.4299999	-0.13211547	3.9200001	-2.0140828	6.4200001	-2.2905418	8.9200001	-1.9998263
1.4400001	-0.13091802	3.9300001	-1.9423397	6.4299998	-2.2681034	8.9300003	-2.0606562
1.45	-0.12976087	3.9400001	-1.8743349	6.4400001	-2.2465362	8.9399996	-2.1249583
1.46	-0.12867327	3.95	-1.8100226	6.4499998	-2.225776	8.9499998	-2.1926732
1.47	-0.12768455	3.96	-1.7493548	6.46	-2.2057761	8.96	-2.2636683
1.48	-0.12682005	3.97	-1.6922719	6.4699998	-2.1865071	8.9700003	-2.3377312
1.49	-0.12610202	3.98	-1.6386946	6.48	-2.1679596	8.9799995	-2.4145602
1.5	-0.12554924	3.99	-1.588524	6.4899998	-2.1501496	8.9899998	-2.4937645
1.51	-0.12517431	4	-1.5416341	6.5	-2.1331152	9	-2.5748603
1.52	-0.12498402	4.0100002	-1.4978728	6.5100002	-2.1169204	9.0100002	-2.6572693
1.53	-0.12497895	4.02	-1.4570651	6.52	-2.1016511	9.0200005	-2.7403234
1.54	-0.1251542	4.0300002	-1.4190082	6.5300002	-2.0874169	9.0299997	-2.8232719
1.55	-0.12549655	4.04	-1.383479	6.54	-2.0743438	9.04	-2.9052903
1.5599999	-0.1259894	4.0500002	-1.3502378	6.5500002	-2.0625753	9.0500002	-2.9854951
1.5700001	-0.12660879	4.0599999	-1.3190308	6.5599999	-2.0522653	9.0600004	-3.0629646
1.58	-0.12732683	4.0700002	-1.2896014	6.5700002	-2.0435766	9.0699997	-3.1367539
1.59	-0.12811288	4.0799999	-1.2616926	6.5799999	-2.0366719	9.0799999	-3.2059306
1.6	-0.12893352	4.0900002	-1.2350552	6.5900002	-2.0317139	9.0900002	-3.2695933
1.61	-0.12975574	4.0999999	-1.2094561	6.5999999	-2.0288581	9.1000004	-3.326905
1.62	-0.13054453	4.1100001	-1.1846816	6.6100001	-2.0282514	9.1099997	-3.37712
1.63	-0.13127041	4.1199999	-1.1605462	6.6199999	-2.0300266	9.1199999	-3.4196142
1.64	-0.13190543	4.1300001	-1.1368975	6.6300001	-2.0343001	9.1300001	-3.4539023
1.65	-0.13242832	4.1399999	-1.1136177	6.6399999	-2.0411721	9.1400003	-3.4796574
1.66	-0.13282067	4.1500001	-1.0906292	6.6500001	-2.0507245	9.1499996	-3.4967234
1.67	-0.13307265	4.1599998	-1.0678908	6.6599998	-2.0630227	9.1599998	-3.5051145
1.6799999	-0.13318283	4.1700001	-1.0454018	6.6700001	-2.0781131	9.1700001	-3.5050116
1.6900001	-0.13315541	4.1799998	-1.0231957	6.6799998	-2.0960298	9.1800003	-3.4967499
1.7	-0.13300522	4.1900001	-1.0013367	6.6900001	-2.1167961	9.1899996	-3.4808013
1.71	-0.13275054	4.1999998	-0.97991939	6.6999998	-2.1404291	9.1999998	-3.4577509
1.72	-0.13242065	4.21	-0.95905462	6.71	-2.1669413	9.21	-3.4282691
1.73	-0.13204782	4.2199998	-0.93886944	6.7199998	-2.1963512	9.2200003	-3.393084
1.74	-0.13166925	4.23	-0.91949514	6.73	-2.2286833	9.2299995	-3.352956
1.75	-0.13132652	4.2399998	-0.9010649	6.7399998	-2.2639789	9.2399998	-3.3086521
1.76	-0.13106243	4.25	-0.88369938	6.75	-2.3022972	9.25	-3.2609204
1.77	-0.13091714	4.2600002	-0.86750625	6.7600002	-2.3437232	9.2600002	-3.2104788
1.78	-0.13093346	4.27	-0.85257333	6.77	-2.3883713	9.2700005	-3.1579923
1.79	-0.13114543	4.2800002	-0.83896092	6.7800002	-2.4363892	9.2799997	-3.1040666
1.8	-0.13158526	4.29	-0.82670056	6.79	-2.4879596	9.29	-3.0492413
1.8099999	-0.13227768	4.3000002	-0.81579038	6.8000002	-2.5433045	9.3000002	-2.9939882
1.8200001	-0.13323975	4.3099999	-0.8061992	6.8099999	-2.6026812	9.3100004	-2.9387091
1.83	-0.13447878	4.3200002	-0.79786057	6.8200002	-2.6663887	9.3199997	-2.8837407
1.84	-0.13599521	4.3299999	-0.79067985	6.8299999	-2.7347538	9.3299999	-2.8293578
1.85	-0.13777631	4.3400002	-0.78453463	6.8400002	-2.8081386	9.3400002	-2.7757825

1.86	-0.1398052	4.3499999	-0.77928134	6.8499999	-2.8869284	9.3500004	-2.723187
1.87	-0.14205202	4.3600001	-0.77475939	6.8600001	-2.9715289	9.3599997	-2.6717028
1.88	-0.14448253	4.3699999	-0.77080088	6.8699999	-3.062353	9.3699999	-2.6214325
1.89	-0.14705572	4.3800001	-0.76723275	6.8800001	-3.1598209	9.3800001	-2.5724506
1.9	-0.14972591	4.3899999	-0.76388881	6.8899999	-3.2643406	9.3900003	-2.5248117
1.91	-0.15244451	4.4000001	-0.76061841	6.9000001	-3.376303	9.3999996	-2.4785595
1.92	-0.15516331	4.4099998	-0.7572871	6.9099998	-3.4960667	9.4099998	-2.433729
1.9299999	-0.15783492	4.4200001	-0.75379004	6.9200001	-3.6239475	9.4200001	-2.390349
1.9400001	-0.1604171	4.4299998	-0.75005485	6.9299998	-3.7601973	9.4300003	-2.3484444
1.95	-0.16287237	4.4400001	-0.74604649	6.9400001	-3.9049965	9.4399996	-2.308043
1.96	-0.1651716	4.4499998	-0.74176635	6.9499998	-4.0584297	9.4499998	-2.2691663
1.97	-0.16729486	4.46	-0.73726034	6.96	-4.2204665	9.46	-2.2318374
1.98	-0.16923216	4.4699998	-0.73261039	6.9699998	-4.3909441	9.4700003	-2.1960741
1.99	-0.1709858	4.48	-0.72793678	6.98	-4.5695391	9.4799995	-2.1618905
2	-0.17256895	4.4899998	-0.72339183	6.9899998	-4.7557407	9.4899998	-2.1292919
2.01	-0.1740057	4.5	-0.71915554	7	-4.9488297	9.5	-2.0982736
2.02	-0.1753318	4.5100002	-0.71542493	7.0100002	-5.1478437	9.5100002	-2.068821
2.03	-0.17659263	4.52	-0.71241091	7.02	-5.3515497	9.5200005	-2.0409034
2.04	-0.17784071	4.5300002	-0.71032657	7.0300002	-5.5584215	9.5299997	-2.0144743
2.05	-0.17913454	4.54	-0.70937842	7.04	-5.7666174	9.54	-1.9894728
2.0599999	-0.18053775	4.5500002	-0.7097579	7.0500002	-5.9739699	9.5500002	-1.9658198
2.0699999	-0.18211268	4.5599999	-0.71163338	7.0599999	-6.1779855	9.5600004	-1.9434219
2.0799999	-0.18392294	4.5700002	-0.71514191	7.0700002	-6.3758752	9.5699997	-1.9221714
2.0899999	-0.18602412	4.5799999	-0.72038204	7.0799999	-6.5645986	9.5799999	-1.9019485
2.0999999	-0.18846994	4.5900002	-0.72740897	7.0900002	-6.7409476	9.5900002	-1.882624
2.1099999	-0.19130075	4.5999999	-0.73622905	7.0999999	-6.9016596	9.6000004	-1.8640648
2.1199999	-0.19454995	4.6100001	-0.74679712	7.1100001	-7.0435638	9.6099997	-1.8461367
2.1300001	-0.19823408	4.6199999	-0.75901504	7.1199999	-7.1637509	9.6199999	-1.8287089
2.1400001	-0.20236025	4.6300001	-0.77273461	7.1300001	-7.2597516	9.6300001	-1.8116572
2.1500001	-0.20691844	4.6399999	-0.7877537	7.1399999	-7.3297061	9.6400003	-1.7948726
2.1600001	-0.21188547	4.6500001	-0.80382658	7.1500001	-7.3724982	9.6499996	-1.778261
2.1700001	-0.21722532	4.6599998	-0.8206673	7.1599998	-7.3878401	9.6599998	-1.7617472
2.1800001	-0.2228879	4.6700001	-0.83795346	7.1700001	-7.3762886	9.6700001	-1.7452804
2.1900001	-0.22881533	4.6799998	-0.85534264	7.1799998	-7.3391975	9.6800003	-1.7288326
2.2	-0.23493832	4.6900001	-0.87247308	7.1900001	-7.2786037	9.6899996	-1.7124019
2.21	-0.24118514	4.6999998	-0.88898276	7.1999998	-7.1970774	9.6999998	-1.6960085
2.22	-0.24747983	4.71	-0.90451669	7.21	-7.0975456	9.71	-1.6796989
2.23	-0.25374834	4.7199998	-0.91874008	7.2199998	-6.983121	9.7200003	-1.6635373
2.24	-0.25992065	4.73	-0.93134895	7.23	-6.8569435	9.7299995	-1.6476059
2.25	-0.26593585	4.7399998	-0.9420805	7.2399998	-6.7220571	9.7399998	-1.6320006
2.26	-0.2717415	4.75	-0.95072459	7.25	-6.5813107	9.75	-1.6168231
2.27	-0.27730215	4.7600002	-0.95712757	7.2600002	-6.4373012	9.7600002	-1.6021789
2.28	-0.28259502	4.77	-0.96120275	7.27	-6.2923356	9.7700005	-1.5881713
2.29	-0.28761844	4.7800002	-0.96292577	7.2800002	-6.1484259	9.7799997	-1.5748963
2.3	-0.29238681	4.79	-0.96234253	7.29	-6.0072904	9.79	-1.5624387
2.3099999	-0.29693545	4.8000002	-0.95956064	7.3000002	-5.8703742	9.8000002	-1.5508639
2.3199999	-0.30131718	4.8099999	-0.95474924	7.3099999	-5.7388724	9.8100004	-1.5402222
2.3299999	-0.30560115	4.8200002	-0.94812914	7.3200002	-5.6137591	9.8199997	-1.5305381
2.3399999	-0.30987298	4.8299999	-0.93996311	7.3299999	-5.4958113	9.8299999	-1.5218137
2.3499999	-0.31422722	4.8400002	-0.93055054	7.3400002	-5.3856408	9.8400002	-1.5140292
2.3599999	-0.31876895	4.8499999	-0.9202112	7.3499999	-5.2837106	9.8500004	-1.5071388
2.3699999	-0.32360853	4.8600001	-0.90927704	7.3600001	-5.1903646	9.8599997	-1.5010782
2.3800001	-0.32885144	4.8699999	-0.8980829	7.3699999	-5.1058393	9.8699999	-1.4957622
2.3900001	-0.33460435	4.8800001	-0.88695225	7.3800001	-5.0302821	9.8800001	-1.4910933
2.4000001	-0.34096178	4.8899999	-0.87618948	7.3899999	-4.9637604	9.8900003	-1.4869606
2.4100001	-0.34800816	4.9000001	-0.86607557	7.4000001	-4.9062722	9.8999996	-1.4832519
2.4200001	-0.3558077	4.9099998	-0.85685557	7.4099998	-4.857752	9.9099998	-1.4798511
2.4300001	-0.36440827	4.9200001	-0.8487368	7.4200001	-4.8180723	9.9200001	-1.4766483
2.4400001	-0.37383442	4.9299998	-0.84188789	7.4299998	-4.7870479	9.9300003	-1.4735461
2.45	-0.38408694	4.9400001	-0.83643238	7.4400001	-4.7644345	9.9399996	-1.4704579
2.46	-0.39514335	4.9499998	-0.83245274	7.4499998	-4.7499275	9.9499998	-1.4673189
2.47	-0.40695556	4.96	-0.82998674	7.46	-4.7431578	9.96	-1.4640861
2.48	-0.41945342	4.9699998	-0.82903816	7.4699998	-4.7436895	9.9700003	-1.4607392

	4.98	-0.8295704		7.48	-4.7510154		9.9799995	-1.4572826
							9.9899998	-1.4537464
							10	-1.4501807

b. Rl 4 elemen

c. Rl 16 elemen

d. Hpbw 1 elemen

Theta [deg.]	Phi [deg.]	Abs(Dir.)[dBi]	Abs(Theta)[dBi]	Phase(Theta)[deg.]	Abs(Phi)[dBi]	Phase(Phi)[deg.]	Ax.Ratio[dB]
0	90	6.56E+00	5.35E+00	168.248	4.32E-01	199.224	1.27E+01
1	90	6.56E+00	5.35E+00	168.211	4.30E-01	199.222	1.26E+01
2	90	6.55E+00	5.34E+00	168.173	4.26E-01	199.216	1.26E+01
3	90	6.55E+00	5.33E+00	168.135	4.18E-01	199.205	1.26E+01
4	90	6.54E+00	5.32E+00	168.095	4.07E-01	199.19	1.26E+01
5	90	6.52E+00	5.31E+00	168.055	3.94E-01	199.17	1.26E+01
6	90	6.50E+00	5.29E+00	168.014	3.77E-01	199.147	1.26E+01
7	90	6.48E+00	5.27E+00	167.973	3.57E-01	199.119	1.26E+01
8	90	6.46E+00	5.25E+00	167.93	3.34E-01	199.086	1.26E+01
9	90	6.43E+00	5.22E+00	167.887	3.08E-01	199.05	1.26E+01
10	90	6.41E+00	5.19E+00	167.842	2.78E-01	199.008	1.26E+01
11	90	6.37E+00	5.16E+00	167.797	2.46E-01	198.963	1.26E+01
12	90	6.34E+00	5.12E+00	167.751	2.11E-01	198.913	1.26E+01
13	90	6.30E+00	5.09E+00	167.705	1.73E-01	198.859	1.26E+01
14	90	6.26E+00	5.05E+00	167.657	1.31E-01	198.8	1.26E+01
15	90	6.22E+00	5.00E+00	167.609	8.70E-02	198.737	1.26E+01
16	90	6.17E+00	4.96E+00	167.559	3.97E-02	198.669	1.26E+01
17	90	6.12E+00	4.91E+00	167.509	-1.05E-02	198.597	1.26E+01
18	90	6.07E+00	4.85E+00	167.458	-6.37E-02	198.52	1.26E+01
19	90	6.01E+00	4.80E+00	167.406	-1.20E-01	198.439	1.26E+01
20	90	5.95E+00	4.74E+00	167.353	-1.79E-01	198.352	1.27E+01
21	90	5.89E+00	4.68E+00	167.299	-2.41E-01	198.262	1.27E+01
22	90	5.83E+00	4.62E+00	167.244	-3.05E-01	198.166	1.27E+01
23	90	5.76E+00	4.55E+00	167.188	-3.73E-01	198.066	1.27E+01
24	90	5.69E+00	4.48E+00	167.131	-4.43E-01	197.961	1.27E+01
25	90	5.62E+00	4.41E+00	167.073	-5.17E-01	197.851	1.27E+01
26	90	5.55E+00	4.33E+00	167.014	-5.93E-01	197.736	1.27E+01
27	90	5.47E+00	4.26E+00	166.954	-6.71E-01	197.616	1.28E+01
28	90	5.39E+00	4.18E+00	166.893	-7.53E-01	197.492	1.28E+01
29	90	5.30E+00	4.09E+00	166.831	-8.37E-01	197.362	1.28E+01
30	90	5.22E+00	4.01E+00	166.768	-9.24E-01	197.227	1.28E+01
31	90	5.13E+00	3.92E+00	166.704	-1.01E+00	197.088	1.28E+01
32	90	5.04E+00	3.83E+00	166.639	-1.11E+00	196.943	1.29E+01
33	90	4.95E+00	3.74E+00	166.572	-1.20E+00	196.793	1.29E+01
34	90	4.85E+00	3.64E+00	166.504	-1.30E+00	196.638	1.29E+01
35	90	4.75E+00	3.54E+00	166.435	-1.40E+00	196.477	1.29E+01
36	90	4.65E+00	3.44E+00	166.365	-1.50E+00	196.311	1.30E+01
37	90	4.55E+00	3.34E+00	166.294	-1.60E+00	196.14	1.30E+01
38	90	4.44E+00	3.23E+00	166.221	-1.71E+00	195.964	1.30E+01
39	90	4.33E+00	3.13E+00	166.147	-1.82E+00	195.782	1.31E+01
40	90	4.22E+00	3.02E+00	166.072	-1.93E+00	195.595	1.31E+01
41	90	4.11E+00	2.90E+00	165.996	-2.05E+00	195.402	1.31E+01
42	90	3.99E+00	2.79E+00	165.918	-2.16E+00	195.204	1.32E+01
43	90	3.88E+00	2.67E+00	165.839	-2.28E+00	195	1.32E+01
44	90	3.76E+00	2.55E+00	165.758	-2.40E+00	194.791	1.32E+01
45	90	3.63E+00	2.43E+00	165.676	-2.52E+00	194.576	1.33E+01
46	90	3.51E+00	2.30E+00	165.592	-2.65E+00	194.356	1.33E+01
47	90	3.38E+00	2.18E+00	165.507	-2.77E+00	194.13	1.34E+01
48	90	3.25E+00	2.05E+00	165.42	-2.90E+00	193.899	1.34E+01
49	90	3.12E+00	1.92E+00	165.331	-3.03E+00	193.662	1.35E+01

50	90	2.99E+00	1.78E+00	165.241	-3.17E+00	193.42	1.35E+01
51	90	2.85E+00	1.65E+00	165.149	-3.30E+00	193.172	1.36E+01
52	90	2.72E+00	1.51E+00	165.056	-3.44E+00	192.919	1.36E+01
53	90	2.58E+00	1.37E+00	164.961	-3.57E+00	192.66	1.36E+01
54	90	2.44E+00	1.23E+00	164.863	-3.71E+00	192.396	1.37E+01
55	90	2.29E+00	1.09E+00	164.764	-3.86E+00	192.127	1.38E+01
56	90	2.15E+00	9.40E-01	164.663	-4.00E+00	191.853	1.38E+01
57	90	2.00E+00	7.93E-01	164.56	-4.14E+00	191.573	1.39E+01
58	90	1.85E+00	6.43E-01	164.454	-4.29E+00	191.288	1.39E+01
59	90	1.70E+00	4.91E-01	164.347	-4.44E+00	190.998	1.40E+01
60	90	1.55E+00	3.37E-01	164.237	-4.59E+00	190.704	1.40E+01
61	90	1.40E+00	1.81E-01	164.125	-4.74E+00	190.405	1.41E+01
62	90	1.24E+00	2.32E-02	164.01	-4.89E+00	190.101	1.42E+01
63	90	1.08E+00	-1.37E-01	163.892	-5.04E+00	189.793	1.42E+01
64	90	9.20E-01	-2.99E-01	163.772	-5.19E+00	189.48	1.43E+01
65	90	7.59E-01	-4.62E-01	163.649	-5.35E+00	189.164	1.43E+01
66	90	5.95E-01	-6.28E-01	163.523	-5.51E+00	188.844	1.44E+01
67	90	4.30E-01	-7.96E-01	163.394	-5.66E+00	188.52	1.45E+01
68	90	2.63E-01	-9.66E-01	163.262	-5.82E+00	188.193	1.45E+01
69	90	9.39E-02	-1.14E+00	163.126	-5.98E+00	187.863	1.46E+01
70	90	-7.67E-02	-1.31E+00	162.986	-6.14E+00	187.53	1.46E+01
71	90	-2.49E-01	-1.49E+00	162.843	-6.30E+00	187.195	1.47E+01
72	90	-4.23E-01	-1.67E+00	162.696	-6.46E+00	186.857	1.48E+01
73	90	-5.99E-01	-1.85E+00	162.544	-6.63E+00	186.518	1.48E+01
74	90	-7.77E-01	-2.03E+00	162.388	-6.79E+00	186.178	1.49E+01
75	90	-9.56E-01	-2.21E+00	162.226	-6.95E+00	185.837	1.49E+01
76	90	-1.14E+00	-2.40E+00	162.06	-7.12E+00	185.496	1.50E+01
77	90	-1.32E+00	-2.59E+00	161.889	-7.28E+00	185.154	1.50E+01
78	90	-1.51E+00	-2.78E+00	161.711	-7.45E+00	184.814	1.51E+01
79	90	-1.69E+00	-2.98E+00	161.528	-7.61E+00	184.474	1.51E+01
80	90	-1.88E+00	-3.17E+00	161.337	-7.78E+00	184.136	1.52E+01
81	90	-2.07E+00	-3.37E+00	161.14	-7.95E+00	183.801	1.52E+01
82	90	-2.27E+00	-3.57E+00	160.936	-8.11E+00	183.468	1.52E+01
83	90	-2.46E+00	-3.78E+00	160.723	-8.28E+00	183.14	1.53E+01
84	90	-2.66E+00	-3.99E+00	160.502	-8.45E+00	182.816	1.53E+01
85	90	-2.86E+00	-4.20E+00	160.271	-8.61E+00	182.497	1.53E+01
86	90	-3.06E+00	-4.41E+00	160.031	-8.78E+00	182.184	1.53E+01
87	90	-3.26E+00	-4.63E+00	159.78	-8.95E+00	181.877	1.53E+01
88	90	-3.47E+00	-4.85E+00	159.518	-9.12E+00	181.579	1.53E+01
89	90	-3.67E+00	-5.07E+00	159.243	-9.28E+00	181.289	1.53E+01
90	90	-3.89E+00	-5.30E+00	158.955	-9.45E+00	181.008	1.52E+01
91	90	-4.10E+00	-5.53E+00	158.653	-9.62E+00	180.739	1.52E+01
92	90	-4.31E+00	-5.76E+00	158.335	-9.78E+00	180.48	1.51E+01
93	90	-4.53E+00	-6.00E+00	158.001	-9.95E+00	180.234	1.51E+01
94	90	-4.75E+00	-6.25E+00	157.649	-1.01E+01	180.002	1.50E+01
95	90	-4.98E+00	-6.49E+00	157.277	-1.03E+01	179.785	1.49E+01
96	90	-5.20E+00	-6.75E+00	156.884	-1.05E+01	179.584	1.48E+01
97	90	-5.43E+00	-7.01E+00	156.468	-1.06E+01	179.399	1.46E+01
98	90	-5.67E+00	-7.27E+00	156.027	-1.08E+01	179.234	1.45E+01
99	90	-5.90E+00	-7.54E+00	155.558	-1.09E+01	179.087	1.43E+01
100	90	-6.14E+00	-7.81E+00	155.06	-1.11E+01	178.962	1.42E+01
101	90	-6.39E+00	-8.09E+00	154.529	-1.13E+01	178.859	1.40E+01
102	90	-6.63E+00	-8.38E+00	153.962	-1.14E+01	178.779	1.37E+01
103	90	-6.88E+00	-8.67E+00	153.356	-1.16E+01	178.725	1.35E+01
104	90	-7.14E+00	-8.98E+00	152.707	-1.18E+01	178.696	1.32E+01
105	90	-7.39E+00	-9.29E+00	152.01	-1.19E+01	178.695	1.29E+01
106	90	-7.65E+00	-9.60E+00	151.261	-1.21E+01	178.724	1.26E+01
107	90	-7.92E+00	-9.93E+00	150.454	-1.22E+01	178.782	1.23E+01
108	90	-8.19E+00	-1.03E+01	149.582	-1.24E+01	178.873	1.20E+01
109	90	-8.46E+00	-1.06E+01	148.64	-1.25E+01	178.996	1.16E+01
110	90	-8.73E+00	-1.10E+01	147.618	-1.27E+01	179.154	1.12E+01
111	90	-9.01E+00	-1.13E+01	146.508	-1.29E+01	179.348	1.08E+01
112	90	-9.28E+00	-1.17E+01	145.3	-1.30E+01	179.579	1.03E+01

113	90	-9.57E+00	-1.21E+01	143.981	-1.32E+01	179.848	9.88E+00
114	90	-9.85E+00	-1.25E+01	142.539	-1.33E+01	180.156	9.41E+00
115	90	-1.01E+01	-1.29E+01	140.959	-1.34E+01	180.505	8.91E+00
116	90	-1.04E+01	-1.33E+01	139.224	-1.36E+01	180.895	8.40E+00
117	90	-1.07E+01	-1.37E+01	137.315	-1.37E+01	181.327	7.87E+00
118	90	-1.10E+01	-1.41E+01	135.211	-1.39E+01	181.802	7.33E+00
119	90	-1.13E+01	-1.46E+01	132.891	-1.40E+01	182.32	6.77E+00
120	90	-1.15E+01	-1.50E+01	130.328	-1.41E+01	182.882	6.20E+00
121	90	-1.18E+01	-1.54E+01	127.499	-1.42E+01	183.488	5.63E+00
122	90	-1.20E+01	-1.59E+01	124.378	-1.44E+01	184.138	5.07E+00
123	90	-1.23E+01	-1.63E+01	120.942	-1.45E+01	184.831	4.51E+00
124	90	-1.25E+01	-1.67E+01	117.174	-1.46E+01	185.567	3.99E+00
125	90	-1.27E+01	-1.71E+01	113.065	-1.47E+01	186.346	3.52E+00
126	90	-1.29E+01	-1.74E+01	108.619	-1.48E+01	187.166	3.15E+00
127	90	-1.31E+01	-1.77E+01	103.858	-1.49E+01	188.025	2.94E+00
128	90	-1.32E+01	-1.79E+01	98.825	-1.50E+01	188.922	2.95E+00
129	90	-1.33E+01	-1.81E+01	93.584	-1.51E+01	189.856	3.18E+00
130	90	-1.34E+01	-1.82E+01	88.222	-1.51E+01	190.823	3.62E+00
131	90	-1.34E+01	-1.82E+01	82.834	-1.52E+01	191.822	4.22E+00
132	90	-1.34E+01	-1.81E+01	77.521	-1.53E+01	192.849	4.94E+00
133	90	-1.34E+01	-1.80E+01	72.376	-1.53E+01	193.901	5.76E+00
134	90	-1.34E+01	-1.78E+01	67.475	-1.54E+01	194.975	6.66E+00
135	90	-1.33E+01	-1.75E+01	62.871	-1.54E+01	196.068	7.64E+00
136	90	-1.32E+01	-1.72E+01	58.599	-1.54E+01	197.176	8.69E+00
137	90	-1.31E+01	-1.69E+01	54.671	-1.54E+01	198.295	9.81E+00
138	90	-1.29E+01	-1.65E+01	51.084	-1.55E+01	199.421	1.10E+01
139	90	-1.28E+01	-1.61E+01	47.825	-1.55E+01	200.551	1.23E+01
140	90	-1.26E+01	-1.58E+01	44.874	-1.55E+01	201.68	1.38E+01
141	90	-1.24E+01	-1.54E+01	42.205	-1.55E+01	202.805	1.53E+01
142	90	-1.22E+01	-1.50E+01	39.795	-1.54E+01	203.923	1.71E+01
143	90	-1.20E+01	-1.47E+01	37.619	-1.54E+01	205.029	1.92E+01
144	90	-1.18E+01	-1.43E+01	35.652	-1.54E+01	206.121	2.17E+01
145	90	-1.16E+01	-1.40E+01	33.873	-1.54E+01	207.196	2.48E+01
146	90	-1.14E+01	-1.36E+01	32.262	-1.53E+01	208.25	2.93E+01
147	90	-1.12E+01	-1.33E+01	30.802	-1.53E+01	209.282	3.78E+01
148	90	-1.09E+01	-1.30E+01	29.477	-1.52E+01	210.288	4.00E+01
149	90	-1.07E+01	-1.27E+01	28.273	-1.52E+01	211.268	3.20E+01
150	90	-1.05E+01	-1.24E+01	27.177	-1.51E+01	212.218	2.76E+01
151	90	-1.03E+01	-1.21E+01	26.179	-1.51E+01	213.139	2.48E+01
152	90	-1.01E+01	-1.19E+01	25.268	-1.50E+01	214.028	2.29E+01
153	90	-9.95E+00	-1.16E+01	24.438	-1.49E+01	214.884	2.14E+01
154	90	-9.77E+00	-1.14E+01	23.68	-1.49E+01	215.707	2.03E+01
155	90	-9.59E+00	-1.12E+01	22.988	-1.48E+01	216.496	1.93E+01
156	90	-9.42E+00	-1.09E+01	22.356	-1.47E+01	217.251	1.85E+01
157	90	-9.26E+00	-1.07E+01	21.78	-1.47E+01	217.972	1.78E+01
158	90	-9.11E+00	-1.06E+01	21.254	-1.46E+01	218.658	1.73E+01
159	90	-8.96E+00	-1.04E+01	20.774	-1.45E+01	219.31	1.68E+01
160	90	-8.82E+00	-1.02E+01	20.338	-1.45E+01	219.927	1.63E+01
161	90	-8.69E+00	-1.00E+01	19.942	-1.44E+01	220.51	1.59E+01
162	90	-8.56E+00	-9.89E+00	19.584	-1.43E+01	221.06	1.56E+01
163	90	-8.44E+00	-9.76E+00	19.26	-1.43E+01	221.576	1.53E+01
164	90	-8.33E+00	-9.63E+00	18.969	-1.42E+01	222.06	1.51E+01
165	90	-8.23E+00	-9.51E+00	18.71	-1.42E+01	222.511	1.48E+01
166	90	-8.14E+00	-9.40E+00	18.479	-1.41E+01	222.93	1.46E+01
167	90	-8.05E+00	-9.30E+00	18.276	-1.41E+01	223.318	1.44E+01
168	90	-7.97E+00	-9.21E+00	18.1	-1.40E+01	223.674	1.43E+01
169	90	-7.90E+00	-9.13E+00	17.949	-1.40E+01	224	1.41E+01
170	90	-7.84E+00	-9.06E+00	17.823	-1.39E+01	224.297	1.40E+01
171	90	-7.78E+00	-9.00E+00	17.72	-1.39E+01	224.563	1.39E+01
172	90	-7.73E+00	-8.95E+00	17.64	-1.39E+01	224.8	1.38E+01
173	90	-7.69E+00	-8.91E+00	17.582	-1.38E+01	225.009	1.37E+01
174	90	-7.66E+00	-8.87E+00	17.546	-1.38E+01	225.189	1.37E+01
175	90	-7.64E+00	-8.85E+00	17.531	-1.38E+01	225.341	1.36E+01

176	90	-7.62E+00	-8.83E+00	17.538	-1.38E+01	225.465	1.36E+01
177	90	-7.61E+00	-8.82E+00	17.566	-1.37E+01	225.561	1.35E+01
178	90	-7.61E+00	-8.82E+00	17.614	-1.37E+01	225.63	1.35E+01
179	90	-7.61E+00	-8.83E+00	17.684	-1.37E+01	225.671	1.35E+01
180	90	-7.63E+00	-8.85E+00	17.775	-1.37E+01	225.685	1.35E+01
179	270	-7.65E+00	-8.88E+00	197.888	-1.37E+01	45.672	1.36E+01
178	270	-7.68E+00	-8.92E+00	198.022	-1.37E+01	45.632	1.36E+01
177	270	-7.72E+00	-8.96E+00	198.178	-1.37E+01	45.564	1.37E+01
176	270	-7.76E+00	-9.02E+00	198.358	-1.38E+01	45.469	1.37E+01
175	270	-7.81E+00	-9.08E+00	198.561	-1.38E+01	45.346	1.38E+01
174	270	-7.87E+00	-9.16E+00	198.788	-1.38E+01	45.195	1.39E+01
173	270	-7.94E+00	-9.24E+00	199.041	-1.38E+01	45.016	1.40E+01
172	270	-8.02E+00	-9.33E+00	199.32	-1.39E+01	44.809	1.41E+01
171	270	-8.10E+00	-9.44E+00	199.627	-1.39E+01	44.573	1.43E+01
170	270	-8.20E+00	-9.55E+00	199.964	-1.39E+01	44.308	1.45E+01
169	270	-8.30E+00	-9.67E+00	200.331	-1.40E+01	44.014	1.47E+01
168	270	-8.40E+00	-9.80E+00	200.732	-1.40E+01	43.689	1.49E+01
167	270	-8.52E+00	-9.95E+00	201.167	-1.41E+01	43.335	1.52E+01
166	270	-8.65E+00	-1.01E+01	201.64	-1.41E+01	42.949	1.55E+01
165	270	-8.78E+00	-1.03E+01	202.153	-1.42E+01	42.532	1.58E+01
164	270	-8.92E+00	-1.04E+01	202.71	-1.42E+01	42.084	1.62E+01
163	270	-9.07E+00	-1.06E+01	203.314	-1.43E+01	41.603	1.66E+01
162	270	-9.22E+00	-1.08E+01	203.968	-1.43E+01	41.089	1.72E+01
161	270	-9.39E+00	-1.10E+01	204.678	-1.44E+01	40.543	1.78E+01
160	270	-9.56E+00	-1.13E+01	205.448	-1.45E+01	39.963	1.85E+01
159	270	-9.74E+00	-1.15E+01	206.285	-1.45E+01	39.349	1.94E+01
158	270	-9.92E+00	-1.17E+01	207.195	-1.46E+01	38.701	2.04E+01
157	270	-1.01E+01	-1.20E+01	208.185	-1.47E+01	38.019	2.17E+01
156	270	-1.03E+01	-1.23E+01	209.264	-1.47E+01	37.302	2.34E+01
155	270	-1.05E+01	-1.26E+01	210.442	-1.48E+01	36.552	2.57E+01
154	270	-1.07E+01	-1.29E+01	211.729	-1.49E+01	35.767	2.93E+01
153	270	-1.09E+01	-1.32E+01	213.139	-1.49E+01	34.949	3.62E+01
152	270	-1.12E+01	-1.35E+01	214.685	-1.50E+01	34.098	4.00E+01
151	270	-1.14E+01	-1.38E+01	216.383	-1.50E+01	33.215	3.13E+01
150	270	-1.16E+01	-1.42E+01	218.253	-1.51E+01	32.301	2.57E+01
149	270	-1.18E+01	-1.45E+01	220.313	-1.52E+01	31.356	2.21E+01
148	270	-1.20E+01	-1.49E+01	222.587	-1.52E+01	30.383	1.94E+01
147	270	-1.23E+01	-1.53E+01	225.099	-1.53E+01	29.382	1.72E+01
146	270	-1.25E+01	-1.57E+01	227.873	-1.53E+01	28.357	1.53E+01
145	270	-1.27E+01	-1.60E+01	230.936	-1.53E+01	27.31	1.36E+01
144	270	-1.29E+01	-1.64E+01	234.313	-1.54E+01	26.242	1.21E+01
143	270	-1.30E+01	-1.68E+01	238.023	-1.54E+01	25.156	1.07E+01
142	270	-1.32E+01	-1.71E+01	242.081	-1.54E+01	24.057	9.46E+00
141	270	-1.33E+01	-1.74E+01	246.487	-1.54E+01	22.946	8.28E+00
140	270	-1.34E+01	-1.77E+01	251.228	-1.54E+01	21.827	7.17E+00
139	270	-1.35E+01	-1.79E+01	256.267	-1.54E+01	20.704	6.14E+00
138	270	-1.35E+01	-1.80E+01	261.546	-1.54E+01	19.58	5.18E+00
137	270	-1.35E+01	-1.81E+01	266.985	-1.54E+01	18.46	4.31E+00
136	270	-1.35E+01	-1.81E+01	272.488	-1.54E+01	17.347	3.53E+00
135	270	-1.35E+01	-1.80E+01	277.952	-1.54E+01	16.244	2.90E+00
134	270	-1.34E+01	-1.78E+01	283.277	-1.53E+01	15.156	2.49E+00
133	270	-1.33E+01	-1.76E+01	288.38	-1.53E+01	14.087	2.38E+00
132	270	-1.31E+01	-1.73E+01	293.196	-1.52E+01	13.038	2.57E+00
131	270	-1.30E+01	-1.69E+01	297.686	-1.52E+01	12.015	2.99E+00
130	270	-1.28E+01	-1.66E+01	301.83	-1.51E+01	11.019	3.55E+00
129	270	-1.26E+01	-1.62E+01	305.627	-1.50E+01	10.055	4.18E+00
128	270	-1.23E+01	-1.57E+01	309.087	-1.50E+01	9.123	4.84E+00
127	270	-1.21E+01	-1.53E+01	312.23	-1.49E+01	8.227	5.51E+00
126	270	-1.18E+01	-1.49E+01	315.08	-1.48E+01	7.369	6.18E+00
125	270	-1.16E+01	-1.45E+01	317.663	-1.47E+01	6.55	6.85E+00
124	270	-1.13E+01	-1.40E+01	320.004	-1.46E+01	5.772	7.52E+00
123	270	-1.10E+01	-1.36E+01	322.127	-1.45E+01	5.036	8.17E+00
122	270	-1.07E+01	-1.32E+01	324.056	-1.44E+01	4.342	8.81E+00

121	270	-1.04E+01	-1.28E+01	325.812	-1.42E+01	3.692	9.44E+00
120	270	-1.02E+01	-1.24E+01	327.413	-1.41E+01	3.085	1.01E+01
119	270	-9.88E+00	-1.20E+01	328.876	-1.40E+01	2.521	1.07E+01
118	270	-9.61E+00	-1.17E+01	330.216	-1.39E+01	2.001	1.12E+01
117	270	-9.33E+00	-1.13E+01	331.445	-1.37E+01	1.524	1.18E+01
116	270	-9.06E+00	-1.10E+01	332.575	-1.36E+01	1.09	1.23E+01
115	270	-8.79E+00	-1.06E+01	333.617	-1.34E+01	0.697	1.29E+01
114	270	-8.52E+00	-1.03E+01	334.579	-1.33E+01	0.346	1.34E+01
113	270	-8.26E+00	-9.96E+00	335.468	-1.32E+01	0.035	1.39E+01
112	270	-8.00E+00	-9.64E+00	336.293	-1.30E+01	359.763	1.43E+01
111	270	-7.74E+00	-9.34E+00	337.058	-1.29E+01	359.529	1.48E+01
110	270	-7.49E+00	-9.05E+00	337.77	-1.27E+01	359.332	1.52E+01
109	270	-7.24E+00	-8.76E+00	338.433	-1.26E+01	359.171	1.56E+01
108	270	-7.00E+00	-8.48E+00	339.052	-1.24E+01	359.044	1.60E+01
107	270	-6.76E+00	-8.21E+00	339.629	-1.22E+01	358.95	1.63E+01
106	270	-6.53E+00	-7.94E+00	340.17	-1.21E+01	358.888	1.67E+01
105	270	-6.29E+00	-7.68E+00	340.676	-1.19E+01	358.857	1.70E+01
104	270	-6.07E+00	-7.43E+00	341.151	-1.18E+01	358.854	1.72E+01
103	270	-5.84E+00	-7.18E+00	341.597	-1.16E+01	358.879	1.75E+01
102	270	-5.62E+00	-6.94E+00	342.016	-1.14E+01	358.93	1.77E+01
101	270	-5.40E+00	-6.70E+00	342.41	-1.13E+01	359.006	1.79E+01
100	270	-5.19E+00	-6.47E+00	342.781	-1.11E+01	359.106	1.81E+01
99	270	-4.97E+00	-6.24E+00	343.13	-1.10E+01	359.227	1.83E+01
98	270	-4.76E+00	-6.01E+00	343.46	-1.08E+01	359.37	1.84E+01
97	270	-4.56E+00	-5.79E+00	343.771	-1.06E+01	359.533	1.85E+01
96	270	-4.35E+00	-5.58E+00	344.065	-1.05E+01	359.714	1.86E+01
95	270	-4.15E+00	-5.36E+00	344.343	-1.03E+01	359.912	1.87E+01
94	270	-3.95E+00	-5.15E+00	344.606	-1.01E+01	0.126	1.87E+01
93	270	-3.76E+00	-4.95E+00	344.855	-9.96E+00	0.354	1.87E+01
92	270	-3.56E+00	-4.75E+00	345.09	-9.80E+00	0.597	1.88E+01
91	270	-3.37E+00	-4.55E+00	345.313	-9.63E+00	0.852	1.88E+01
90	270	-3.18E+00	-4.35E+00	345.524	-9.46E+00	1.119	1.87E+01
89	270	-2.99E+00	-4.16E+00	345.725	-9.30E+00	1.396	1.87E+01
88	270	-2.81E+00	-3.96E+00	345.915	-9.13E+00	1.683	1.87E+01
87	270	-2.63E+00	-3.77E+00	346.095	-8.96E+00	1.979	1.86E+01
86	270	-2.44E+00	-3.59E+00	346.266	-8.79E+00	2.282	1.86E+01
85	270	-2.26E+00	-3.40E+00	346.428	-8.63E+00	2.592	1.85E+01
84	270	-2.08E+00	-3.22E+00	346.582	-8.46E+00	2.908	1.84E+01
83	270	-1.91E+00	-3.04E+00	346.728	-8.29E+00	3.23	1.83E+01
82	270	-1.73E+00	-2.86E+00	346.867	-8.12E+00	3.555	1.82E+01
81	270	-1.56E+00	-2.69E+00	346.999	-7.96E+00	3.885	1.81E+01
80	270	-1.38E+00	-2.51E+00	347.124	-7.79E+00	4.218	1.80E+01
79	270	-1.21E+00	-2.34E+00	347.243	-7.63E+00	4.553	1.79E+01
78	270	-1.04E+00	-2.17E+00	347.356	-7.46E+00	4.89	1.78E+01
77	270	-8.75E-01	-2.00E+00	347.463	-7.29E+00	5.228	1.77E+01
76	270	-7.08E-01	-1.83E+00	347.565	-7.13E+00	5.567	1.76E+01
75	270	-5.42E-01	-1.67E+00	347.662	-6.96E+00	5.906	1.75E+01
74	270	-3.78E-01	-1.50E+00	347.754	-6.80E+00	6.245	1.74E+01
73	270	-2.16E-01	-1.34E+00	347.841	-6.64E+00	6.583	1.72E+01
72	270	-5.41E-02	-1.18E+00	347.923	-6.47E+00	6.92	1.71E+01
71	270	1.06E-01	-1.02E+00	348.002	-6.31E+00	7.255	1.70E+01
70	270	2.65E-01	-8.61E-01	348.076	-6.15E+00	7.588	1.69E+01
69	270	4.22E-01	-7.04E-01	348.146	-5.99E+00	7.919	1.68E+01
68	270	5.78E-01	-5.49E-01	348.213	-5.83E+00	8.247	1.67E+01
67	270	7.33E-01	-3.96E-01	348.276	-5.67E+00	8.572	1.65E+01
66	270	8.86E-01	-2.44E-01	348.335	-5.52E+00	8.894	1.64E+01
65	270	1.04E+00	-9.31E-02	348.391	-5.36E+00	9.213	1.63E+01
64	270	1.19E+00	5.59E-02	348.445	-5.20E+00	9.527	1.62E+01
63	270	1.34E+00	2.03E-01	348.495	-5.05E+00	9.838	1.61E+01
62	270	1.49E+00	3.49E-01	348.542	-4.90E+00	10.144	1.60E+01
61	270	1.63E+00	4.94E-01	348.586	-4.75E+00	10.447	1.59E+01
60	270	1.78E+00	6.37E-01	348.628	-4.60E+00	10.744	1.58E+01
59	270	1.92E+00	7.78E-01	348.667	-4.45E+00	11.037	1.57E+01

58	270	2.06E+00	9.18E-01	348.703	-4.30E+00	11.325	1.56E+01
57	270	2.20E+00	1.06E+00	348.737	-4.15E+00	11.609	1.55E+01
56	270	2.34E+00	1.19E+00	348.769	-4.01E+00	11.887	1.54E+01
55	270	2.48E+00	1.33E+00	348.798	-3.86E+00	12.16	1.53E+01
54	270	2.61E+00	1.46E+00	348.826	-3.72E+00	12.428	1.52E+01
53	270	2.74E+00	1.59E+00	348.851	-3.58E+00	12.691	1.51E+01
52	270	2.88E+00	1.72E+00	348.874	-3.45E+00	12.948	1.50E+01
51	270	3.01E+00	1.85E+00	348.895	-3.31E+00	13.2	1.49E+01
50	270	3.13E+00	1.98E+00	348.914	-3.17E+00	13.447	1.48E+01
49	270	3.26E+00	2.10E+00	348.932	-3.04E+00	13.688	1.47E+01
48	270	3.39E+00	2.22E+00	348.947	-2.91E+00	13.923	1.47E+01
47	270	3.51E+00	2.34E+00	348.961	-2.78E+00	14.154	1.46E+01
46	270	3.63E+00	2.46E+00	348.974	-2.66E+00	14.378	1.45E+01
45	270	3.75E+00	2.58E+00	348.984	-2.53E+00	14.598	1.44E+01
44	270	3.86E+00	2.70E+00	348.993	-2.41E+00	14.811	1.44E+01
43	270	3.98E+00	2.81E+00	349	-2.29E+00	15.019	1.43E+01
42	270	4.09E+00	2.92E+00	349.006	-2.17E+00	15.222	1.42E+01
41	270	4.20E+00	3.03E+00	349.011	-2.05E+00	15.42	1.41E+01
40	270	4.31E+00	3.13E+00	349.014	-1.94E+00	15.611	1.41E+01
39	270	4.42E+00	3.24E+00	349.015	-1.83E+00	15.798	1.40E+01
38	270	4.52E+00	3.34E+00	349.015	-1.72E+00	15.979	1.39E+01
37	270	4.62E+00	3.44E+00	349.014	-1.61E+00	16.155	1.39E+01
36	270	4.72E+00	3.54E+00	349.012	-1.51E+00	16.325	1.38E+01
35	270	4.82E+00	3.64E+00	349.008	-1.40E+00	16.49	1.38E+01
34	270	4.91E+00	3.73E+00	349.003	-1.30E+00	16.65	1.37E+01
33	270	5.01E+00	3.82E+00	348.997	-1.21E+00	16.805	1.37E+01
32	270	5.10E+00	3.91E+00	348.99	-1.11E+00	16.954	1.36E+01
31	270	5.19E+00	3.99E+00	348.982	-1.02E+00	17.098	1.36E+01
30	270	5.27E+00	4.08E+00	348.972	-9.29E-01	17.238	1.35E+01
29	270	5.35E+00	4.16E+00	348.961	-8.42E-01	17.372	1.35E+01
28	270	5.43E+00	4.24E+00	348.95	-7.58E-01	17.501	1.34E+01
27	270	5.51E+00	4.32E+00	348.937	-6.76E-01	17.625	1.34E+01
26	270	5.59E+00	4.39E+00	348.923	-5.97E-01	17.744	1.33E+01
25	270	5.66E+00	4.46E+00	348.908	-5.21E-01	17.859	1.33E+01
24	270	5.73E+00	4.53E+00	348.892	-4.48E-01	17.968	1.32E+01
23	270	5.80E+00	4.60E+00	348.875	-3.77E-01	18.073	1.32E+01
22	270	5.86E+00	4.66E+00	348.858	-3.09E-01	18.172	1.32E+01
21	270	5.92E+00	4.72E+00	348.839	-2.44E-01	18.268	1.31E+01
20	270	5.98E+00	4.78E+00	348.819	-1.82E-01	18.358	1.31E+01
19	270	6.04E+00	4.83E+00	348.799	-1.23E-01	18.444	1.31E+01
18	270	6.09E+00	4.89E+00	348.777	-6.67E-02	18.525	1.30E+01
17	270	6.14E+00	4.94E+00	348.755	-1.34E-02	18.601	1.30E+01
16	270	6.19E+00	4.98E+00	348.732	3.70E-02	18.673	1.30E+01
15	270	6.24E+00	5.03E+00	348.708	8.44E-02	18.741	1.29E+01
14	270	6.28E+00	5.07E+00	348.683	1.29E-01	18.804	1.29E+01
13	270	6.32E+00	5.11E+00	348.657	1.70E-01	18.862	1.29E+01
12	270	6.35E+00	5.14E+00	348.63	2.09E-01	18.916	1.29E+01
11	270	6.39E+00	5.18E+00	348.603	2.44E-01	18.966	1.28E+01
10	270	6.42E+00	5.21E+00	348.575	2.77E-01	19.011	1.28E+01
9	270	6.45E+00	5.23E+00	348.546	3.06E-01	19.052	1.28E+01
8	270	6.47E+00	5.26E+00	348.516	3.32E-01	19.088	1.28E+01
7	270	6.49E+00	5.28E+00	348.485	3.56E-01	19.12	1.28E+01
6	270	6.51E+00	5.30E+00	348.454	3.76E-01	19.148	1.27E+01
5	270	6.53E+00	5.31E+00	348.421	3.93E-01	19.171	1.27E+01
4	270	6.54E+00	5.33E+00	348.388	4.07E-01	19.191	1.27E+01
3	270	6.55E+00	5.34E+00	348.354	4.18E-01	19.205	1.27E+01
2	270	6.56E+00	5.34E+00	348.32	4.26E-01	19.216	1.27E+01
1	270	6.56E+00	5.35E+00	348.284	4.30E-01	19.222	1.27E+01